Using of Di- and Triorganotin(IV) complexes as photostabilizer for poly(vinyl chloride)

A Thesis
Submitted to the College of Science Al-Nahrain University as a Partial Fulfillment of the Requirements for the Degree of M.Sc. in Chemistry

By

Mustafa Mohammed Ali

B.Sc. Chemistry/College of Science/Al-Nahrain University (2014)

Supervised by

Prof. Dr. Emad Al-Sarraj

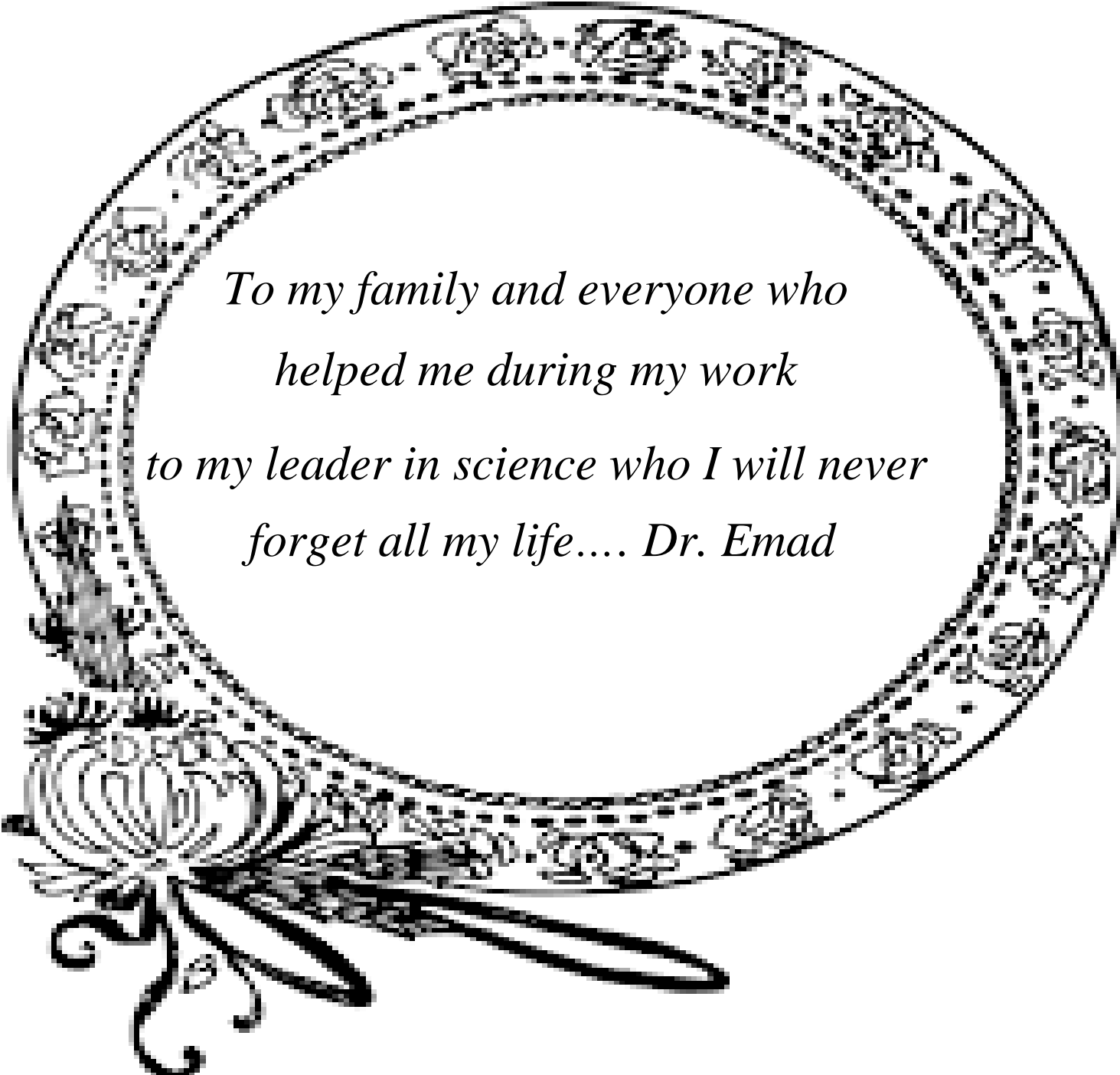**2017 A.D.**   **1438 A.H.**

١

بِسْمِ اللَّهِ الرَّحْمَنِ الرَّحِيمِ

إِنَّا فَتَحْنَا لَكَ فَتْحًا مُبِينًا (١) لِيَغْفِرَ لَكَ اللَّهُ مَا تَقَدَّمَ مِن ذَنبِكَ وَمَا تَأَخَّرَ وَيُتِمَّ نِعْمَتَهُ عَلَيْكَ وَيَهْدِيَكَ صِرَاطًا مُّسْتَقِيمًا (٢) وَيَنصُرَكَ اللَّهُ نَصْرًا عَزِيزًا (٣)

صدق الله العظيم

سورة الفتح

To my family and everyone who

helped me during my work

to my leader in science who I will never

forget all my life…. Dr. Emad

Acknowledgements

I would like to express my sincere thanks and gratitude to my supervisor, Prof. **Dr. Emad A. Yousif** for suggesting the subject of this thesis and supervision in my work. His enthusiasm, encouragement, and faith in me throughout have been extremely helpful. Without him this work would not be completed.

I would like to thank my **father**, my **mother**, my **wife**, my **brothers** and all of my **friends** for their supporting me during the course of the study and work.

Special thanks go to the staff of **Chemistry Department**, **College of Science, Al-Nahrain University** for their support and teaching me for all the six years.

Finally, I wish to thank all the people who helped me during my work.

Mustafa

Abstract

Four organotin complexes containing furosemide as a ligand (L), Ph_3SnL, Me_2SnL_2, Bu_2SnOHL and Bu_2SnL_2, were synthesized in alcoholic medium.

These complexes are:

Dimethyltin di-[4-hloro-2-(furan-2-ylmethylamino)-5-sulfamoylbenzoic acid], Me_2SnL_2

Dibutyltin di-[4-chloro-2-(furan-2-ylmethylamino)-5-sulfamoylbenzoic acid], Bu_2SnL_2

Dibutyltin hydroxy [4-chloro-2-(furan-2-ylmethylamino)-5-sulfamoylbenzoic acid], Bu_2SnOHL

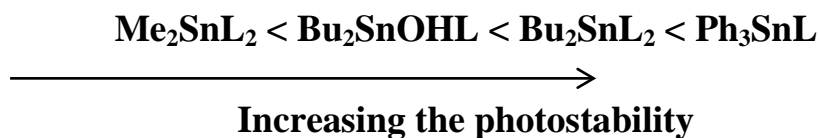Triphenyltin [4-chloro-2-(furan-2-ylmethylamino)-5-sulfamoylbenzoic acid], Ph_3SnL

The ligand and its organotin complexes were characterized by using: FTIR, UV-visible spectroscopy, ^{1}H-NMR, conductivity measurements and melting point. According to the spectral data of the complexes an octahedral geometry was proposed for the Me_2SnL_2 and Bu_2SnL_2, while the Ph_3SnL and Bu_2SnOhL complex has trigonal bipyramid geometry.

The synthesized organotin complexes (0.5% by weight) were used as additives to improve the photostability of poly(vinyl chloride), (40 μm thickness) upon irradiation. The photostabilization of poly(vinyl chloride) films were studied at room temperature under irradiation of light(λ= 313)nm wave length with light intensity of $7.75*10^{-7}$ Einstein $Dm^{-3} Sec^{-1}$.

The photostabilization activity of organotin(IV) complexes were determined by monitoring the hydroxyl (I_{OH}) , polyene ($I_{c=c}$) and carbonyl ($I_{C=O}$) indexes, weight loss method with irradiation time. It was found that carbonyl, polyene and hydroxyl indexes values increased with irradiation time and this increase depend on the type of additives. The surface morphology for these films was studied during irradiation time and changes in viscosity average molecular weight of PVC with irradiation time were also tracked. The

quantum yield of the chain scission (Φ_{cs}) of these complexes in PVC films was also evaluated.

The following trend was obtained for the photostabilization effect on PVC films in presence of additives as shown below:

$$\text{Me}_2\text{SnL}_2 < \text{Bu}_2\text{SnOHL} < \text{Bu}_2\text{SnL}_2 < \text{Ph}_3\text{SnL}$$

$\longrightarrow$

Increasing the photostability

According to the experimental results obtained several mechanisms were suggested depending on the structures of the organotin complexes. Among these mechanisms, HCl scavenging, UV absorption, peroxide decomposer and radical scavenger for photostabilizer additives.

Table of Contents

List of Figures

List of Tables

Symbols and Abbreviations

AFM	Atomic Force Microscopy
R·	Alkyl radical
RO·	Alkoxy radical
ASTM	American Standard Methods
BDH	British Drug House
ROO·	Peroxy radical
DMF	DiMethylFormamide
DP	Degree of Polymerization
hv	Energy, ultraviolet or solar radiation
FTIR	Fourier Transform Infra-Red
HNMR	Proton Nuclear Magnetic Resonance
H·	Hydrogen radical
HCl	Hydrogen chloride
HO·	Hydroxide radical
HOO$^-$	Hydroperoxy group
mm	Millimetre
μm	Micrometer
nm	nanometre

$^1O_2$	Singlate oxygen
P·	Polymer radical
PE	PolyEthylene
PO·	Polymer Oxy Radical
POOH	Polymer Hydroperoxy groups
PVC	Poly Vinyl Chloride
ROO·	Peroxy radical
HOOH	Hydrogen peroxide
THF	Tetrahydrofuran
UV-VIS	Ultra Violet-Visible
VCM	Vinyl Chloride Monomer

Chapter One

INTRODUCTION

INTRODUCTION

1.1 Organotin compounds

Organotins are compounds which have at least one organic substituent linked directly to the tin atom *via* the carbon atom of the organic substituent. Organotin(II) and organotin(IV) compounds are known since tin has two stable oxidation states, that is +2 and +4. However, organotin(II) compounds are not very stable and tends to polymerize rapidly [1,2]. The organotin(II) compounds are also easily oxidized to organotin(IV) that is more stable. Bis(cyclopentadienyl)tin(II) is the only known stable organotin(II) derivative. The tin atom of this organotin(II) compound is sp^2 hybridized, with two of the hybrid orbitals involved in

bonding with cyclopentadienyl ligands and the third containing the unshared pair of electrons as illustrated in Figure (1.1).
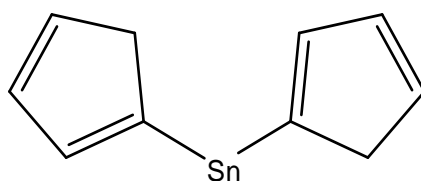
Figure 1.1 Bis(cyclopentadienyl)tin(II)

Most known tin compounds are derivatives of organotin(IV) due to its stability. In organotin(IV) compounds, sp^3 hybridization of the valence orbital resulted in tetrahedral oriented bonds. The four principal classes of organotin(IV) compounds are mono-, di-, tri-, and tetraorganotins, which are represented by R_nSnX_{4-n}, where R is any organic group and X is anionic residue.

Organotin(IV) compounds with electronegative groups such as organotin halides or pseudohalides are prone to use its empty 5d orbital to expand its coordination number beyond four. Hence, formation of 5-coordinate trigonal bipyramidal sp^3d or six-coordinate octahedral sp^3d^2 coordination geometries are commonly observed in organotin(IV) complexes. In the case of tetraorganotin compounds, where there is absence of any electronegative groups, evidence for higher coordination in such compounds are also known. In particular, if the tetraorganotin contained organic groups with donor substituents such as 3-(2-pyridyl)-2-thiophene. These types of higher than four coordination compounds are observed in bis[3-(2-pyridyl)-2-thienyl-C,N]diphenyltin(IV), where the intramolecular coordination of the donor nitrogen atoms to the tin atom resulted in two additional coordination bonds in the tetraorganotin compounds [3,4].

1.2 Synthesis of tetraorganotin

1.2.1 Grignard method

Tetraalkyls, tetraaryls, tetravinyl and tetraethyltin compounds are prepared in coordinating solvents such as diethyl ether (Et_2O) or tetrahydrofuran (THF) [5].

$$SnCl_4 + 4\ RMgCl \xrightarrow{\ THF\ } R_4Sn + 4\ MgCl_2$$

[R = aryl or alkyl]
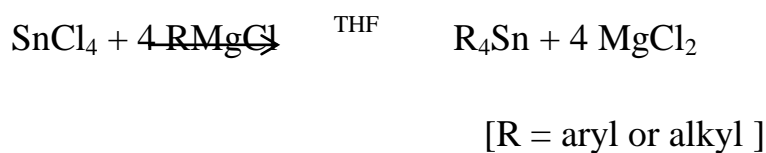
1.2.2 Wurtz method

The reaction of alkyl halide with alkali metal such as sodium, followed by the addition of stannic chloride also yield the tetraorganotin.

$$SnCl_4 + 4\ RCl \xrightarrow{\ 8Na\ } R_4Sn + 8\ NaCl$$

[R= alkyl or aryl]
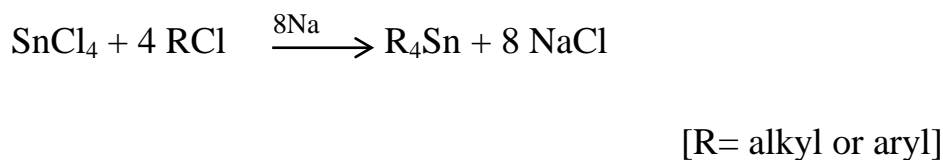
1.2.3 Aluminium alkyl method

Organoaluminium compounds can be reacted with stannic chloride to produce tetraorganotin. The reactions are carried out in the absence of solvents. The addition of a complexing agent such as ether is required for high efficiency [6].

$$3\ SnCl_4 + 4\ R_3Al \xrightarrow{\ R_2O\ } 3\ R_4Sn + 4\ AlCl_3$$

[R= alkyl or aryl]
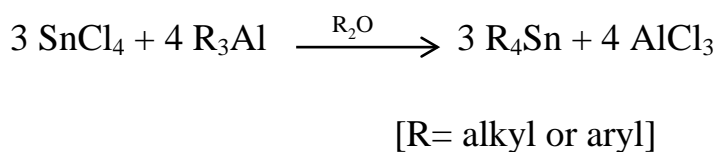
1.3 Synthesis of mono-, di- and triorganotins

The first organotin derivative which isolated by Frankland some 130 years ago was diethyltin diiodide. This organotin compound was synthesized by direct synthesis method. The direct synthesis method was later extended for preparation of other organotin halides

that involves the direct alkylation of metallic tin or tin halides by alkyl halides, in the presence of suitable catalyst [7].

$$Sn + 2\ RX \xrightarrow{\text{catalyst}} R_2SnX_2$$
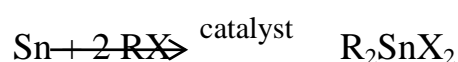
[R= alkyl or aryl]

The direct synthesis may be carried out in the absence of a catalyst. The reaction of benzyl chloride with tin powder represents an example, in which the toluene or water used as the solvent to gave good yield of dibenzyltin chloride. and tribenzyltin chloride [8], respectively.

$$2\ BzCl + Sn \xrightarrow{\text{PhMe}} Bz_2SnCl_2$$

$$3\ BzCl + 2\ Sn \xrightarrow{\text{H}_2\text{O}} Bz_3SnCl + SnCl_2$$

$$3\ Bz_2SnCl_2 + Sn \xrightarrow{\text{H}_2\text{O}} 2\ Bz_3SnCl + 2\ SnCl_2$$
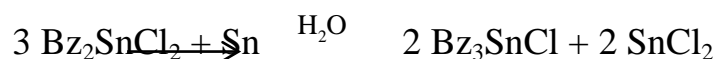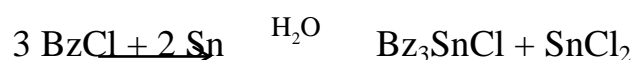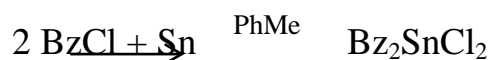
The conventional method of preparing tri-, di- and monoorganotins is by the comproportionation reaction of tetraorganotins using different stoichiometric amounts of stannic chloride.

$$3\ R_4Sn + SnX_4 \longrightarrow 4\ R_3SnX$$

$$R_4Sn + SnX_4 \longrightarrow 2\ R_2SnX_2$$

$$R_4Sn + 3\ SnX_4 \longrightarrow 4\ RSnX_3$$
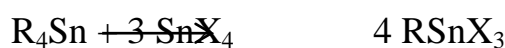
[R= alkyl or aryl]

The organotin halides particularly triorganotin halides, R_3SnX and diorganotin halides, R_2SnX_2 can be easily converted to organotin hydroxides and oxides by base hydrolysis using sodium hydroxide or ammonium hydroxide.

$$R_3SnX + OH^- \longrightarrow R_3SnOH + X^-$$

$$R_2SnX_2 + OH^- \longrightarrow R_2SnO + 2X^-$$
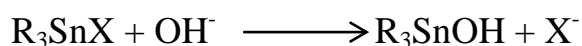
[R= alkyl or aryl]

1.4 Organotin structures and bonding

Both the Sn(II) and Sn(IV) state are stable. The Sn(II) state uses mainly the 5p orbitals for bonding leaving the unshared singlet pair in the largely 5s state, with a little p character SnX_2 is compound shown in figure (1.2) (1, the stannylenes) with XSnX angle of about 90-100^0. These compound are most stable when there are strongle electron-attracting ligands, which make loss of the remaining electron pair more difficult (e.g. :SnF_2, :$SnCl_2$), or when the ligands X are very bulky, and sterically protect the tin against further ligation (e.g. :$Sn[N(SiMe_3)_2]_2$). Otherwise, oxidation readily occurs to the Sn(IV) state, where the tin is sp^3 hybridized and the SnX_4 (4, stannane) molecule has tetrahedral geometry.

However, both the stannylenes and stannanes have vacant 5d orbitals, which can accept one or more further ligands. The stannylenes readily form the trigonal pyramid sp^3 complexes :SnX3 (2), and the seesaw sp^{3}d complexes :SnX_4 (3), and the stannens form the trigonal bipyramidal sp^{3}d complexes SnX_5 (5) or octahedral SP^{3}d^2 complexes SnX_6 (6). All of these may carry charges corresponding to the charge of the new ligands X [9].
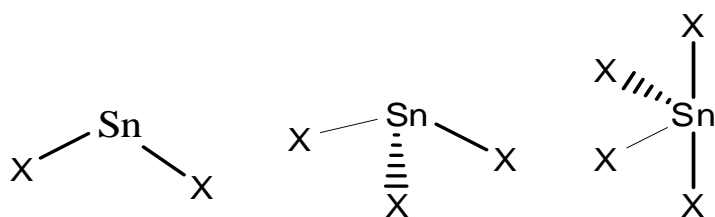
1 (sp^2)   2 (sp^3)   3 (sp^{3}d)

Structures of Sn(II) compounds
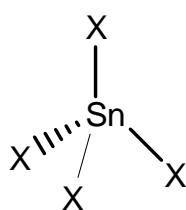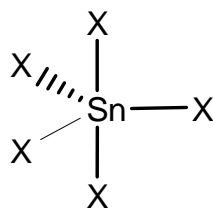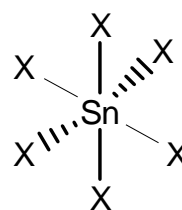
(4) Sp^3 (5) Sp^{3}d   (6) sp^{3}d^2

Structures of Sn(IV) compounds

Figure 1.2 Proposed structure of organotin(IV) compounds.

1.5 Application of Organotin Compounds

The synthesis, characterization and structural study of organotin(IV) complexes have been well-known. These procedures was established and documented since the first organotin(IV) compound was successfully isolated in 1850s. The interest and application of organotin(IV) carboxylate complexes have also received considerable attention as these complexes display a large array of applications in industries as catalysts, antifouling agents, wood preservatives, crop protection agents, etc. [10].

1.5.1 Biological Application of Organotin Compounds

The use of organotin(IV) carboxylates for any specific biological activity is related to the nature and number of organic groups R directly attached to the tin atom and carboxylate groups attached to the tin atom through Sn-O bonds. These factors decide the effectiveness of organotin(IV) compounds for required purposes. The nature of the R group decides its site of attack for organotin(IV), binding to the different locations in the body, e.g. carbohydrates, nucleic acid derivatives, amino acids [11] and to proteins.

The presence of hetero atoms such as N, O or S in the ligand play a key role in the geometry, and thus effect the biological activity of these complexes [12]. Higher biological

activity of organotin(IV) compounds encourage their applications in pharmaceutical. Some of the biological applications are discussed below.

(I) *Pharmaceutical Applications*

Metal ions have a significant role in various physicochemical processes that take place in the living body and they are known for their metallopharmaceutical applications. Organotin(IV) compounds are used as potential biologically agent against various diseases [13,14]. Study of organotin(IV) activity and their mode of effect by interaction with different parts like ATPase and hemoglobin's are a model for studying interactions of drugs with the human body [15].

The synthesis of organotin(IV) complexes with new ligands and different coordination geometries are attempt to develop new drugs for different purposes. Potential biological activities of organotin(IV) compounds encouraged their applications in the fields of veterinary science, antibacterial, antifungal, antitumour and antimalarial [16] agents.

(II) *Antifouling agents*

Organotin(IV) compounds, particularly tributyltin (TBT), are used as a part of paint to protect the underwater surface of ships against the attack of microorganism. The ship without this paint causes higher fuel consumption, premature dry docking, and raise the cost of cleaning due to increase weight and roughness of the hull [17].

(III) *Wood protection*

Insects, fungi and bacteria decompose the cellulose of wood. Tributyltin(IV) complexes show potential biological activities against microorganism (fungi and bacteria), which are used for treatment and preservations of wood. In this approach the wood is treated with organotin(IV) compounds in a vacuum. Releasing the vacuum result in a flow of

organotin(IV) into the wood in which the organotin(IV) compound is attached with terminal OH groups of cellulose preventing the damage of wood by microorganisms [18].

(IV) *Antiviral agents*

Organotin(IV) compounds can be applied as metal-based drugs used for the treatment of tumor and some compounds show a higher activity than cis-platin. This encourage scientists to make attempts for designing tin based drugs having good activity and low toxicity for cancer chemotherapy, due to their apoptotic inducing character, which is linked to the inhibition of mitochondrial oxidative phosphorylation. There are a number of reviews available that dealing with potential anti-tumor application of organotin(IV) compounds [19]. The diorganotin(IV) complexes against tumor is geometry based as their coordination to target site depends on their geometry. The anticancer of drugs can be evaluated by their ability of hydrolysis in a suitable medium. Drug molecules produce cis-configuration with at least two water molecules and have both hydrophobic and hydrophilic groups. Both the anticancer complex and its active intermediate species should be polar. The metal should be capable of bonding with DNA. Organotin(IV) compounds fulfilled all the above cited rules and show activity by changing the gene sequence in the DNA [20].

1.5.2 Non-biological applications

Organotin(IV) compounds have wide ranging industrial and synthetic applications, which attract the interest of scientists to develop methods that meet the increasing demands in production.

(I) *As a PVC stabilizer*

One important uses of organotin(IV) compounds is to stabilize PVC at high temperatures. During its processing at higher temperatures, HCl is eliminated that catalyses further elimination and generating conjugated polyene as an end product. This also causes changes of color and the physical state of the resin. Organotin(IV) stabilizers are good oxidation catalysts and they fulfill all the requirements necessary for an ideal stabilizer [21,22].

(II) *Catalytic activity*

Mono and diorganotin(IV) compounds possess outstanding catalytic activities because of the bonding capability of lone pair electrons on tin [22]. They are utilizing in the field of chemical synthesis. In chemical synthesis, the organotin(IV) compounds are used as catalysts for the esterification and transesterification. The tin-based catalysts show no decomposition at high temperatures. Organotin(IV) based catalysts are used for the formation of various types of polymers, which are used for coating purposes [23].

(III) *Glass coating*

Organotin(IV) halides are used to form electrically conductive thin films on the surface of glass by using Atmospheric Pressure Chemical Vapor Deposition (AP-CVD) technique [24] due to its economical reason and wide range commercial applications. Tin chloride is used as a precursor for the formation of transparent conductive oxide (TCO) films.

$$SnCl_4 + 2H_2O \rightarrow SnO_2 + 4HCl$$
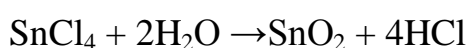
The coatings of 10 nm thickness provide strength, thermal stability and resistance to oxidation. Coated glass is used in deicing wind shield screens, security glass, or display systems [25]. This is due to their low electrical resistance and high resistance to chemicals. TCO film also control the loss of heat through glass, which is due to the metal oxide film deposition on glass surface. Coating also acts as a p-type or n-type semiconductor or conductor.

1.7 Poly(vinyl chloride)

Poly(vinyl chloride) (PVC) has unique physical and mechanical properties and it is widely utilized as a thermoplastic material [26]. PVC polymeric materials come next to polyolefins in terms of global production and consumption [27]. It has various outdoor applications, mainly in construction materials [28-30].

PVC however, undergoes photochemical degradation when exposed to sunlight or high temperatures for long periods of time [31]. This photodegradation process can lead to changes in the mechanical and physical properties of PVC [32]. Conjugated double bonds

could be formed within PVC chains due to dehydrochlorination. This process commonly takes place due to the presence of impurities and/or defects produced within the polymeric chains during synthesis [34]. Cross-linking and a reduction in the average molecular weight also occur within PVC chains due to photodegradation processes [31–33]. The poor stability of PVC hinders its use in outdoor applications. Therefore it is important to photostabilize PVC to enable its uses in harsh conditions such as high temperatures.

Commercial stabilizers such as plasticizers can be used to enhance photostability of PVC . Photostabilizers including Schiff base complexes [35-37], aromatics [38,39] and heterocycles [40-42] have been used in various studies in order to increase PVC photostability. Other additives include inorganic salts and metal complexes are also common for this application [43-45].

Organotin complexes can be used in a variety of different applications. The diorganotin(IV) additives containing benzamidoacetic acid have been used to stabilize PVC [46]. In this work, we report the use of di- and triorganotin(IV) complexes containing furosemide as photostabilizers for PVC as part of our general interest in the field of polymeric materials [47-51].

1.7.1 *Production of Poly(vinyl chloride)*

PVC is fabricated using three different procedures: suspension, bulk or mass and emulsion polymerization. The suspension process, however, grasps 80% of all commercial productions of PVC [52]. Polymerization of VCM occurs according to a free radical addition process, which includes initiation, propagation, chain transfer to monomer and bimolecular termination steps [53], (Scheme 1.1).

Decomposition initiator:

$$I \longrightarrow 2R$$

Initiation monomer:

$$R + H_2C=CHCl \longrightarrow R\text{-}CH_2\text{-}CHCl$$

Propagation:

$$R\text{-}CH_2\text{-}CHCl + n\ H_2C=CHCl \longrightarrow R(CH_2\text{-}CHCl)_n CH_2\text{-}CHCl$$

Chain transfer to monomer:

$$\sim\!\!\sim\!CH_2\text{-}CHCl + H_2C=CHCl \longrightarrow \sim\!\!\sim\!CH_2\text{-}CH_2Cl + H_2C=CCl$$

$$\longrightarrow \sim\!\!\sim\!CH=CHCl + H_3C\text{-}CHCl$$

Termination:

$$2\ \sim\!\!\sim\!CH_2\text{-}CHCl \longrightarrow \overset{\overset{\displaystyle Cl}{|}}{\sim\!CH_2\text{-}CH}\text{-}CH2\text{-}\overset{\overset{\displaystyle Cl}{|}}{CH}\!\sim\!\!\sim$$

(combination of radicals)

$$\longrightarrow \sim\!\!\sim\!CH_2\text{-}CH_2Cl + \sim\!\!\sim\!CH=CHCl$$

(disproportionation)

$$\sim\!\!\sim\!CH_2\text{-}CHCl + R \longrightarrow \sim\!CH_2\text{-}CHCl\text{-}R$$

(combination with primary radical)
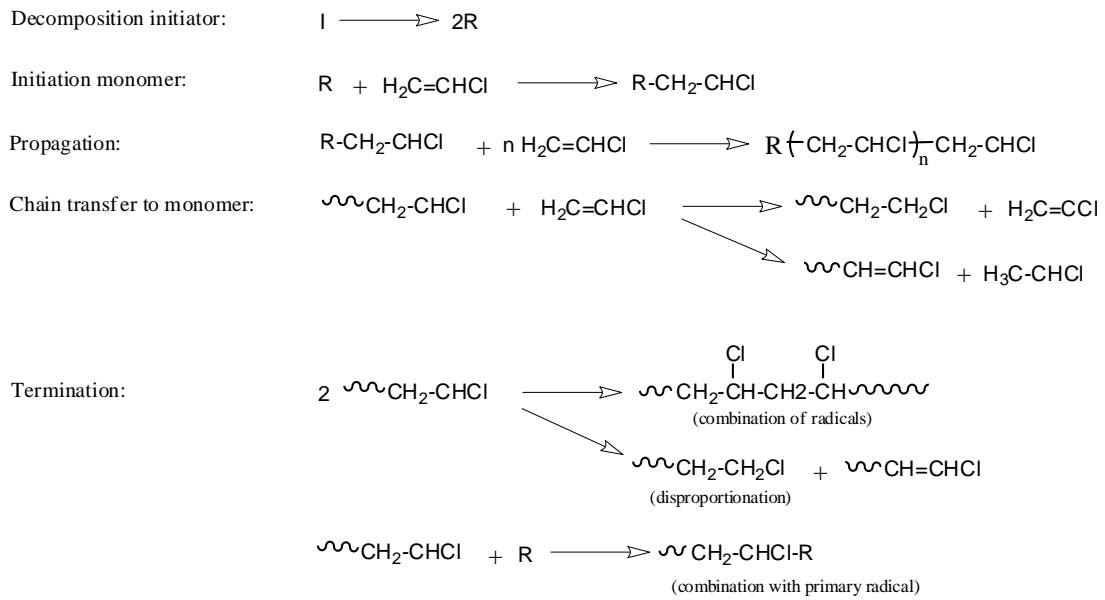
Scheme 1.1 VCM polymerization

The general reaction describing the PVC polymerization is appeared in Figure (1.3)

vinyl chloride

Polymerization

Poly(vinyl chloride) or PVC

n = a very large integer
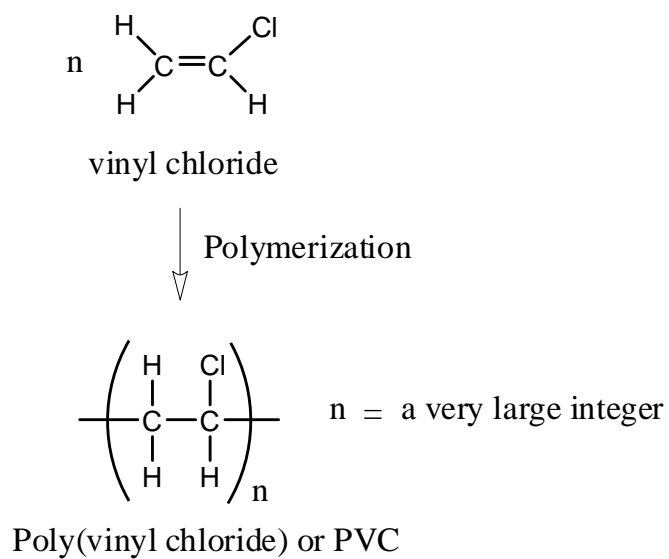
Figure 1.3 PVC formation

1.7.2 Uses of poly(vinyl chloride)

The low generation costs and the great versatility of vinyl chloride polymers are the two main reasons for their large share on the plastic market. The good performance of poly(vinyl chloride) products have increased the utilization of this polymer in building, mainly in exterior applications, such as window profiles, cladding structure and siding [54]. The polymer can be converted into wide range of different products exhibiting an extremely many properties both physical and chemical by using modifying agents, such as plasticizers, fillers and stabilizers [55].

PVC compositions have succeeded in materials such as rubber, metals, wood, leather, textiles, conventional paints and coatings, ceramics, glass.

In North America, PVC is mainly used for pipes and sidings, while in Europe and Asia, most use is for pipes and window frames. Builders in Japan have begun to use more PVC windows, in part because of their superior insulating properties to reduce heating and cooling costs. Demand in using PVC is growing strongly in China for construction materials as well as consumer goods. Flexible PVC is used for film and sheet, wire and cable insulation, floorcoverings, synthetic leather products, coatings and many other consumer goods.
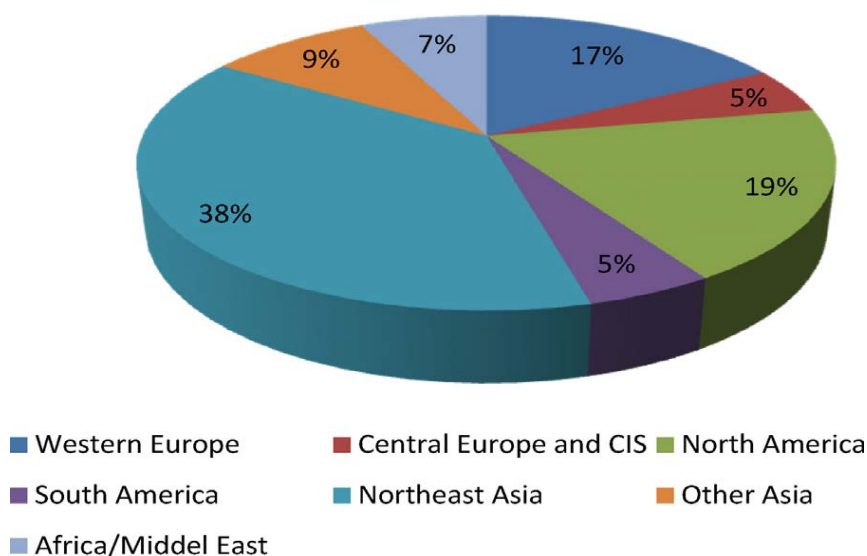
Figure1.4 World consumption of poly(vinyl chloride) in 2007.

1.7.3 Degradation of poly(vinyl chloride)

There is an abundant interest at present in the photodegradation of polymeric systems, and this is reflected in the great number of research papers and other scientific publications that show up each year in this area. A main reason for this interest is that macromolecular materials have progressively wide commercial applications where outdoor toughness is an important consideration. In this context, all commercial organic polymers will break down in air when exposed to sunlight, although there is a very wide range of photo-oxidative sensibilities. It is usually the absorption of near ultraviolet (UV) wavelengths which leads to bond-breaking reactions and the concomitant loss of useful physical properties and/or discoloration [56].

Under UV light, and within the presence of oxygen and moisture, PVC undergoes a fast dehydrochlorination and peroxidation process with the formation of polyenes. Degradation also causes a severe change in the mechanical properties of the polymer, which is accompanied by a decrease or increase in its average molecular weight as a consequence of either chain scission or crosslinking of the polymer molecules, respectively [57].

1.8 Factors that lead to the photodegradation

Generally, numerous variables are in charge of bringing about photodegradation of polymeric materials. They might be divided into two classifications [58].

I) Internal impurities, which might contain chromophoric groups that are brought into macromolecules during polymerization handling and storage; they include:

a- Hydroperoxide (H_2O_2).

b- Unsaturated bonds (C=C).

c- Catalyst residue.

d- Carbonyl

II) External impurities, which might contain chromophoric groups, are:

a- Traces of solvents, catalyst, ……..etc.

b- Compounds from urban environment and exhaust cloud, e.g. polynuclear hydrocarbons such as naphthalene and anthracene in polypropylene and polybutadiene.

c- Additives (dyes, pigment, thermal stabilizers, photostabilizers, .…… etc.).

d- Traces of metals and metal oxides from preparing hardware and containers, such as Fe, Ni or Cr.

1.9 Types of polymers degradation

The degradation of polymers usually start at the outer surface and penetrates gradually into the bulk of the material.

Polymer degradation can be caused by heat (thermal degradation), light (photodegradation), ionizing radiation (radio degradation), mechanical action, or by fungi, bacteria, yeasts, algae, and their enzymes (biodegradation). The deleterious effects of weathering on polymers generally has been ascribed to a complex set of processes, in which the combined action of UV light and oxygen predominant. The overall light-initiated process in the presence of oxygen generally is referred to as oxidative photodegradation or photooxidation. A pure thermal effect   in possible because oxygen is always present and so the process is thermaloxidative degradation [59].

There are many different modes of polymer degradation. These are very similar since they all involve chemical reactions that result in bond scission. These modes are:

1.9.1 Chemical degradation

Chemical degradation indicates exclusively to processes, which involved under the influence of chemical reagent (e.g. bases, acids, solvents gases, etc.) [60].

1.9.2 Thermal degradation

Thermal degradation is an ideal degradation situation for commercial polymer products in addition to industrial products. The thermal degradation divided into two classes; the thermal degradation in the absence of oxygen (thermal decomposition) and the thermal degradation in the presence of oxygen (thermal oxidation). The principle reason of thermal decomposition was the high temperature influence on the polymer [61].

1.9.3 Mechanical degradation

Generally indicate to macroscopic effects brought about under the effect of shear forces. These forces lead to the formation of macro radicals as follows:

Polymer chain   Macro free radical
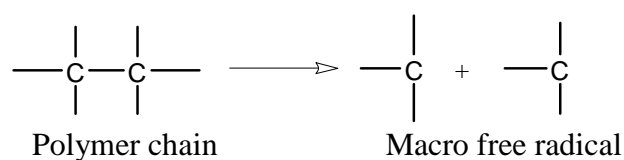
Such radicals could recombine in the absence of oxygen. In the presence of oxygen peroxy radicals can be created, which result in the degradation of polymeric chains [62].
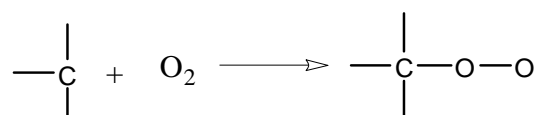
1.9.4 Biological degradation

The polymer product utilized in outdoor circumstances is exposed to environmental bacteria and a part of polymer material was biodegradable because of the chemical structure as formerly described. Microorganisms produce diffrent of enzymes which are able to react with natural and synthetic polymers [63].

1.9.5 Radiolytic degradation

When polymers are exposed to high energy radiation (e.g. gamma radiation) changes are occurred on their molecular structure, fundamentally chain scission, which leads to reduction in molar mass [64].

1.9.6 Photodegradation

Photodegradation is degradation of a photodegradable molecule occurred by the photon absorption. In particularly those wavelengths found in solar light, such as infrared radiation, ultraviolet light, and visible light. So, other forms of electromagnetic radiation could lead to photodegradation. Photodegradation involves photodissociation, the separate of molecules into smaller pieces by photons. It also involves the change of a molecular shape to make it irreversibly change, such as the denaturing of proteins, and the addition of other atoms or molecules [65].

Light - stimulate polymer degradation, or photodegradation, involves the physical and chemical changes occurred by irradiation of polymers with ultraviolet or visible light. In order to be effective, light should be absorbed by the polymeric material. Thus, the presence of chromophoric groups in the macromolecules is a prerequisite for the initiation of any photochemical reaction [66].

Photodegradation could happen in the absence of oxygen (chain breaking or cross-linking) and the existence of oxygen (photooxidative) degradation. The photooxidative degradation process is occurred by UV radiation and other catalysts, and also can be accelerated at elevated temperatures.

1.10 Polymer Oxidation

The degradation operation of the different types of polymer possess specific mechanisms and depend on both the major macromolecular chain nature, structure and on the chemical origin of the branched groups. It is outstanding for the oxidation of polyolefins or rubber (natural and   some synthetic types) that peroxy and the hydroperoxides radicals are intermediates in a chain mechanism. In the case of the halogenated polymers, the dehydrohalogenation is the first reaction stage followed by the thermal oxidation. Whereas for the polyamides or cellulose the oxidation take place by hydroperoxides within a short chain mechanism. [67].

The polymer degradation is brought on by two primary classes of factors, physical factors: light, heat, mechanical processing, ionizing radiation, ultrasonic…etc.;

Chemical factors: ozone, oxygen, chemicals, polymerization catalysts…. etc.

Also these degradation processes will be approached together with the polymer preservation methods, as shown in Figure (1.5)
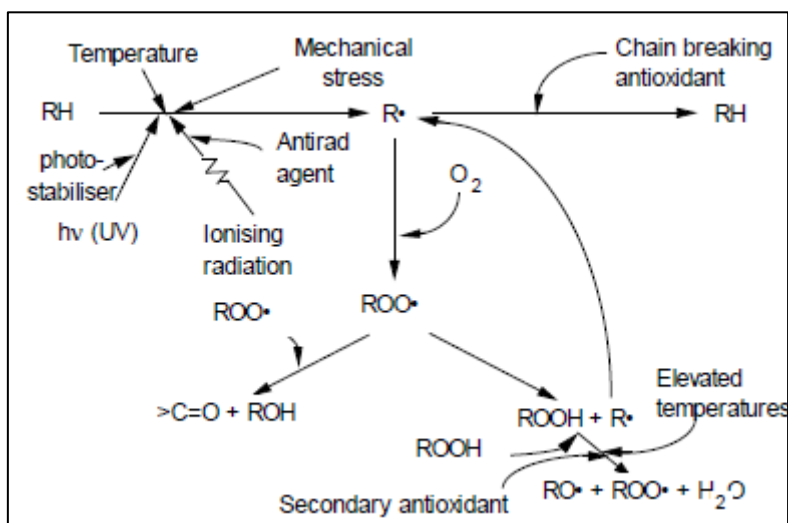
Figure 1.5 Oxidation of polymers and routes for their preservation

1.10.1 Therml-Oxidation

The thermal-oxidation (or thermo-oxidation) of the macromolecular materials is defined as their thermally initiated reaction with the molecular oxygen. The general planner of the polymers therml-oxidation indicates the radical character of the process [68], see figure (1.6).
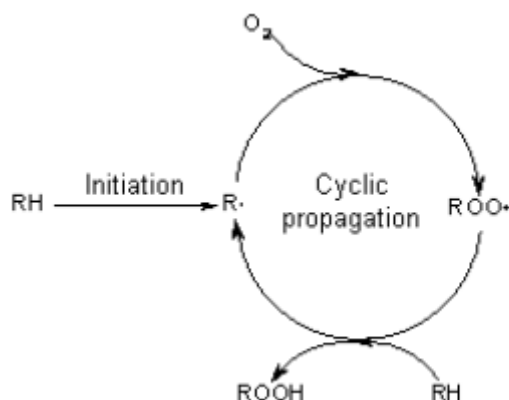
Figure 1.6 Therml-oxidation process in a polymeric material.

The therml-oxidation of a hydrocarbon polymer begins with a H atom extraction by excited oxygen or a radical. The organic radical created reacts with the polymer prompting a peroxy radical and further to a hydroperoxide accompanied by a macromolecular radical, and thus propagates the chain reaction process:

$$R\text{-}H + I^{\bullet} \rightarrow R^{\bullet} + IH \quad \text{Initiation} \tag{1.1}$$

$$R^{\bullet} + O_2 \rightarrow ROO^{\bullet} \qquad \left.\begin{array}{l} \\ \\ \end{array}\right\} \quad \text{Propagation} \tag{1.2}$$

$$ROO^{\bullet} + RH \rightarrow ROOH + R^{\bullet}$$
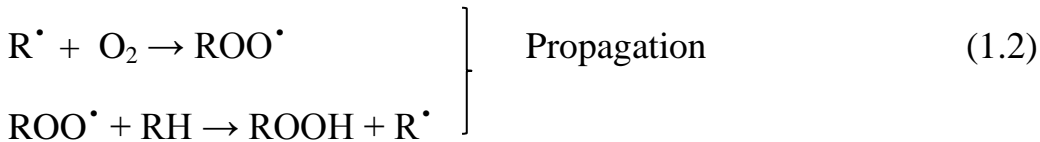
The major reaction incharge of the chain termination reactions is the peroxy radical recombination:

$$\tag{1.3}$$
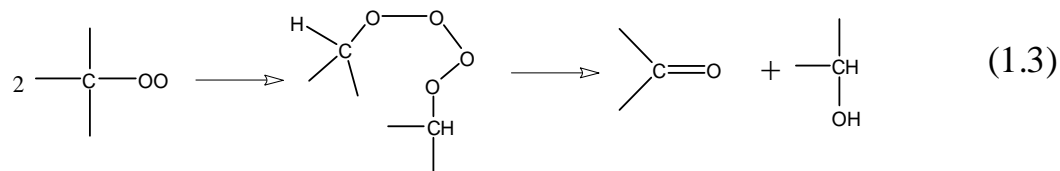
The unstable hydroperoxides is shown in reaction 1.2, which decomposes as appeared below:

$$ROOH \rightarrow R^{\bullet} + HOO^{\bullet} \tag{1.4}$$

$$ROOH \rightarrow RO^{\bullet} + HO^{\bullet} \tag{1.5}$$
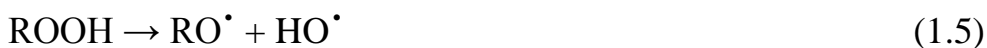
The alcoxy radicals from the reaction step 1.5 might react with the present hydroperoxides promoting alcohols and peroxy radicals:

$$ROOH + RO^{\bullet} \rightarrow ROO^{\bullet} + ROH \tag{1.6}$$

To be seen that the free radicals $R^{\bullet}$ react in (1.2) and (1.4) with hydroperoxides and/or molecular oxygen in this manner starting new response chains.

The initiating reaction is very important in the therml-oxidation process. If the H is bonded to a benzyl, tertiary or allyl type carbon atom, its extraction is simpler compared with that attaching to a primary or secondary type atom carbon. This explains the marked

propensity towards oxidation of the diene type polymers and in addition of the unsaturated polyesters and the higher stability of the linear polyolefins.

The therml-oxidation at ambient temperature (auto-oxidation) was considered by Bolland and Gee beginning from the hydrocarbon oxidation and reached out to polyolefins [69], as demonstrated as follows (1.7) - (1.19):

Intiation steps

$$RH \longrightarrow R^{\bullet} + H^{\bullet} \qquad (1.7)$$

$$ROOH \longrightarrow RO^{\bullet} + HO^{\bullet} \qquad (1.8)$$

$$2ROOH \longrightarrow ROO^{\bullet} + RO^{\bullet} + H_2O \qquad (1.9)$$

$$ROOH + M^{n+} \longrightarrow RO^{\bullet} + M^{(n+1)+} OH^- \qquad (1.10)$$

$$ROOH + M^{(n+1)+} \longrightarrow ROO^{\bullet} + M^{n+} + H^+ \qquad (1.11)$$

Propagation

$$R^{\bullet} + O_2 \longrightarrow ROO^{\bullet} \qquad (1.12)$$

$$ROO^{\bullet} + RH \longrightarrow ROOH + R^{\bullet} \qquad (1.13)$$

Transfer

$$RO^{\bullet} + RH \longrightarrow ROH + R^{\bullet} \qquad (1.14)$$

$$HO^{\bullet} + RH \longrightarrow H_2O + R^{\bullet} \qquad (1.15)$$

Termination

$$2R^{\bullet} \longrightarrow R - R \qquad (1.16)$$

$$ROO^{\bullet} + R^{\bullet} \longrightarrow ROOR \qquad (1.17)$$

$$2ROO^{\bullet} \longleftrightarrow ROOOOR \qquad (1.18)$$

$$ROOOOR \longrightarrow R^{'}OH + R''R'''C=O + O_2 \qquad (1.19)$$
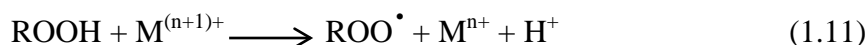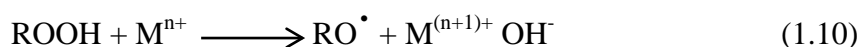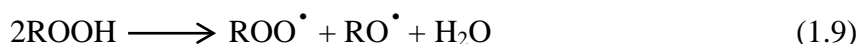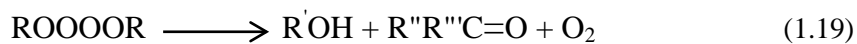
The stability of polymeric material towards thermal oxidation depends upon the C-H bonds strength, the crystallinity point, the presence of substituents, the catalysts traces and heteroatoms.

1.10.2 Photo-Oxidation

The sun energy is an essential physical degradation factor for polymers and elastomers. The joined effect of the sun light and of the oxygen may result in discoloration, modification, scission and/or crosslinking. Appearance of oxygenated chemical groups that reduced the electrical properties [70].

The photo-oxidation mechanisms, the incident photons in UV-visible spectral range resulted in excited molecular species that involving excited molecular oxygen. The photochemical reactions are chain reactions, that based on three types of different photophysical operations: fluorescence, internal energy conversion and phosphorescence (intermolecular energy transfer). The molecular excited oxygen (oxygen singlet, $_1O^2$) is included in numerous reactions because of its high reactivity. The resulted chemical species relied on the chemical nature of the material, environmental conditions and temperature.

The initiation reaction rate is higher in comparsion to the thermal oxidation initiation rate. The essential kinetic mechanism is similar to the therml-oxidation [71], reactions (1.7) – (1.19). The variance consists in a variant mechanism of the initiation step, as shown in the reaction (1.20) [72]:

$$
\left.\begin{array}{l} ROOH \\ \diagdown C{=}O \diagup \\ RH\ldots O_2 \end{array}\right\} \xrightarrow{\ h\nu\ } R\,,\ RO^{\bullet}\,,\ RO^{\bullet}_2 \qquad\qquad (1.20)
$$
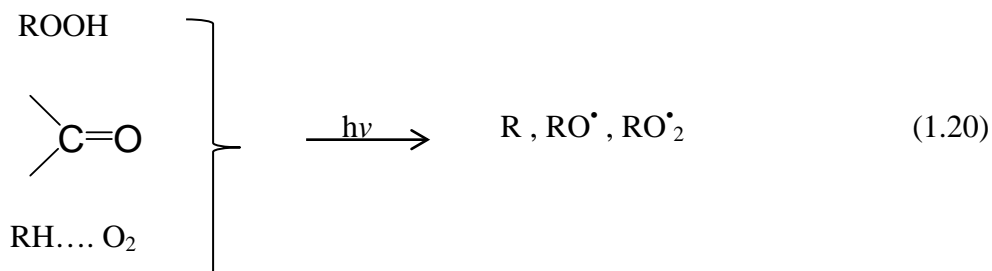
1.11 Aim of the present work

The aims of the present research are:

i- Synthesis and characterization of Di- and Triorganotin(IV) complexes with furosemide as a ligand.

ii- Evaluation the photostabilization activity of these organotin(IV) complexes by UV light in the presence poly(vinyl chloride) polymer.

Chapter Two

EXPEREMENTAL

2. EXPERIMENTAL PART

2.1 Chemicals

All reagents, starting materials and solvents used in this work were of highest purity available and used without any further purification as shown in Table 2.1.

Table 2.1 Chemicals used in the experimental work, their purity and the companies suppliers

No.	Compound	Formula	M.wt.	State	Purity	Company
1	Furosemide	$C_{12}H_{11}ClN_2O_5S$	330.74	solid	92%	Scharlau
2	Ethanol	CH_3CH_2OH	46.07	liquid	99%	Scharlau
3	Tetrahydrofuran	C_4H_8O	72.11	liquid	99.5%	Romil
4	PVC	$(C_2H_3Cl)_n$	$(62.5)_n$	solid	97%	BDH
5	Methanol	CH_3OH	32.4	liquid	99%	GCC
6	Triphenyltin chloride	$C_{18}H_{15}ClSn$	385.46	Solid	97%	Fluka
7	Dibutyltin oxide	$C_8H_{18}OSn$	248.92	Solid	97%	Fluka

8	di-n-butyltin dichloride	$C_8H_{18}SnCl_2$	303.84	Solid	97%	Alfa Aesar
9	Dimethyltin dichloride	$C_2H_6SnCl_2$	219.67	Solid	95%	Fluka
10	DMSO	C_2H_6OS	78.13	liquid	98%	BDH

2.2 Instruments

2.2.1 Melting point

Melting point apparatus of Electro thermal capillary, was used to measure melting points of all prepared compounds. The measurements were carried out in the laboratories of the Chemistry Department /College of Science /Al-Nahrain University.

2.2.2 Fourier Transform Infrared Spectroscopy (FT-IR)

FTIR spectra were recorded using FTIR 8300 Shimadzu spectrophotometer as KBr disc in the frequency range of (400-4000) cm^{-1}. The spectra were recorded in the laboratories of Ibn Sina State Company.

2.2.3 Ultraviolet-Visible Spectroscopy (UV-VIS)

The ultraviolet-visible (UV-VIS) spectra were recorded using Shimadzu UV-VIS. 160 A-Ultra-Violet spectrophotometer using (1.0 cm) quartz cell at room temperature in the range

of wavelength (200-600) nm. All the prepared compounds were dissolved in DMF. These were carried out in the laboratories of Chemistry Department / College of Science / Al-Nahrain University.

2.2.4 Conductivity measurements

The conductivity measurements were obtained using WTW conductometer at (25 °C) with concentration of 10^{-3} M. All the prepared complexes were dissolved in ethanol. These were carried out in the laboratories of Chemistry Department / College of Science / Al-Nahrain University.

2.2.5 Nuclear Magnetic Resonance (NMR)

The spectra of ^{1}H-NMR was recorded on a Bruker spectrophotometer model ultra-shield at 300 MHz using deuterated DMSO-$d6$ as a solvent and tetramethylsilane, TMS as an internal standard. The measurement were carried out in the AL-Bait University/ Amman, Jordan.

2.2.6 Metal analysis

The metal percentage of the complexes were determined using atomic absorption technique type Shimadzu Atomic Absorption 680 Flame Spectrophotometer. These were carried out in the laboratories of Ibn Sina State Company.

2.2.7 Elemental analysis (CHNS)

The elemental microanalyses (CHNS) for the prepared compounds were determined using EM-017mth instrument. These were carried out in the Chemistry Department/ College of Science /Al-Nahrain university.

2.2.8 Microscope and atomic force microscopy (AFM)

Surface topography of samples were analyzed by Atomic Force Microscopy (AFM) (Veeco, USA), and using microscope (MEIJI TECHNO microscope, Japan), in the Chemistry Department / College of Science / Al-Nahrain University.

2.3 Synthesis of organotin(IV) complexes

2.3.1 synthesis of triphenyltin (IV) complexe

Triphenyltin (IV) and dibutyltin hydroxide complexes were synthesized by dissolving the free ligand (0.33 gm,1 mmol) in methanol (15 ml) and adding drop wise a methanolic solution of Ph_3SnCl (0.385gm, 1 mmol) or Bu_2SnO (0.25 gm,1mmol) with stirring. The resulting solution was stirred at room temperature for 10 min and then refluxed for 6 h. It was filtered and the volatiles were removed in vacuum, which on recrystallization from methanol afforded a white powder.

2.3.2 synthesis of diorganotin (IV) complexes

The free ligand (0.66 gm, 2 mmol) dissolved in 20 ml of methanol was slowly added, with constant stirring, to methanolic solution of Me_2SnCl_2 or Bu_2SnCl_2 (0.22gm and 0.31gm, 1 mmol) respectively. The mixture was refluxed for 8 h. The resulting solution was filtered and concentrated in vacuum. Which on recrystallization from methanol gave a white to pale yellow powder.

2.4 Experimental Technique

2.4.1 Films preparation [73]

The polymer matrix used in this study was PVC (K value = 67, degree of polymerization = 800) supplied by Petkim (Turkey). It was re-precipitated from THF solution by alcohol several times and finally dried under vacuum at room temperature for 24 h. Fixed concentrations of polyvinyl chloride solution (5 g/100 ml) in tetrahydrofuran were used to

prepare polymer films with 40 µm thickness (measured by a micrometer type 2610 A, Germany). The prepared complexes (0.5% concentrations) were added to the films starting at 0 concentrations (control). The films were prepared by evaporation technique at room temperature for 24 h. To remove the possible residual of tetrahydrofuran solvent.

2.4.2 Incident Light Intensity Measurement

The intensity of the incident light (I_o) was measured by the use of potassium ferrioxalate actenometer methods as described by Hatchard and Parker [74]. The actenometer solution (6 x 10^{-3} M) was prepared by dissolving (3.00 gm) of $K_3[Fe(C_2O_4)_3].3H_2O$ in (800 ml) of distilled water, (100 ml) of (1 N) H_2SO_4 was added and the whole solution was dilute to one liter with distilled water. The actenometer solution absorbed 100% of incident light at $\lambda = 510$ nm.

The light intensity measurement involves irradiation of the actenometer solution for known period of time (3 mins); ferrous ion concentration was estimated spectrophotometrically using 1-10-phenathroline (0.1 %) as complexing agent. According to the Hatchard and Parker [74], Ferric ions are reduced to Ferrous ions:

$$\longrightarrow Fe^{3+} \qquad Fe^{2+} \quad ……………….. (2.1)$$
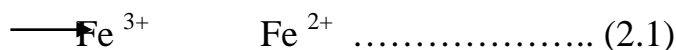
Thus the phenathroline complex is formed with Fe^{2+}, which strongly absorbed at 510 nm. For Fe^{2+} formation (Equation 2.1), the quantum yield (Q) is equal 1.24 [75]. Therefore the intensity of light can be calculated after a calibration curve for Fe^{2+} was obtained using the following solution:

i. $4*10^{-4}$ M of $FeSO_4$ in 0.1 N H_2SO_4

ii. 0.1% w/v phenanthroline monohydrate in water

iii. Buffer solution was prepared from mixing (600 ml) 1N CH_3COONa and (360 ml) of 1N H_2SO_4 dilute to 1L

Solutions of different concentrations of Fe^{2+} were prepared from solution (i) by taking different amount in 25 ml. volumetric flask, to each

a- (2 ml) phenanthroline solution was added,

b- (5ml) of buffer solution,

c- (10 ml) of 0.1 N H_2SO_4 and diluting the whole solution to (25 ml) with distilled water.

The volumetric flasks were covered with aluminum foil, kept in the dark for (30 min). Then the optical densities at $\lambda = 510$ nm were measured. The plot of optical density versus Ferrous ion concentration was a straight line. The slope gave the extinction coefficient of $FeSO_4$ solution, which is equal ($\varepsilon = 1.112 \times 10^4$ L. mol^{-1} cm^{-1}).
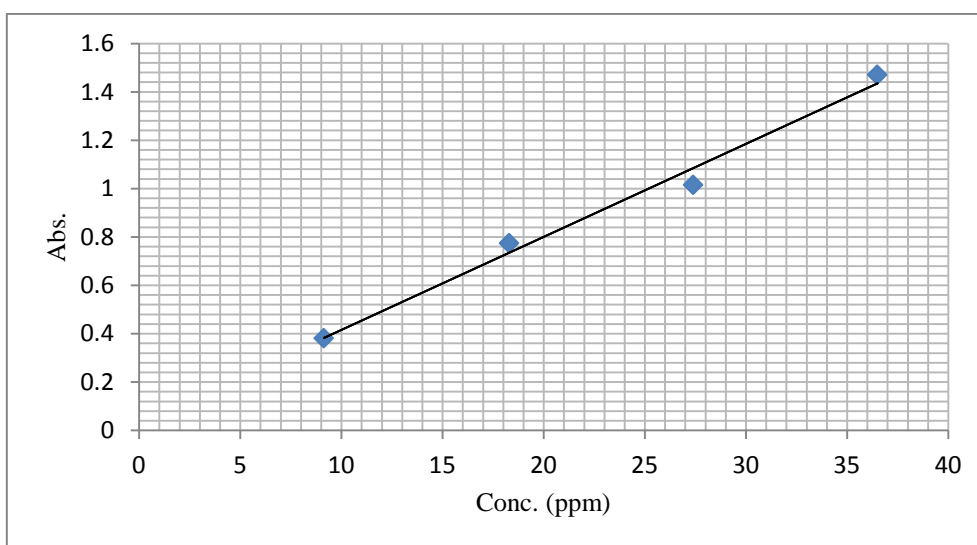
Figure 2.1 Calibration curve

In order to determine the light intensity, (3 ml) of actenometer solution was irradiated. A stream of Nitrogen bubble stirred the solution to exclude the dissolved oxygen gas. The cell was irradiated in the same position used for irradiation samples. After illumination, (1 ml) of irradiated solution was transferred to (25 ml), volumetric flask, (2 ml) of phenanthroline solution and (0.5 ml) of buffer solution then the flask was diluted to (25 ml) with distilled water.

Blank solution was made by mixing 1ml of unirradiated mixture of ferrioxalate solution with other components. The potassium was left in the dark for (30 min). and then the optical density at ($\lambda = 510$ nm.) was measured. The intensity of incident light was calculated using the following relation [76]:

$$I_o = \frac{A \times V_1 \times 10^{-3} \times V_3}{Qy \times \varepsilon \times V_2 \times t} \text{ einstein dm}^{-3} \text{ sec}^{-1} \text{ .... (2.2)}$$

I_o = Intensity of incident light

A = Absorbance at λ = 510

V_1 = Initial volume

V_2 = Volume used of irradiation solution

V_3 = Final volume (25 ml)

Q_y = Quantum yield (1.24)

ε = Molar extinction coefficient (slope of calibration curve)

t = Irradiation time in seconds

2.4.3 Accelerated testing technique

Accelerated weatherometer Q.U.V. tester (Philips, Germany), was used for irradiation of PVC films. These lamps are of the type (UV-B 313) giving wavelength range between (290 to 360 nm) and the maximum wavelength light intensity is at (313 nm). The polymer film samples were fixed parallel to each other and the lamp of the UV incident radiation is vertically incident on the samples. The distance between the polymer films and the source was 25 cm. The irradiation samples were changed place from time to time to insure homogeneous intensity of incident radiation on all the samples

2.5 Method of Evaluation of the Stabilizing Efficiency

2.5.1 Measuring the photodegradation rate of polymer films using infrared spectrophotometry

The degree of photodegradation of polymer film samples was followed by monitoring FTIR spectra in the range $4000 - 400$ cm^{-1} using FTIR 8300 Shimadzu Spectrophotometer. The position of carbonyl absorption is specified at 1722 cm^{-1}, polyene group at 1602 cm^{-1} and the hydroxyl group at 3500 cm^{-1} [77]. The progress of photodegradation during different irradiation times was followed by observing the changes in carbonyl and polyene peaks.

Then carbonyl (I_{co}), polyene (I_{po}) and hydroxyl (I_{OH}) indices were calculated by comparison of the FTIR absorption peak at 1722, 1602 and 3500 cm^{-1} with reference peak at 1328 cm^{-1} attributed to oscillating and bending of CH_2 group, respectively. This method is called band index method [78].

$$I_s = \frac{A_S}{A_r} \quad \text{.............. (2.3)}$$

As = absorbance of peak under study; Ar = absorbance of reference peak; Is = index of group under study.

The absorbance (A) is calculated from the recordered percentage transmittance (%T) using Beer-Lambent law as in the following equation. (2.4):

$$\left. \begin{array}{l} A = \log(100/\%T) \\ A = \log 100 - \log \%T \\ A = 2 - \log \%T \end{array} \right\} \text{..............(2.4)}$$

Actual absorbance, the difference between the absorbance of top peak and the baseline (Top peak — Baseline) is calculated using the baseline method [79].

2.5.2 Measuring the photodegradation rate of polymer films using Ultraviolet-Visible spectrophotometer [80].

A Shimadzu UV-Vis 160A-Ultraviolet Spectrophotometer (Shimadzu Cooperation, Kyoto, Japan) was used to measure the changes in the UV-visible spectra of PVC films during irradiation (λmax = 313 nm). The photodecomposition rate constant (kd) of PVC films were calculated using Equation (2.5).

$$ln(a - x) = lna - k_d\, t \quad \text{………………..(2.5)}$$

Where, $a = A_0 - A_\infty$, $x = A_0 - A_t$

a = stabilizer concentration before irradiation and x = change in stabilizer concentration after irradiation time (t) as shown in Equation (2.6).

A_0 = the absorption intensity of the PVC at t_0, A_∞ = the absorption intensity at t_∞ and A_t = the absorption intensity after irradiation time t.

$$a - x = A_0 - A_\infty - A_0 + A_t = A_t - A_\infty \text{…………. (2.6)}$$

Equation (2.7) was obtained by substituting $a - x$ in Equation (2.5) by its value in Equation (2.6)

$$ln(A_t - A_\infty) = ln(A_0 - A_\infty) - k_d\ t \ldots\ldots\ldots\ldots (2.7)$$

The plot of $ln(A_t - A_\infty)$ *versus* irradiation time (*t*) gives straight line in which the slope equal k_d. The photodecomposition of PVC follows a first order kinetics.

2.5.3 Measuring the photodegradation by weight loss [81].

The stabilizing potency of the stabilizer was determined by measuring the weight-loss percentage of photodegraded PVC films in absence and in presence of additives.The weight loss measurements were carried out according to the following equation;

Weight loss % = (W$_1$ –W$_2$ /W$_1$) 100 …………….. (2.8)

Where W_1 is the weight of the original sample (before irradiation) and W_2 is the weight of sample after irradiation.

2.5.4 Determination of viscosity average molecular weight $\overline{M}_v$ using viscometry method

Viscosity property was used to determine the average molecular weight of PVC polymer using the Mark–Houwink relation. PVC films with and without additives were calculated from intrinsic viscosities measured in the THF solution at 25 °C with an Ostwald U tube viscometer. Eqs. (2.9) and (2.10) were used to deduce the molecular weight [82].

$$[\eta] = K\ \overline{M}_v^\alpha \ldots\ldots\ldots\ldots\ldots(2.9)$$

$$[\eta] = \left(\sqrt{2}\ /c\right)\left(\eta_{sp} - ln\eta_{re}\right)^{1/2} \ldots\ldots\ldots\ldots (2.10)$$

$\overline{M}_v$ = is the molecular weight of polymer, α and k are the constants that depend upon the polymer solvent system at a particle temperature, η is the intrinsic viscosity and C is the concentration of the polymer solution.

Solutions were made by dissolving the polymer in a THF solvent, g/100 ml; the flow times of the polymer solution and pure solvent are t and t_0 respectively. Specific viscosity η_{sp} was calculated as follows Eqs. (2.11) and (2.12).

$$\eta_{re} = \frac{t}{t_0} \quad \text{...........................} \quad (2.11)$$

η_{re} = Relative viscosity.

$$\eta_{sp} = \eta_{re} - 1 \quad \text{...................} \quad (2.12)$$

By applying equation (2.10), the molecular weight of degraded and undegraded polymer can be calculated. Molecular weights of PVC with and without additives were calculated from intrinsic viscosities measured in THF solution using the following equation;

$$[\eta] = 4.17 \times 10^{-4} \, \bar{M}_V^{0.6} \quad \text{........} \quad (2.13)$$

The quantum yield of main chain scission (Φ_{cs}) was calculated from viscosity measurement using the following relation [83].

$$\Phi_{cs} = (CN_A/\bar{M}_{v,o}) \left[([\eta_o]/[\eta])^{1/\alpha} - 1 \right] /I_o \, t \quad \text{...............} \quad (2.14)$$

Where:

C   = concentration.

N_A = Avogadro's number.

$(\bar{M}_{v,o})$ = the initial viscosity – average molecular weight.

$[\eta_o]$ = Intrinsic viscosity of polymer before irradiation.

$[\eta]$ = Intrinsic viscosity of polymer after irradiation.

α = Exponent in the relation: $[\eta] = KM^{\alpha}$.

I_o = Incident intensity

t   = Irradiation time in second.

2.5.5 Measuring the Photodegradation by Morphology Study [84]

Microscope and Atomic Force Microscopy (AFM) were used to determine the morphology of the sample surfaces before and after 300 hour irradiation time. This device

was used to provide information concerning polymer morphology and to obderved changes on the studied surface.

Chapter Three

RESULTS & DISCUSSION

Synthesis and characterization of organotin complexes

Four organotin complexes, Ph_3SnL, Me_2SnL_2, Bu_2SnL_2 and Bu_2SnOHL, were synthesized from reactions between diorganotin dichlorides, triorganotin chloride or diorganotin oxide with furosemide as a ligand (L) in methanol under reflux conditions for 6–8 h (Schemes 1, 2 and 3). In the case of Ph_3SnL and Bu_2SnOHL a 1:1 molar ratio of L and Ph_3SnCl or Bu_2SnO was used, while, a 2:1 molar ratio of L and R_2SnCl_2 (R = Me, Bu) was

used for the production of Me$_2$SnL$_2$ and Bu$_2$SnL$_2$. The structures of Sn(IV) complexes were characterized by elemental analysis and various spectroscopic methods.
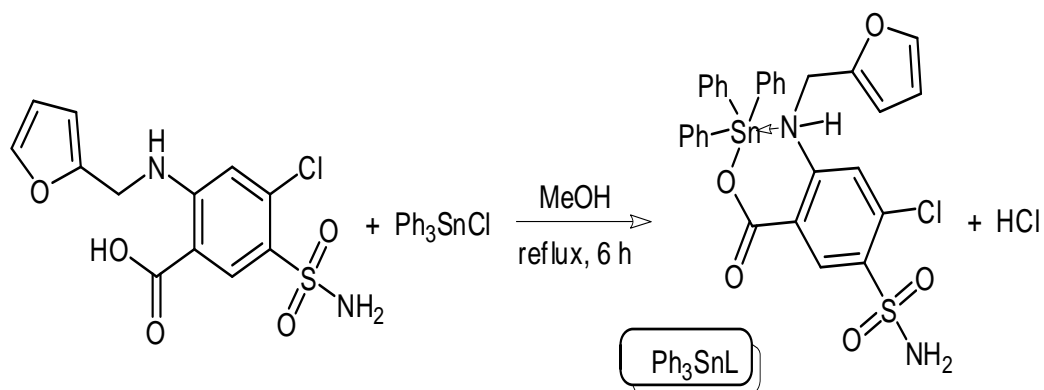
Scheme 1. Synthesis of triphenyltin (Ph₃SnL) complex.
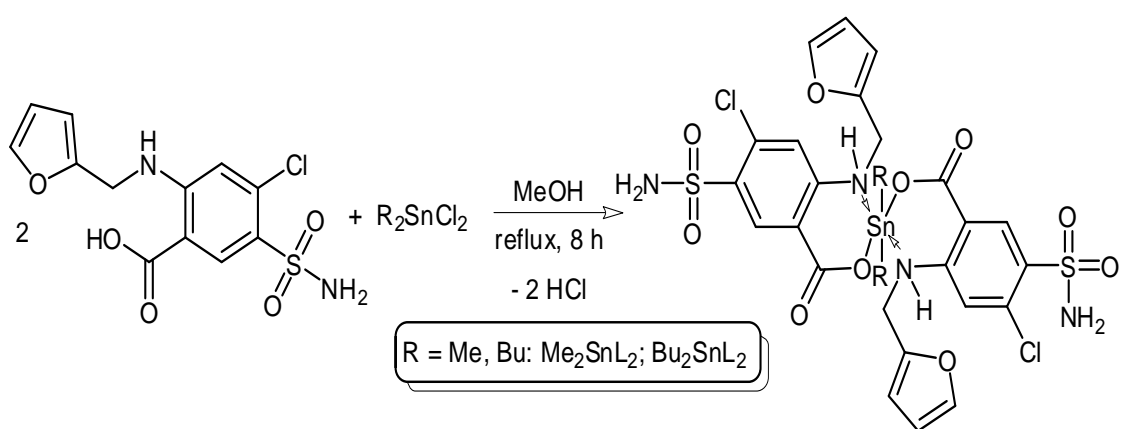
Scheme 2. Synthesis of dimethyltin (Me₂SnL₂) and dibutyltin (Bu₂SnL₂) complexes.
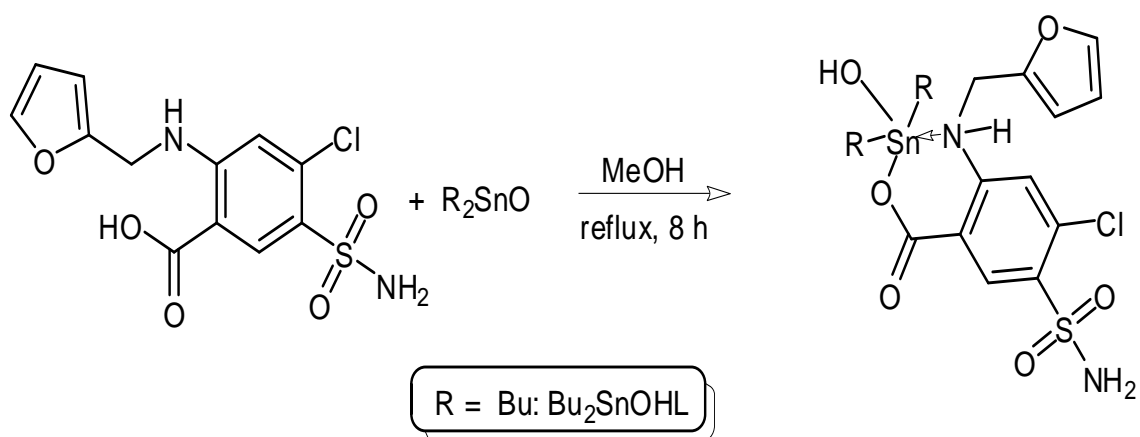
Scheme 3. Synthesis of dibutyltinhydroxide (Bu₂SnOHL) complex.

3.1.1 Elemental Analysis

The composition of the Sn(IV) complexes was checked by elemental analysis. In addition, flame atomic absorption spectroscopy was used to estimate the tin content within the Sn(IV) complexes. The observed values were generally in agreement with the calculated ones, although it should be noted that the observed carbon content in the Ph_3SnL complex was significantly less than the calculated one. The elemental analyses data (C, H, N, S, O and Sn %), yields and melting points for Sn(IV) complexes along with those for the ligand are reported in Table (3.1).

Table 3.1 Melting points, yields and elemental analyses for L and its Sn(IV) complexes.

Compound	Colour	M.P. (°C)	Yield (%)	M. Wt.	Elemental analysis theoretical (Experimental) %					Tin percentage theoretical (experimental) %
					C %	H %	N %	S %	O %	
L	White	205-207	---	330.74	43.58 (43.19)	3.35 (3.34)	8.47 (7.92)	9.69 (9.43)	24.19 (25.38)	-----
Ph₃SnL	White	159-161	73.2	679.77	----	----	----	----	----	17.49 (17.21)
Bu2SnL2	Off white	194-197	80.7	890.03	43.07 (43.32)	4.29 (3.44)	6.28 (7.91)	7.19 (7.94)	17.93 (16.14)	13.28 (12.28)
Bu₂SnOHL	Pale yellow	104-109	61.58	579.45	41.44 (42.35)	5.03 (4.47)	4.83 (4.35)	5.53 (6.02)	16.6 17.42	20.48 (19.21)
Me₂SnL₂	Off whit	184-186	67.4	808.19	38.64 (39.94)	3.47 (3.27)	6.93 (6.31)	7.93 (8.92)	19.8 (18.3)	14.69 (14.77)

3.1.2 *Characterization of ligand and its prepared complexes by Fourier Transform Infrared Spectroscopy (FT-IR)*

FTIR spectroscopy gives valuable information about the coordination modes within organotin complexes. The FTIR measurements (400–4000 cm^{-1}) were performed using KBr

disc. The FTIR spectroscopic data for L and its synthesized organotin(IV) complexes are reported in Table (3.2).

Table 3.2 FTIR spectroscopic data for L and its organotin(IV) complexes.

Vibrational Mode	Compound (Wavenumber; cm^{-1})				
	L	Ph$_3$SnL	Me$_2$SnL$_2$	Bu$_2$SnL$_2$	Bu$_2$SnOHL
v (NH)	3352	3350	3344	3348	3349
v_{as} (COO $^{--}$)	1670	1674	1672	1679	1608
v_s (COO $^{--}$)	1562	1566	1558	1566	1560
v_{as} (SO$_2$NH$_2$)	3398	3396	3398	3398	3397
v_s (SO$_2$NH$_2$)	3282	3282	3282	3282	3286
v (Sn–C)	—	540	536	516	547
v (Sn–O)	—	426	432	447	428
v (Sn–N)	—	416	408	408	412

The IR spectrum for L was compared with those for di- and triorganotin(IV) complexes in order to confirm the binding modes within the synthesized complexes. The IR spectrum of the ligand showed sharp characteristic absorption bands due to asymmetric (sulfonamide SO$_2$NH$_2$) (3398 cm^{-1}) and symmetric (sulfonamide SO$_2$NH$_2$) (3282 cm^{-1}) stretching vibrations. The IR spectra of organotin complexes suggest that the –SO$_2$NH$_2$ group was not involved in the coordination process with the Sn atom because its not shifted in all organotin complexes . The peak appearing at 3352 cm^{-1} (secondary NH stretching) for the ligand was shifted slightly in the organotin complexes, indications the involvement of the NH in the coordinated to the Sn(IV) atom [85]. The asymmetric vibrations band for carboxylate group (v_{as} COO$^-$) in ligand appeared at 1670 cm^{-1}. This peak shifted to higher frequencies for the tin complexes (1672–1679 cm^{-1}), except the Bu$_2$SnOHL was shifted to lower freqency (1608 cm^{-1}) . The symmetric stretching vibrations band (1562 cm^{-1}) for the carboxyl group (v_s COO$^-$) in the ligand has been shifted to higher frequencies (1566 cm^{-1}) in the case of Ph$_3$SnL

and Bu_2SnL_2 and to lower frequency (1558 , 1560) cm^{-1} in the case of Me_2SnL_2 and Bu_2SnOHL, respectivly [85].

Three new absorption bands appeared in the IR spectra of the organotin complexes. These bands are attributed to v (Sn–N), v (Sn–O) and v (Sn–C) that resonate within the 408–416, 447–426 and 516–540 cm^{-1} regions, respectively. The appearance of such peaks provides further evidence for the coordination between ligand and Sn(IV). The coordination thus takes place between the tin atom and the secondary amine, carboxylate and alkyl or phenyl groups [86].
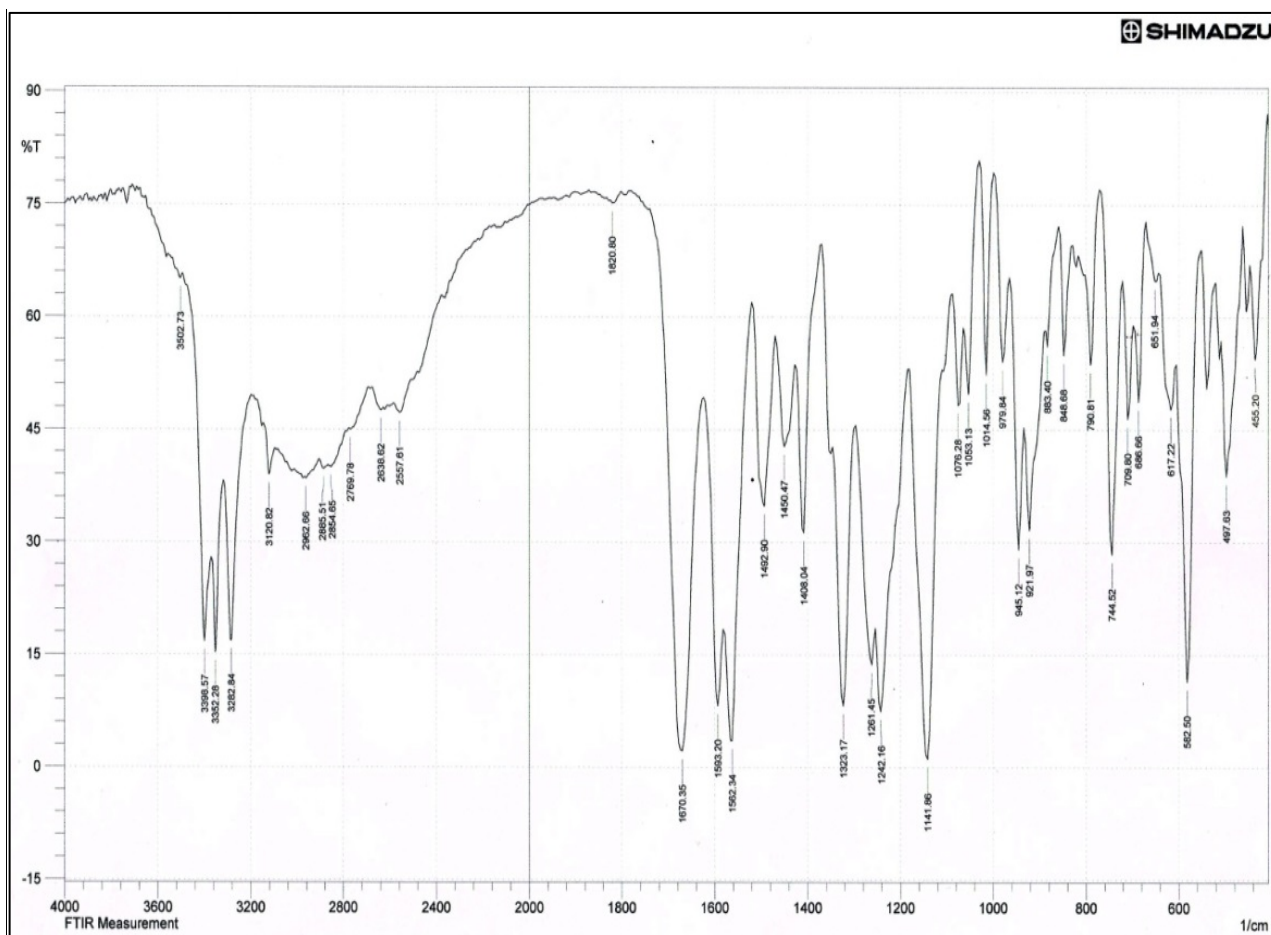
Figure 3.1 FTIR spectrum of ligand
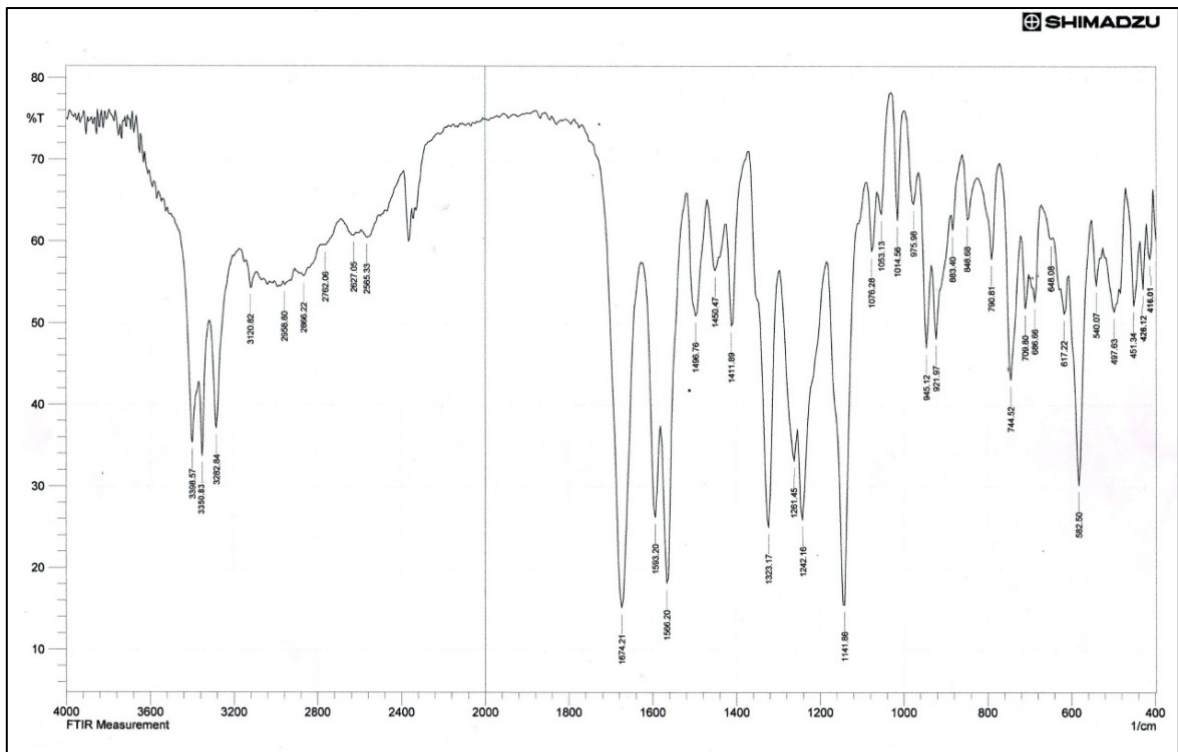
Figure 3.2 FTIR spectrum of Ph₃SnL
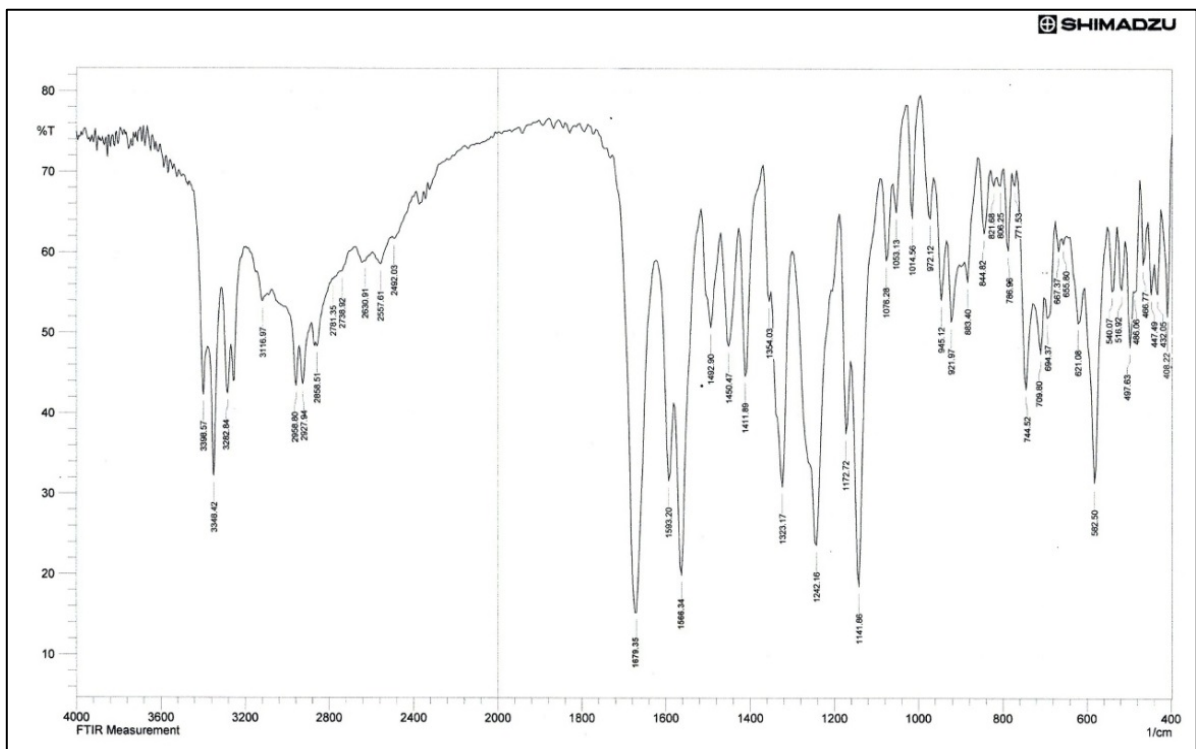
Figure 3.3 FTIR spectrum of Bu₂SnL₂

٥٣
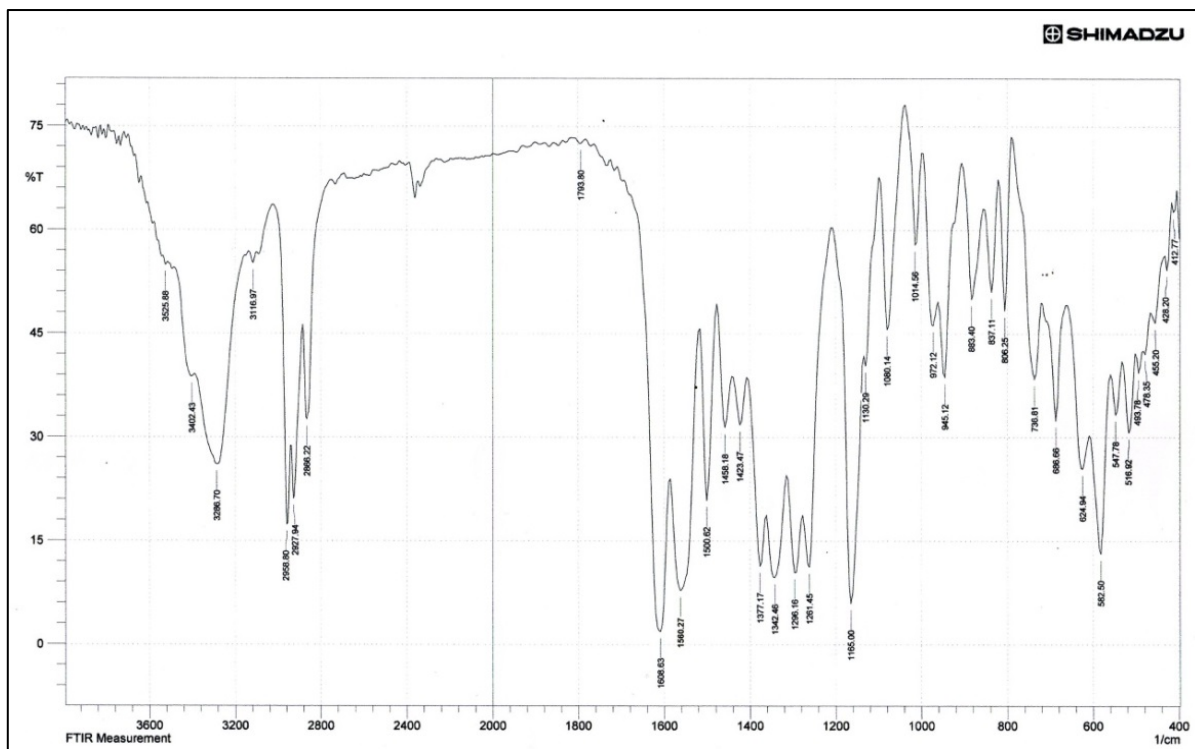
Figure 3.4 FTIR spectrum of Bu$_2$SnOHL
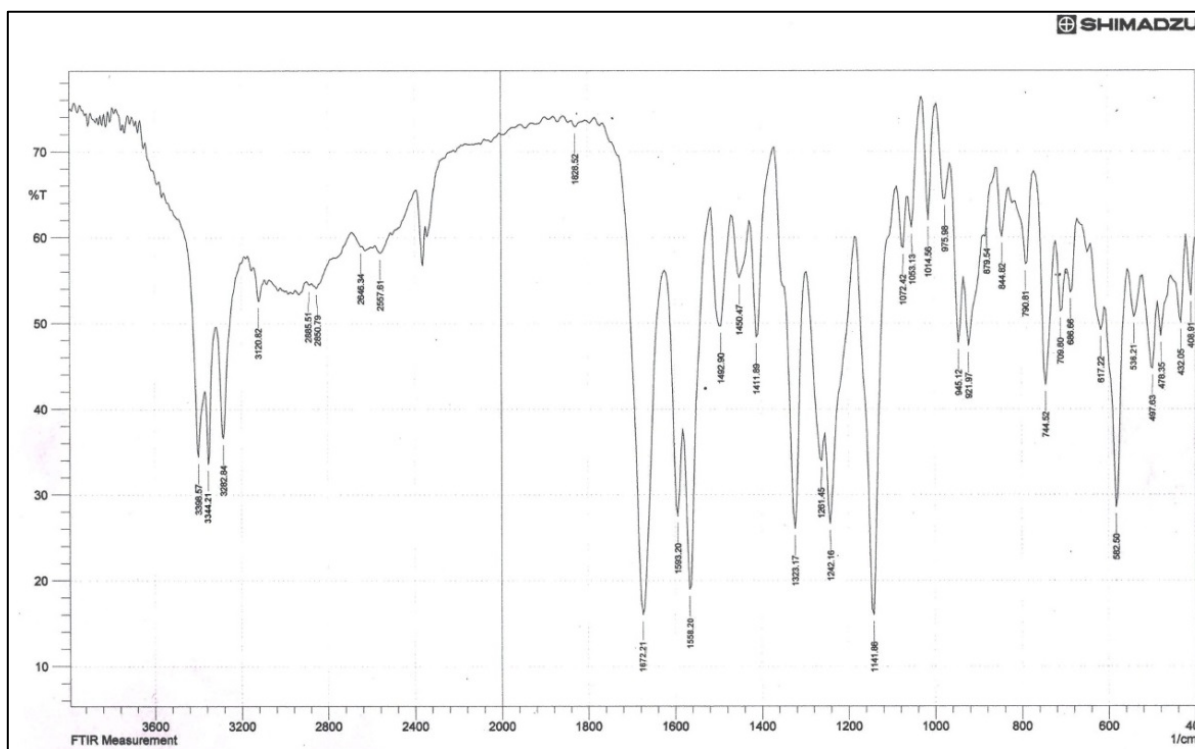
Figure 3.5 FTIR spectrum of Me$_2$SnL$_2$

3.1.3 Characterization of ligand and organotin complexes by Ultraviolet-visible spectroscopy and conductivity measurements

The absorption spectra (200–600 nm) for the ligand and its organotin complexes were recorded in DMF Table (3.3). The electronic spectrum of ligand shows two absorption

bands. The first resonates at 274 nm due to π–π^* electronic transition of the aromatic moieties. This band was slightly shifted to higher wavelength after complexation. The second band resonates at 341 nm due to n–π^* electronic transition for the carbonyl oxygen non-bonding electrons and has been shifted slightly to higher wavelength within organotin complexes [87]. The molar conductivity for organotin complexes (1×10^{-3} M) were measured in ethanol at room temperature. The conductivity for Sn(IV) complexes was found to be in the range of 2.1– 4.4 μS/cm Table (3.3). The organotin complexes were found to be non-electrolyte.

Table 3.3 Electronic spectral data and conductivity for L and its organotin(IV) complexes.

Compound	Wave length nm (n–π^* and π–π^*)	Conductivity(μS/cm)
L	341, 274	----
Ph$_3$SnL	348, 277	2.1
Bu$_2$SnL$_2$	344, 275	2.4
Bu$_2$SnOHL	342, 275	2.2
Me$_2$SnL$_2$	342, 276	4.4
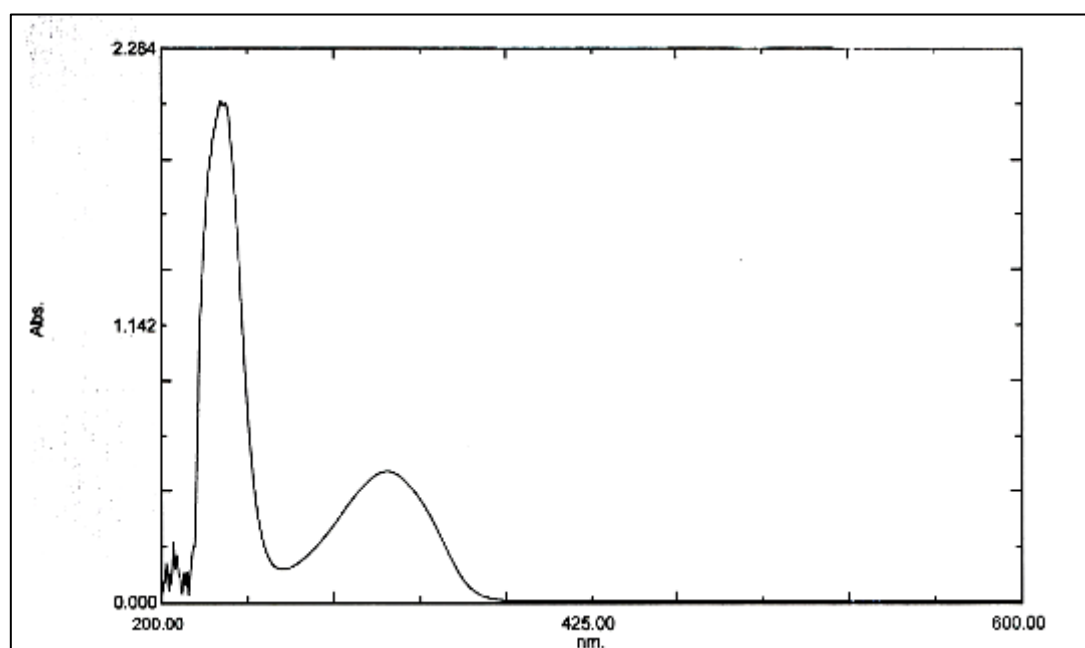
Figure 3.6 Electronic spectrum of ligand in DMF solvent
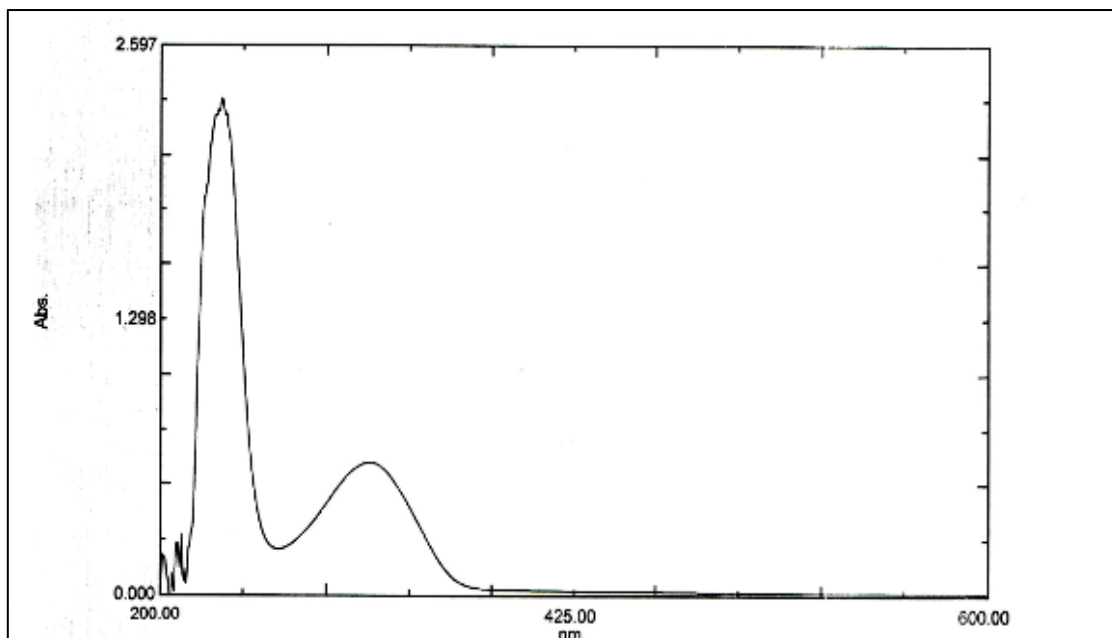
Figure 3.7 Electronic spectrum of Ph₃SnL in DMF solvent
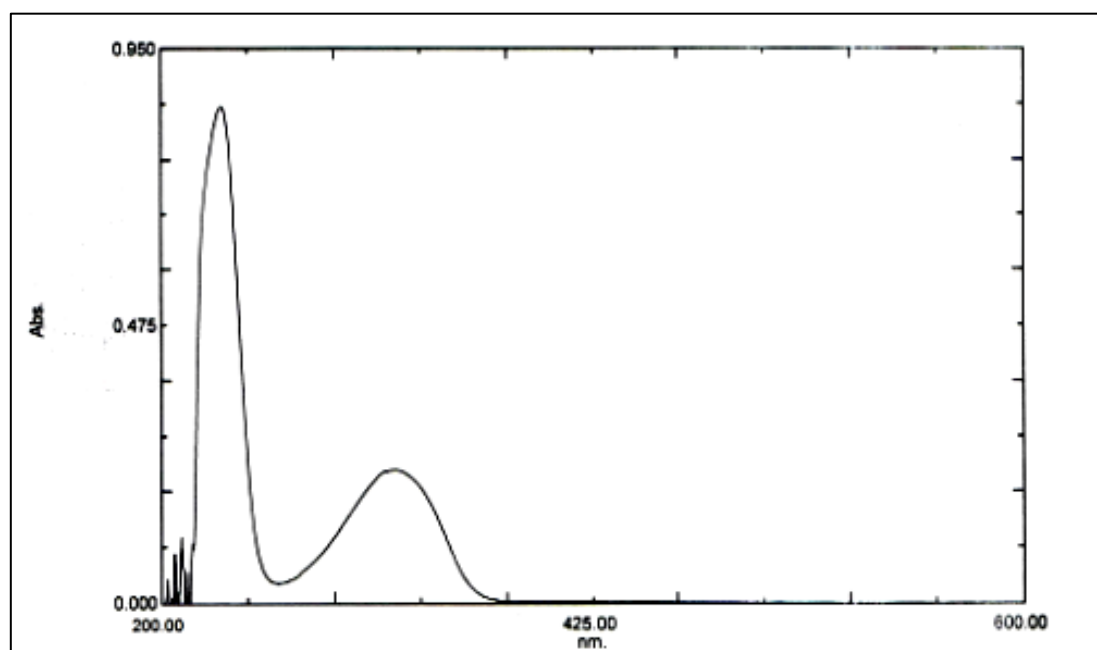
Figure 3.8 Electronic spectrum of (Bu)₂SnL₂ in DMF solvent
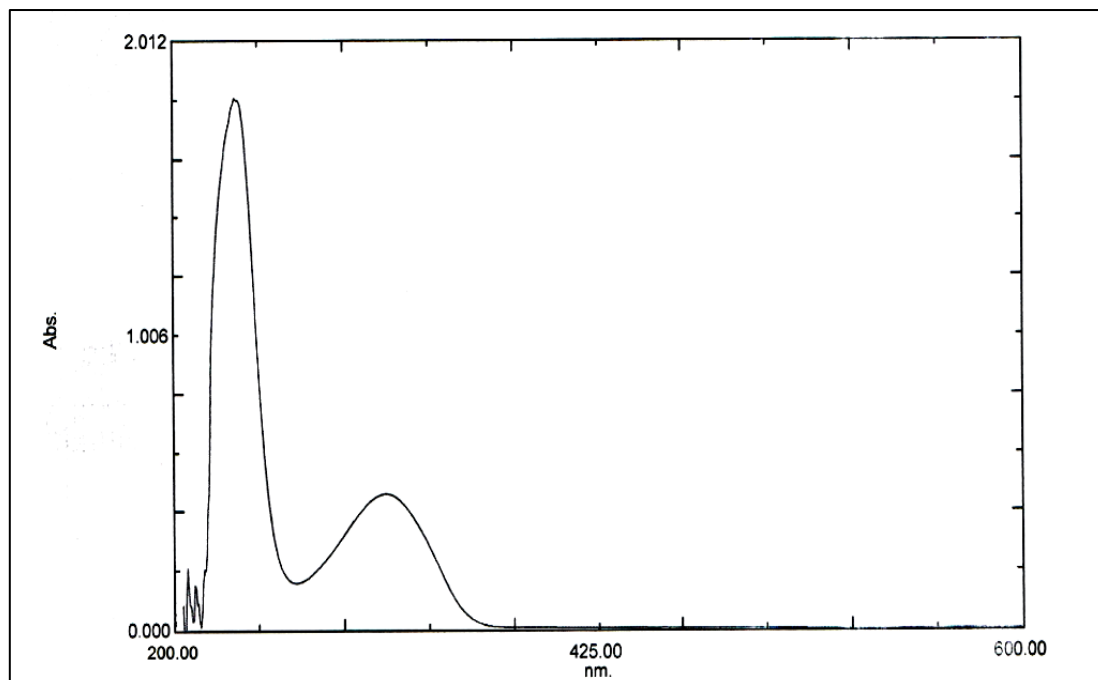
Figure 3.9 Electronic spectrum of Bu$_2$SnOHL in DMF solvent
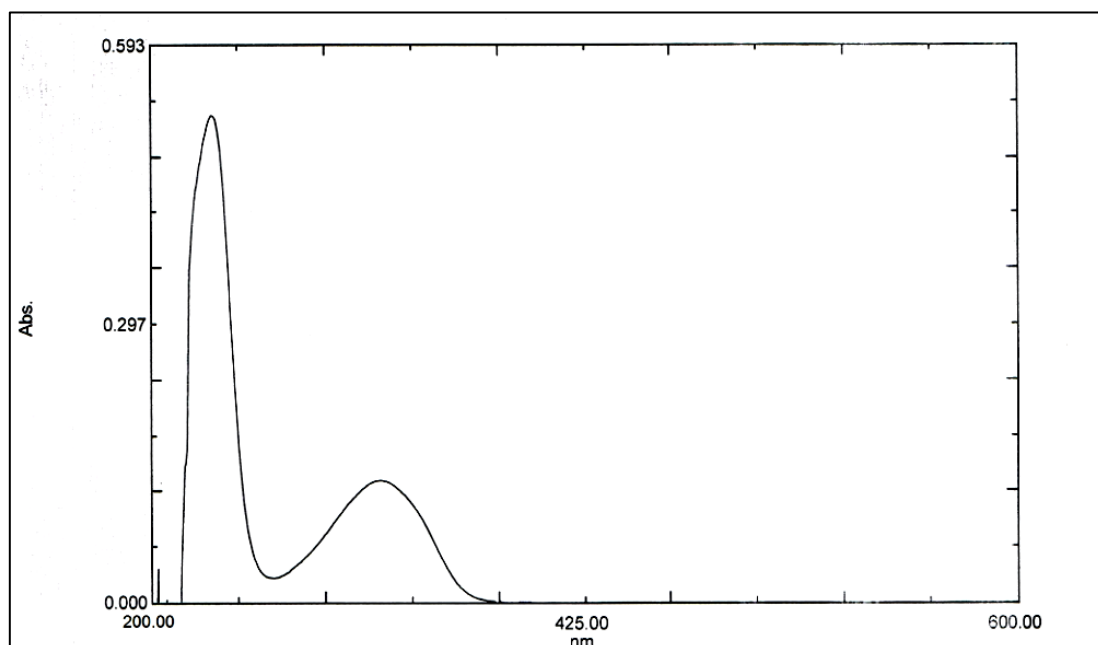
Figure 3.10 Electronic spectrum of Me$_2$SnL$_2$ in DMF solvent

3.1.4 Characterization of ligand and its prepared complexes by Nuclear Magnetic Resonance (HNMR) spectroscopy.

1. The ^{1}H-NMR spectra for L and its Sn(IV) complexes were recorded in DMSO-d_6, see table (3.4). The changes in the chemical shift values between the ligand and its tin complexes are largely dependent on the environment and can be used as an evidence to show that complexation has taken place [88]. The ^{1}H-NMR spectrum of the ligand showed an

exchangeable singlet at 13.35 ppm, due to the carboxyl proton. Such a signal was absent in the ^{1}H-NMR spectra of the organotin complexes. The SO_2NH_2 signal of ligand showed at 7.33 ppm, it was very low shifted upon chelation with organotin complexes this indicate that SO_2NH_2 was not bonded with Sn moitey. The NH signal was shifted down-field upon chelation of ligand with Sn(IV) atom. This could be a result of a charge transfer towards the carboxylate group that binds to the highly electropositive Sn atom [87].

2. The ^{1}H-NMR spectra of organotin complexes showed two singlet aromatic protons that resonated within the 7.06–7.10 and 8.38–8.44 ppm regions, which were attributed to H-3 and H-6, respectively. They also showed an apparent triplet (J = 3.2 Hz) that resonated at 6.38–6.42 ppm which is characteristic for H-4 of a furan. The H-3 of the furan moiety resonated a doublet (J = 3.2 Hz) within the 6.31–6.37 ppm region. Moreover, the CH_2 protons resonated as a doublet (J = ca. 6 Hz) at 4.44–4.58 ppm.

3.

4.

5.
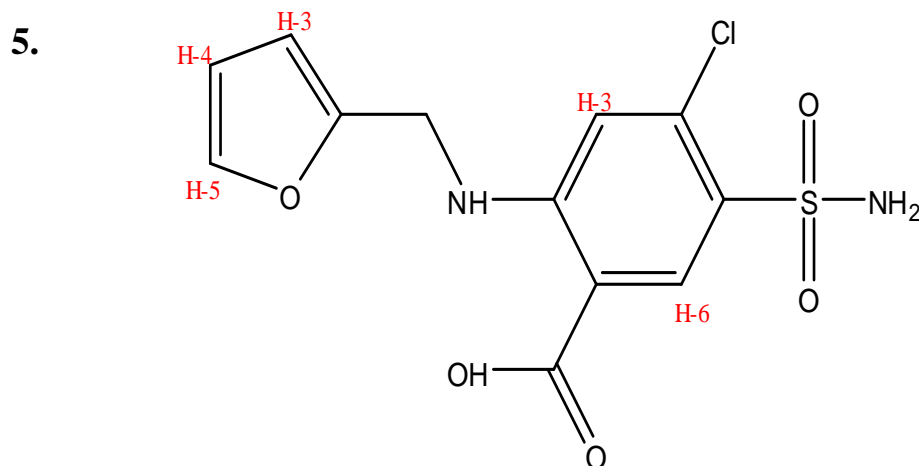
Figure 3.11 ^{1}H NMR numbering scheme of the ligand.

Table 3.4 ^{1}H-NMR spectral data for ligand and organotin complexes.

Compound	^{1}H-NMR (300 MHz: DMSO-d_6, δ, ppm, J in Hz)
L	13.35 (s, exch., CO_2H), 8.51 (t, J = 6.0 Hz, exch., NH), 8.39 (s, H-6), 7.62 (d, J = 3.2 Hz, H-5 of furan), 7.33 (s, exch., SO_2NH_2), 7.05 (s, H-3), 6.40 (app. t, J = 3.2 Hz, H-4 of furan), 6.36 (d, J = 3.2 Hz, H-3 of furan), 4.64 (d, J = 6.0 Hz, CH_2)
Ph₃SnL	8.61 (t, J = 6.2 Hz, exch., NH), 8.41 (s, H-6), 7.82–7.33 (m, 3 Ph and H-5 of furan), 7.22 (s, exch., SO_2NH_2), 7.10 (s, H-3), 6.38 (app. t, J = 3.2 Hz, H-4 of furan), 6.31 (d, J = 3.2 Hz, H-3 of furan), 4.44 (d, J = 6.2 Hz, CH_2)
Me₂SnL₂	8.61 (t, J = 6.1 Hz, exch., NH), 8.44 (s, H-6), 7.62 (d, J = 3.2 Hz, H-5 of furan), 7.34 (s, exch., SO_2NH_2), 7.06 (s, H-3), 6.42 (app. t, J = 3.2 Hz, H-4 of furan), 6.35 (d, J = 3.2 Hz, H-3 of furan), 4.58 (d, J = 6.1 Hz, CH_2), 1.23 (s, Me)
Bu₂SnL₂	8.64 (t, J = 6.0 Hz, exch., NH), 8.38 (s, H-6), 7.61 (d, J = 3.2 Hz, H 5 of furan), 7.29 (s, exch., SO_2NH_2), 7.06 (s, H-3), 6.41 (app. t, J = 3.2 Hz, H-4 of furan), 6.37 (d, J = 3.2 Hz, H-3 of furan), 4.48 (d, J = 6.0 Hz, CH_2), 1.55 (t, J = 7.2 Hz, CH_2), 1.37–1.31 (m, CH_2CH_2Me), 0.85 (t, J = 7.2 Hz, Me)

6.
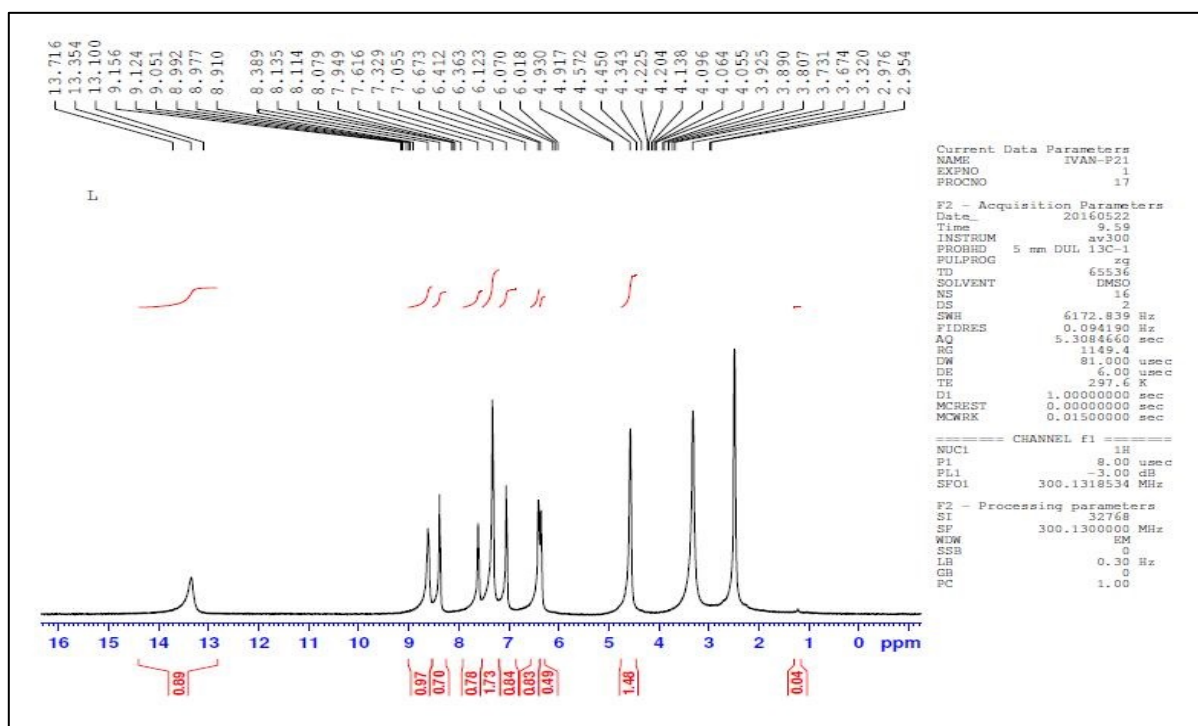
Figure 3.12 ^{1}H-NMR spectrum of ligand
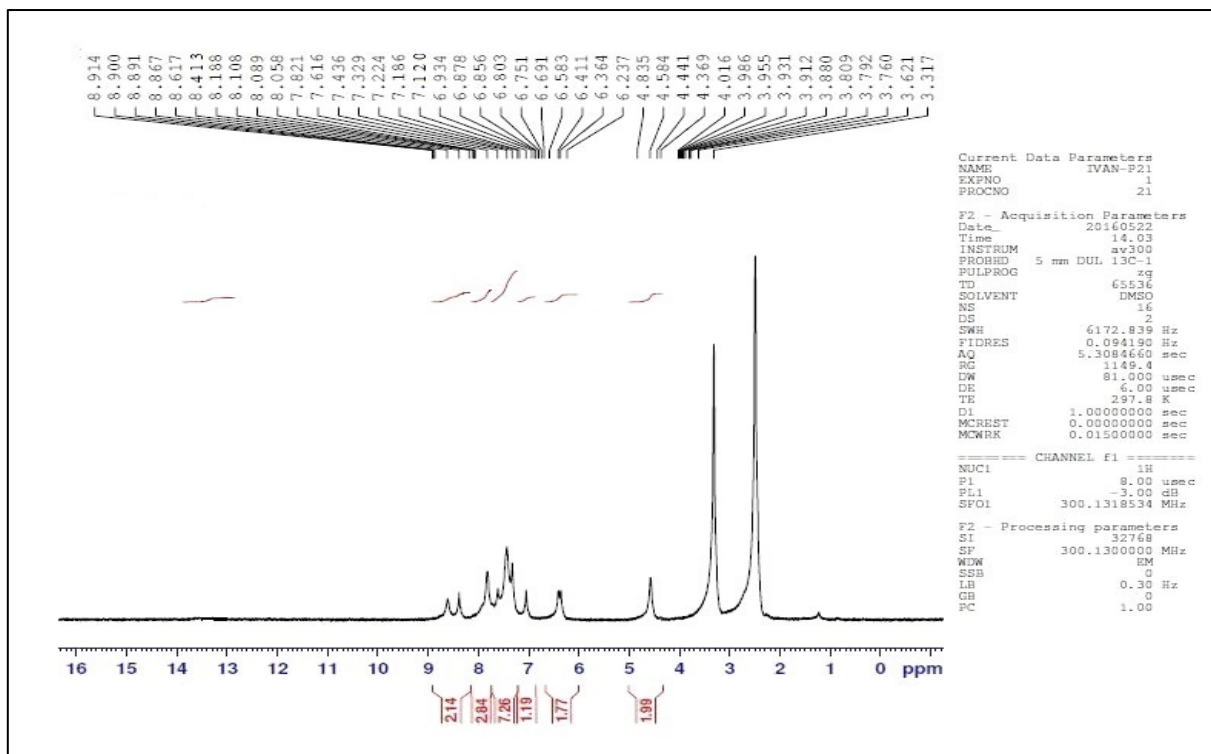
Figure 3.13 ^{1}H-NMR spectrum of Ph$_3$SnL
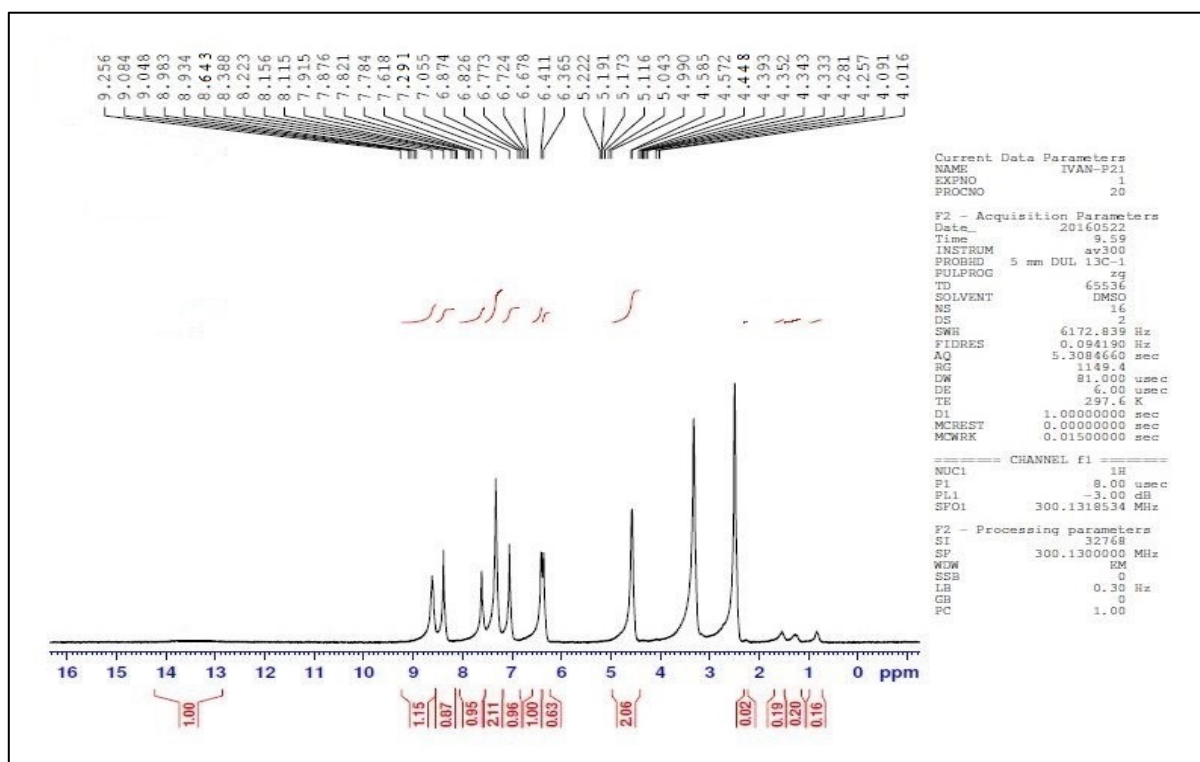
Figure 3.14 ^{1}H-NMR spectrum of Bu$_2$SnL$_2$
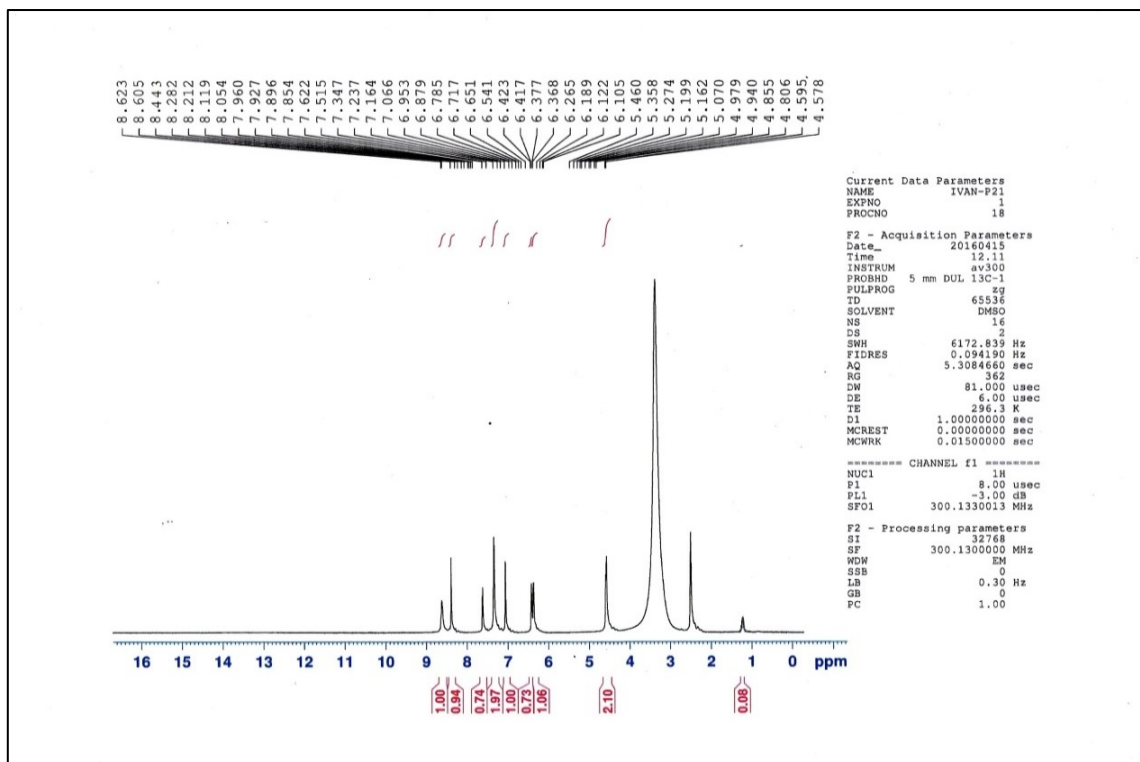
Figure 3.15 ^{1}H-NMR spectrum of Me$_2$SnL$_2$

3.2.1 Evaluation of Stabilizing Efficiency of PVC by FTIR Spectroscopy

The photochemical activity of organotin complexes as additives for PVC films photostabilization was investigated using FTIR spectroscopy. The PVC films were irradiated with UV light (λmax = 313 nm) for 300 h. The irradiation of PVC leads to the formation of various functional groups [89]. The IR spectrum of irradiated PVC shows three absorption bands due to formation of carbonyl, polyene and hydroxyl groups. These bands detected at 1772 (C=O), 1604 (C=C) and 3500 cm^{-1} (OH), respectively [90]. The growth rate of such peaks related to a reference peak (1328 cm^{-1}) could be considered as a measure for the photodegrading of PVC.

The photoactivity of organotin additives in PVC films has been examined and their efficiency in preventing the photo-oxidation reaction has been tested by spectroscopic methods. In order to study the photochemical activity of organotin additives for the photostabilization of PVC films, the carbonyl, polyene and hydroxyl indices were monitored with irradiation time using IR spectrophotometry. The absorption of the carbonyl, polyene and hydroxyl groups was used to follow the extent of polymer degradation during irradiation [91].

The FTIR spectra of PVC films containing Bu_2SnL_2 complex before and after irradiation are represented in Figures (3.16 and 3.17), respectively. The changes in carbonyl group intensity (1722 cm^{-1}) for PVC films containing organotin(IV) was monitored on irradiation. The carbonyl index ($I_{C=O}$) was calculated and plotted against irradiation time. The growth rate of carbonyl group was lower when Ph_3SnL, Me_2SnL_2, Bu_2SnOHL and Bu_2SnL_2 (0.5 wt %) were used as additives compared to PVC without additives Figure (3.18). The Ph_3SnL complex was the most efficient additive amongst the ones used in photostabilization of PVC followed by Bu_2SnL_2, Bu_2SnOHL and Me_2SnL_2.
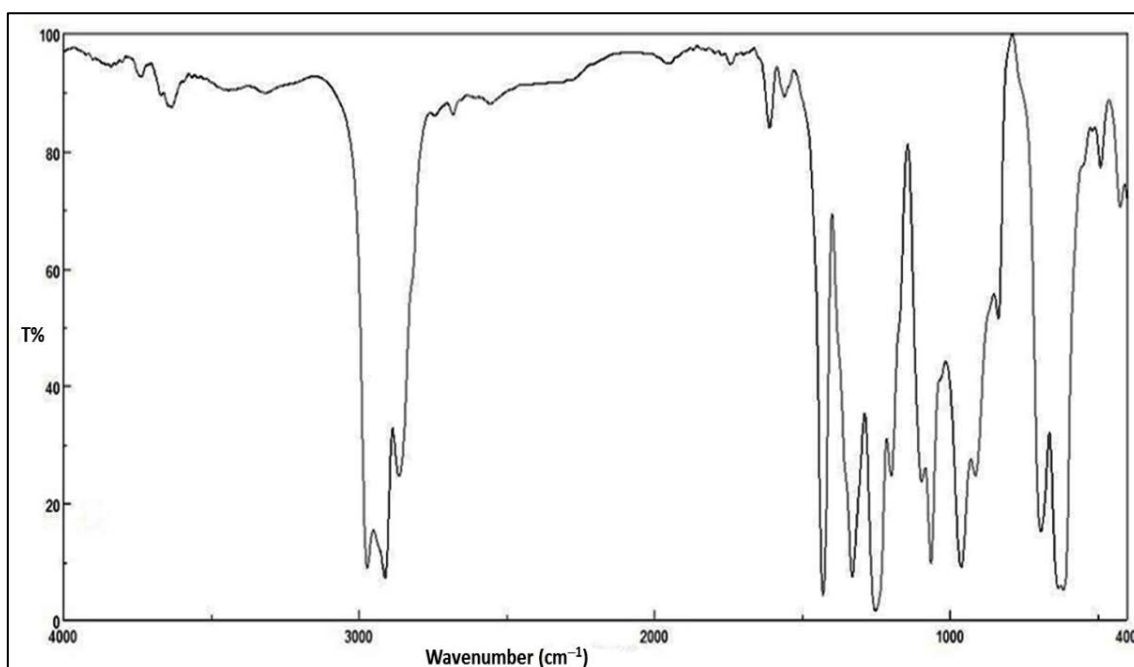
Figure 3.16 FTIR spectrum of PVC film containing Bu₂SnL₂ complex before irradiation.
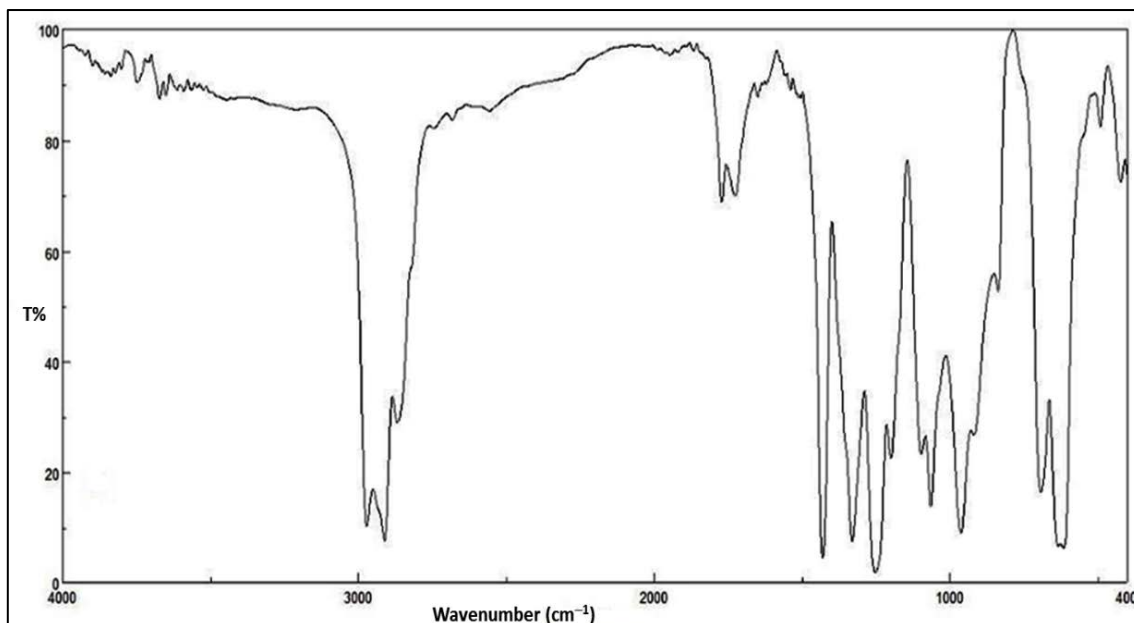
Figure 3.17 FTIR spectrum of PVC film containing Bu_2SnL_2 complex after 300h of irradiation.

Table 3.5 Carbonyl index ($I_{C=O}$) with irradiation time for PVC films in (40μm) thickness containing 0.5% additives

Compound	Irradiation time (h)						
	0	50	100	150	200	250	300
PVC (control)	0.058	0.1319	0.2017	0.2687	0.3274	0.3777	0.4281
PVC + Me_2SnL_2	0.047	0.0971	0.1421	0.1922	0.231	0.2784	0.3192
PVC + Bu_2SnOHL	0.0385	0.0763	0.1212	0.1575	0.2089	0.2531	0.2987
PVC + Bu_2SnL_2	0.0341	0.0583	0.0983	0.1313	0.164	0.1971	0.2361
PVC + Ph_3SnL	0.025	0.0319	0.0703	0.103	0.135	0.1733	0.197
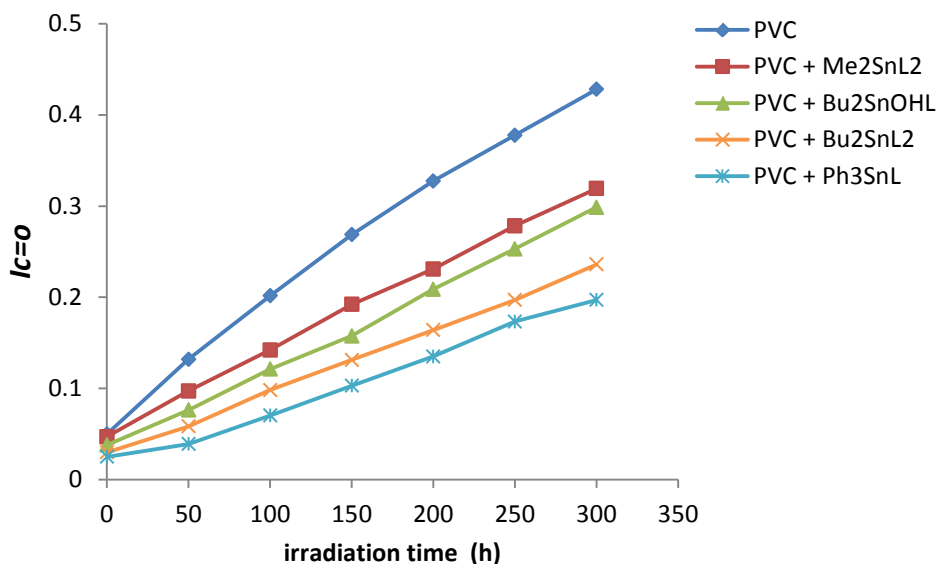
Figure 3.18 Changes in the $I_{C=O}$ index for PVC films versus irradiation time.

Similarly, the changes in the C=C group intensity was monitored and the polyene index ($I_{C=C}$) was calculated. Figure (3.19) shows the changes in $I_{C=C}$ of PVC films upon irradiation. All the additives used show stabilization for PVC on irradiation in which triphenyltin(IV) complex was the most effective additive against photodegradation of PVC.

Table 3.6 polyene index ($I_{C=C}$) with irradiation time for PVC films in (40μm) thickness containing 0.5% additives

Compound	Irradiation time (h)						
	0	50	100	150	200	250	300
PVC (control)	0.121	0.204	0.257	0.311	0.373	0.431	0.499
PVC + Me$_2$SnL$_2$	0.118	0.167	0.191	0.236	0.267	0.291	0.324
PVC + Bu$_2$SnOHL	0.106	0.132	0.165	0.201	0.234	0.264	0.297
PVC + Bu$_2$SnL$_2$	0.089	0.112	0.143	0.184	0.21	0.241	0.275
PVC + Ph$_3$SnL	0.081	0.101	0.132	0.167	0.191	0.212	0.248
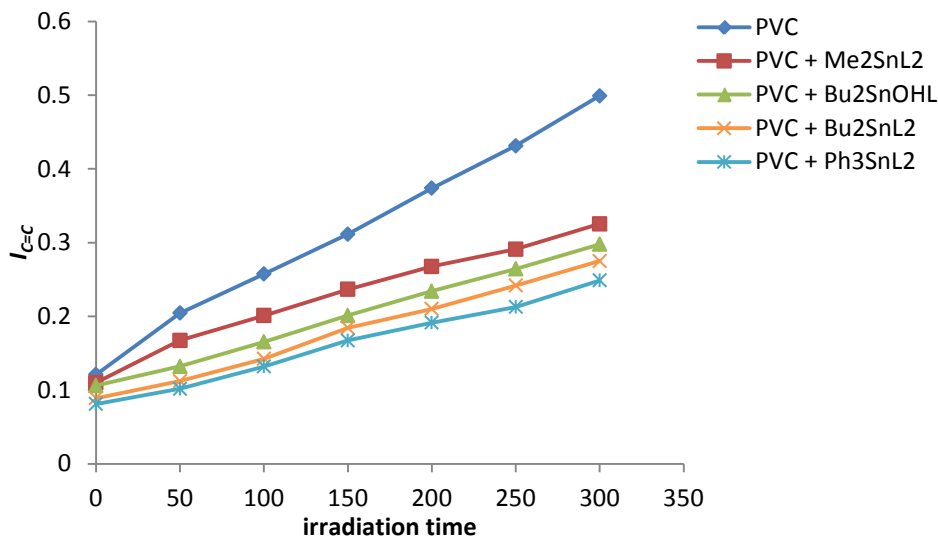
Figure 3.19 Changes in the $I_{C=C}$ index for PVC films versus irradiation time.

Figure (3.20) shows the changes in hydroxyl index (I_{OH}) of PVC films containing organotin(IV) complexes during irradiation. Again the additives used, Ph_3SnL, Bu_2SnL_2, Bu_2SnOHL and Me_2SnL_2, showed lower I_{OH} growth compared to PVC (control).

Table 3.7 hydroxyl index (I_{OH}) with irradiation time for PVC films in (40μm) thickness containing 0.5% additives

Compound	Irradiation time (h)						
	0	50	100	150	200	250	300
PVC (control)	0.0497	0.0644	0.0744	0.0854	0.0960	0.105	0.114
PVC + Me_2SnL_2	0.0468	0.0552	0.0617	0.0661	0.0720	0.0781	0.084
PVC + Bu_2SnOHL	0.0453	0.051	0.0561	0.0619	0.0669	0.071	0.0764
PVC + Bu_2SnL_2	0.0421	0.0463	0.0508	0.0540	0.0587	0.0633	0.0671
PVC + Ph_3SnL	0.0394	0.0421	0.0461	0.0501	0.0542	0.0592	0.063
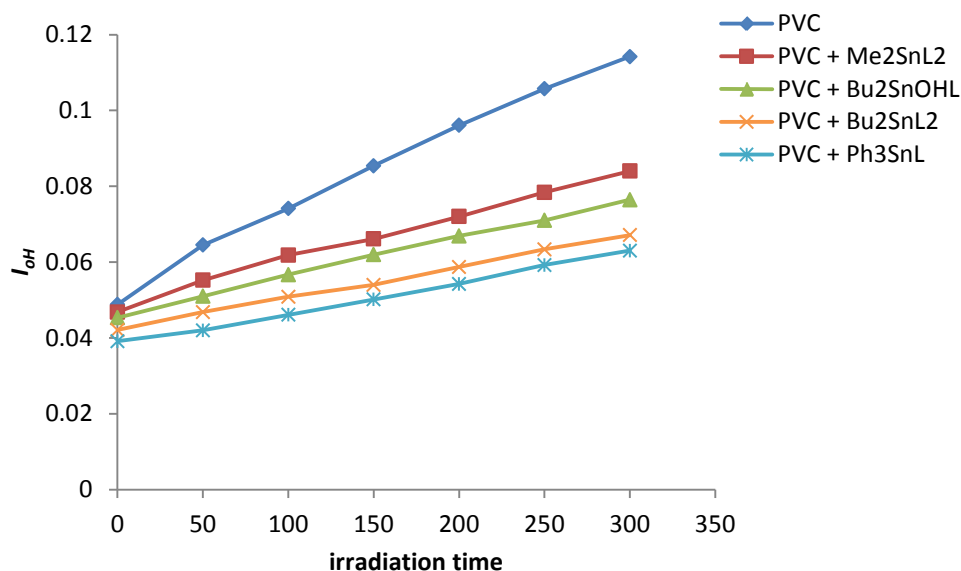
Figure 3.20 Changes in the I_{OH} index for PVC films versus irradiation time.

Again the results confirmed that all these additives are photostabilizer for PVC films, The rate of carbonyl ($I_{C=O}$), polyene ($I_{C=C}$) and hydroxyl indexes (I_{OH}), the Ph$_3$SnL is the most active photostabilizer, followed by Bu$_2$SnL$_2$, Bu$_2$SnOHL and Me$_2$SnL$_2$, respectively.

3.2.2 Evaluation of Stabilizing Efficiency of PVC by Ultra-Violet spectroscopy

The poor light stability of PVC may be caused by structural abnormalities that are existed in different types of commercially available polymer samples, such as unsaturated end groups, and oxidized structures such as hydroperoxide groups and carbonyl groups [92,93]. The PVC contains only C-C, C-H and C-Cl bonds, is not expected to absorb light of wavelength more than (190-220nm). The fact that free radicals are formed after irradiation at longer wavelengths (220-370 nm) indicates that some kinds of chromophores must be presented in a polymer [94].

It is generally accepted that carbonyl and polyene groups formed during UV irradiation of PVC are most probably responsible for the yellow color of the PVC [95].

The effect of organotin(IV) complexes (Me$_2$SnL$_2$, Bu$_2$SnOHL, Bu$_2$SnL$_2$ and Ph$_3$SnL) on the PVC films photodecomposition was investigated. The PVC films (40 μm thickness) containing organotin(IV) complexes (0.5% by weight) were irradiated with a UV light (λ_{max} = 313 nm) for 300 h. The irradiation led to a clear change in PVC films and decomposition took place. The plot of $ln(A_t - A_\infty)$ against irradiation time (t) gave a straight line. The graphs showed a first order kinetics in which the slope equal to the

decomposition rate constant (kd) for PVC films. Figures 3.21 shows the change in $ln(A_t - A_\infty)$ against irradiation time (t) for PVC films in the absence any additives. Figures (3.22–3.25) show the changes in the $ln(A_t - A_\infty)$ against irradiation time for PVC films containing organotin(IV) additives (0.5% by weight) as stabilizers for PVC films on irradiation with light.
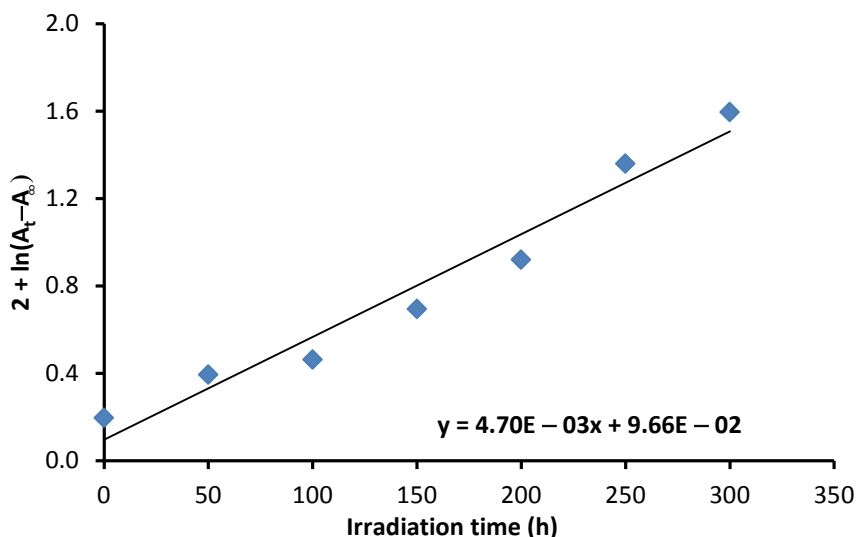
Figure 3.21 Changes in $ln(A_t - A_\infty)$ for PVC (blank) film with irradiation time.
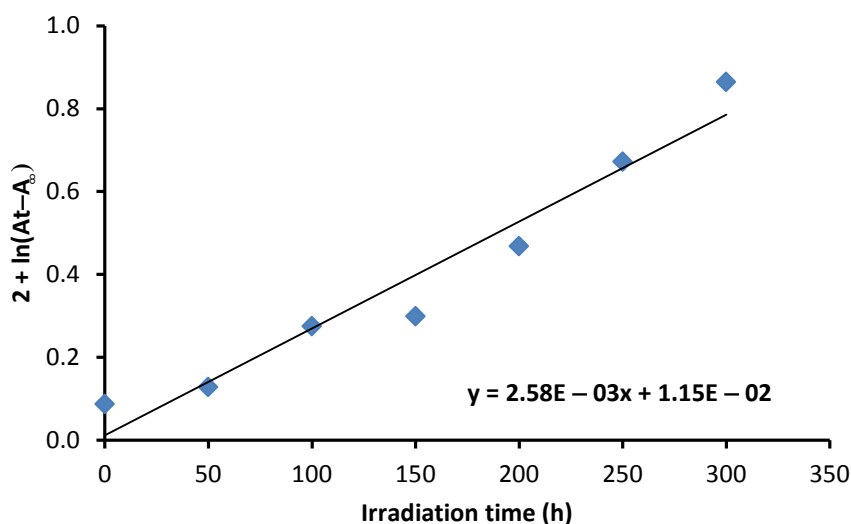
Figure 3.22 Changes in $ln(A_t - A_\infty)$ for PVC film containing Me$_2$SnL$_2$ with irradiation time.
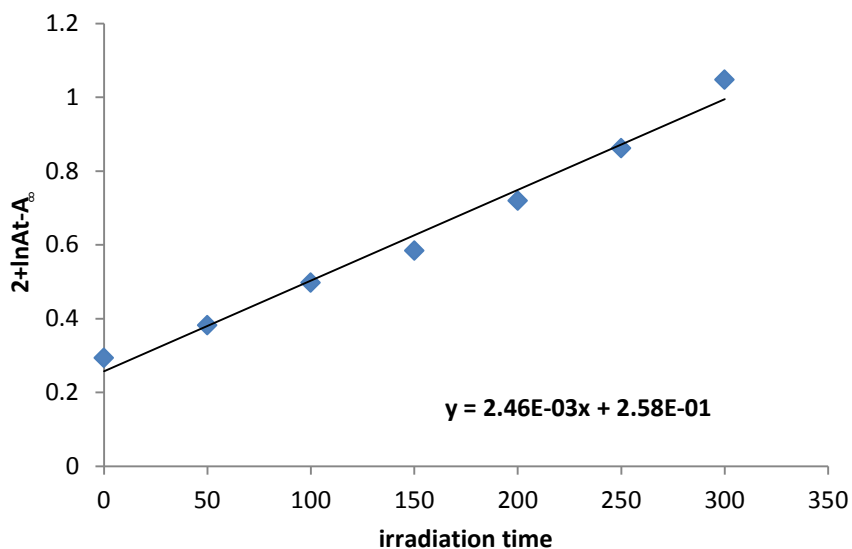
Figure 3.23 Changes in $\ln(A_t - A_\infty)$ for PVC film containing Bu₂SnOHL with irradiation time
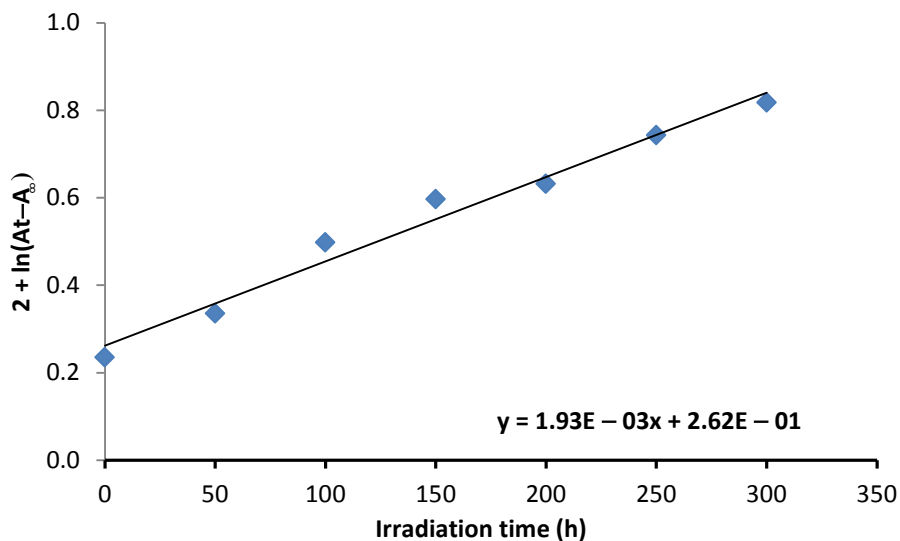
Figure 3.24 Changes in $ln(A_t - A_\infty)$ for PVC film containing Bu₂SnL₂ with irradiation time.
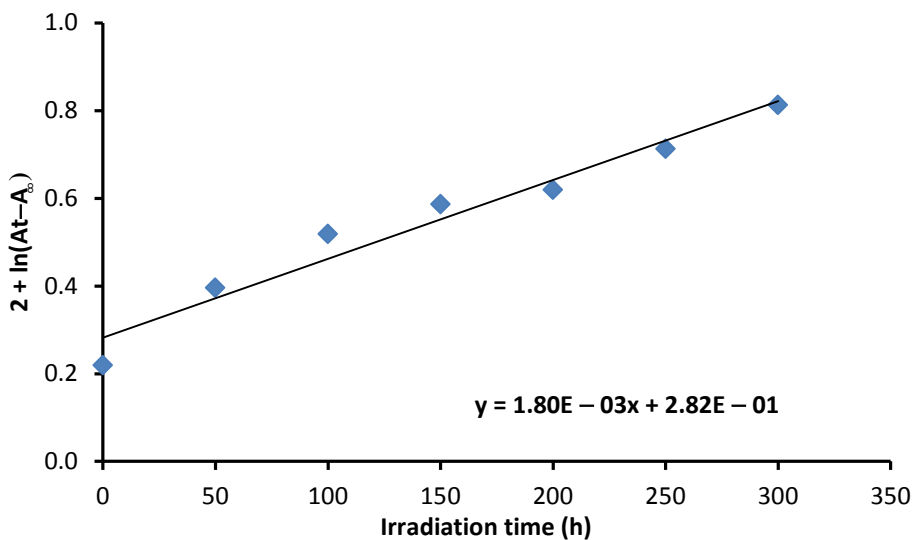
Figure 3.25 Changes in $ln(A_t - A_\infty)$ for PVC film containing Ph₃SnL with irradiation time.

The first order photodecomposition rate constant (k_d) for PVC films in the absence and presence of organotin(IV) complexes (0.5 wt %) is shown in Table (3.8).

Table 3.8 Photodecomposition rate constant (kd) for PVC films on UV irradiation (300 h).

Compound	$K_d(Sec^{-1}) \times 10^{-3}$
PVC (control)	4.70
PVC + Me₂SnL₂	2.58
PVC + Bu₂SnOHL	2.46
PVC + Bu₂SnL₂	1.93
PVC + Ph₃SnL	1.8

Table 3.8 and Figures (3.21–3.25) show that the rate constant (k_d) values are sensitive to the presence of organotin(IV) complex and its type. The PVC photodecomposition rate constant for PVC films was high (4.70×10^{-3} sec^{-1}) in the absence of any additives. Such rate constant has been reduced significantly (1.80×10^{-3} − 2.58×10^{-3} sec^{-1}) when organotin(IV) complexes were used as additives. The photostabilization of PVC in the presence of organotin(IV) complexes follow the order of Ph₃SnL > Bu₂SnL₂ > Bu₂SnOHL > Me₂SnL₂. The triphenyl(IV) complex was the most efficent than the other organotin complexes in photostabilization of PVC films presumely due to the reseonce of the extra phenyl group (*i.e*. acted as a better radical scavenger and UV absorber) [96].

Clearly, organotin(IV) complexes have acted as photostabilizers for the photostabilization of PVC films. The photodecomposition rate constant was highest for PVC (blank) and lowest in the presence of triphenyltin(IV) complex.

One could notice that (k_d) values are sensitive to the type of additives in poly(vinyl chloride) films, which decrease in the following order,

PVC+ Me₂SnL₂ > PVC+ Bu₂SnOHL > PVC+ Bu₂SnL₂ > PVC+ Ph₃SnL

Decrease of photodecomposition rate constasnt
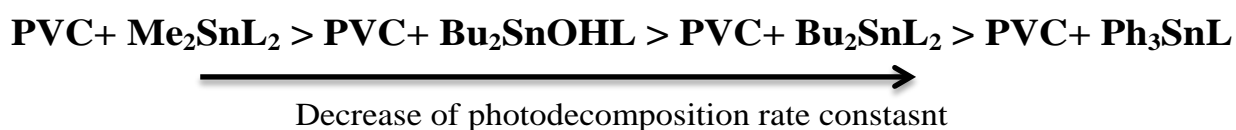
Which might point out the increase of the photo-stability of the additives in this term.

3.2.3 Evaluation of Stabilizing Efficiency of PVC by Weight Loss

Photodegradation of PVC is associated with the evaluation of HCl gas (dehydrochlorination), which leads to weight loss. Therefore, The stabilizing efficiency was determined by measuring the % weight loss of photodegraded PVC films in absence and in presence of additives by applying the following equation:

Weight loss % $= [(W_1 - W_2)/W_1] \times 100$ …….……… (3.1)

Where:

W_1: weight of the film before irradiation

W_2: weight of the film after irradiation

It has been reported that additives with a concentration of 0.5% by weight showed the most efficient photostabilization effect when added to PVC [97]. Therefore, di- and triorganotin(IV) additives (0.5% by weight) were added to PVC to produce the films. Their photostabilization effect was investigated for PVC films (40 μm thickness) on irradiation for up to 300 h. The effect of irradiation time (300 h) on weight loss of PVC films (40 μm thickness) is shown in Figure (3.26) and Table (3.9). Evidently, the PVC weight loss percentage was lower in the presence of organotin complexes, compared to the blank PVC film.

The Ph_3SnL complex shows the most efficient stabilizing effect compared to the other additives. The Ph_3SnL complex is believed to be a better radical scavenger compared to other complexes since the extra phenyl ring increases the photostabilization of PVC films on irradiation via resonance. The PVC photostabilization efficiency of organotin(IV) complexes was found to follow the order $Ph_3SnL > Bu_2SnL_2 > Bu_2SnOHL > Me_2SnL_2$.

Table 3.9 Measurement of weight loss for PVC films (40μm) thickness containing 0.5% from the additives

Compound	Irradiation time (h)					
	50	100	150	200	250	300
PVC (control)	0.815	0.9815	1.212	1.356	1.481	1.592
PVC + Me$_2$SnL$_2$	0.712	0.887	1.097	1.268	1.371	1.431
PVC + Bu$_2$SnOHL	0.542	0.723	0.957	1.127	1.182	1.266
PVC + Bu$_2$SnL$_2$	0.493	0.647	0.84	0.927	0.994	1.115
PVC + Ph$_3$SnL	0.382	0.58	0.695	0.784	0.898	0.974
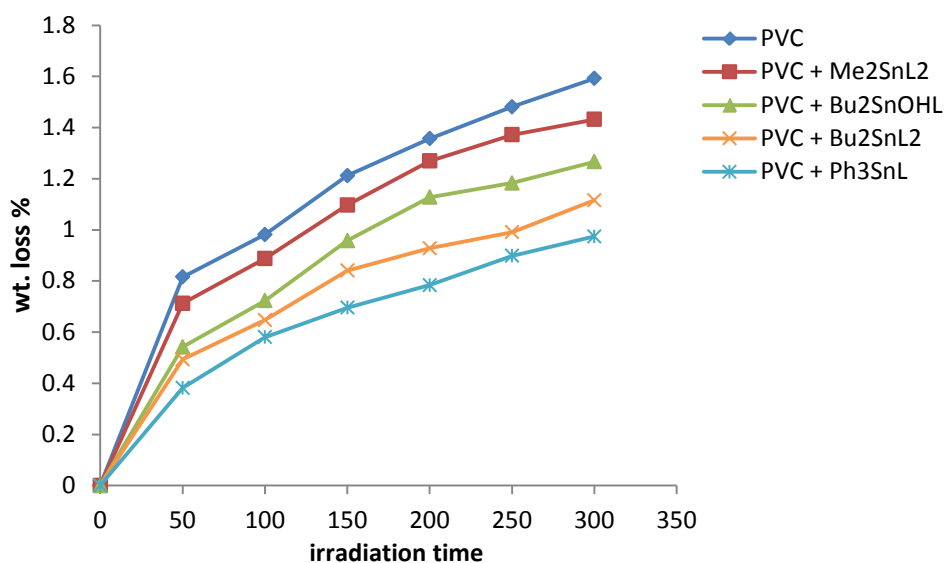
Figure 3.26 Changes in weight loss of PVC films versus irradiation time.

3.2.4 *Evaluation of Stabilizing Efficiency of PVC by Variation in Molecular Weight*

Viscosity average molecular weight ($\bar{M}_V$) can be measured from intrinsic viscosity using (Equation 2.13) in chapter two. The changes in $\bar{M}_V$ for PVC films (40 μm thickness)

containing organotin complexes (0.5 wt %) was plotted against irradiation time Figure (3.27) with a light intensity of 1.052×10^{-8} ein·dm^{-2}·s^{-1} (THF, 25 °C).

The plot indicates a quick decrease in ($\bar{M}_V$) initially then it slows down, suggesting that its due to the main chain scission at various locations along the polymer chain [98]. An additional evidence of the potency of the investigated photostabilizers and how long that stabilizer would protect the polymer, the lower viscosities of the soluble fractions of the degraded polymer in the presence of the investigated organotin stabilizers in comparison with the blank PVC.

Table 3.10 Variation of ($\bar{M}_V$) with irradiation time of PVC films thickness (40µm) containing 0.5 % of additives

Compound	Irradiation time (h)					
	0	50	100	150	200	300
PVC (control)	156281	100987	71132	43230	31420	22612
PVC + Me$_2$SnL$_2$	156651	112009	86230	63077	44582	30434
PVC + Bu$_2$SnOHL	162286	129574	101369	74047	58103	41325
PVC + Bu$_2$SnL$_2$	164445	139987	114411	90568	74500	60122
PVC + Ph$_3$SnL	168879	149720	122841	105764	92907	77430
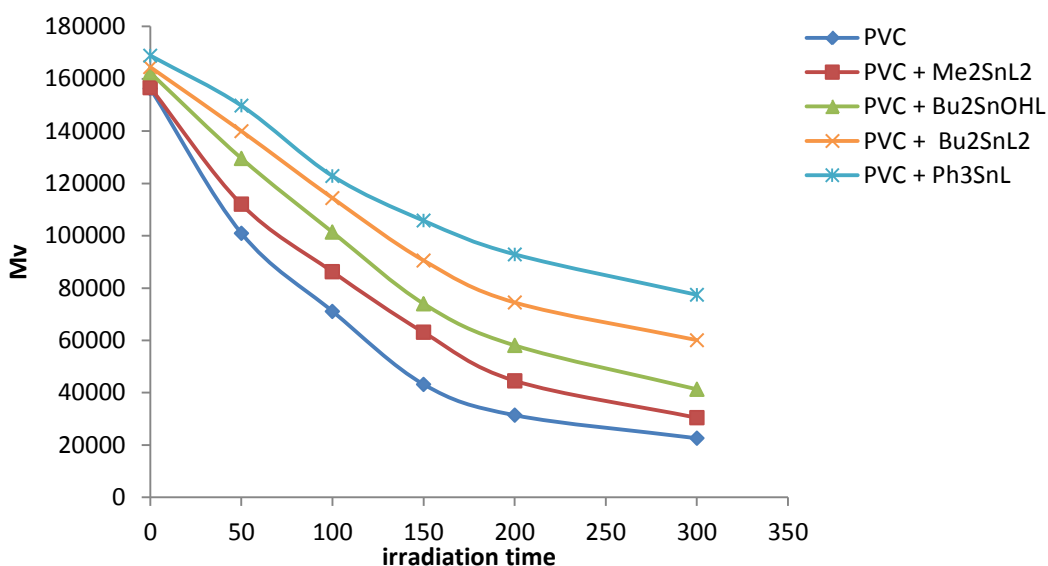
Figure 3.27 Changes in $\bar{M}_V$ for PVC films versus irradiation time.

It was noted that some insoluble PVC traces in THF was produced during photolysis process. It was suggested that these residues could possibly be an indication for PVC crosslinking or branching that occurs on irradiation [99]. To clarify this possibility, the number of average chain scission (S) [100] was calculated using (Equation 3.2). The S value is highly dependent on the viscosity average molecular weight at start ($\bar{M}_{V,O}$) and at t irradiation time ($\bar{M}_{V,t}$).

7. $\quad S = \bar{M}_{V,O} / \bar{M}_{V,t} - 1$ ……… (3.2)

8.

Table (3.11) and Figure (3.28) shows the effect of irradiation time on the value of S for PVC films containing organotin(IV) complexes. The PVC (control) on irradiation shows a higher degree of branching and/or cross-linking compared to the ones containing additives. The increases in S value was sharp for control PVC between 100 and 300 h. Less insoluble residual polymers were observed in PVC containing complexes and in particular those that contain Ph$_3$SnL [100].

Table 3.11 Variation of (S) values with irradiation time of PVC films thickness (40μm) containing 0.5 % of additives

Compound	Irradiation time (h)				
	50	100	150	200	300
PVC (control)	0.468	1.085	2.43	3.719	5.55
PVC + Me$_2$SnL$_2$	0.354	0.758	1.404	2.4	3.98
PVC + Bu$_2$SnOHL	0.26	0.611	1.205	1.81	2.95
PVC + Bu$_2$SnL$_2$	0.193	0.481	0.871	1.2244	1.812
PVC + Ph$_3$SnL	0.153	0.424	0.653	0.882	1.258
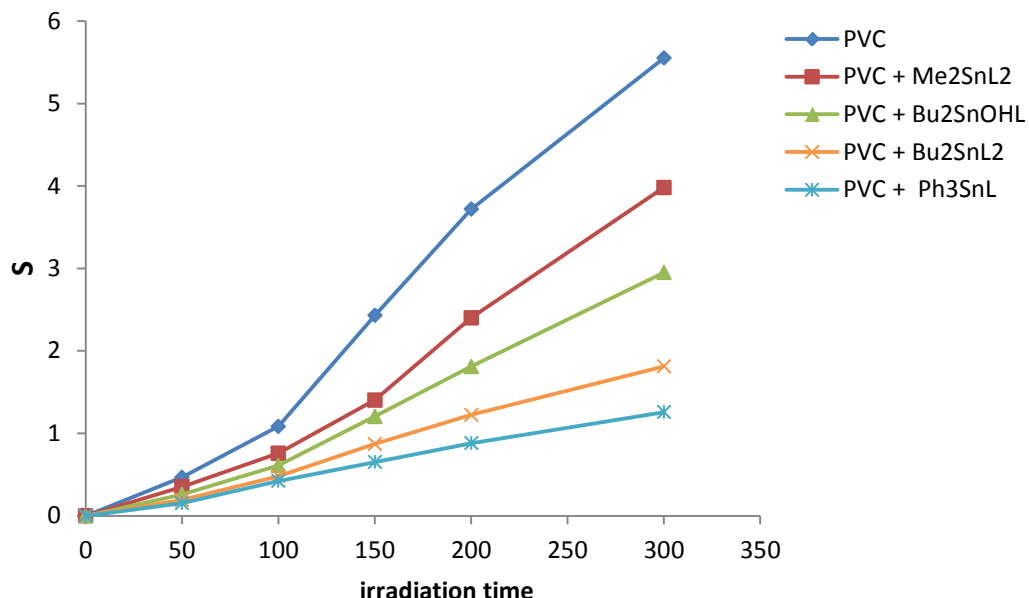
Figure 3.28 Changes in the main chain scission (*S*) for PVC films versus irradiation time.

The degree of deterioration (α) for PVC films can be calculated using (Equation 3.3). It is dependent on the initial molecular weight (*m*), *S* and $\overline{M}_{V,t}$. The value of α is proportional to the break of randomly distributed weak bond which is fast in the initial stage of irradiation.

$$\alpha = m \times S/\overline{M}_{V,t} \quad \ldots\ldots\ldots\ldots \text{ (3.3)}$$

From result in Table (3.12), the effect of irradiation on PVC films is shown in Figure (3.29). The change in α value was increased with irradiation time. The increase in α value for PVC (control) was steep at 150 °C and reached a maximum after 300 h. It seems likely that random bond breakage is occurring within PVC chain. The α value was lower for PVC containing Sn(IV) complexes and was minimum in the case of triphenyltin(IV) complex. It is clear that the use of such additives has reduced the photodegradation of PVC films upon irradiation [101].

Table 3.12 Variation of the (α) value with irradiation time of PVC films thickness (40μm) containing 0.5 % of additives

Compound	Irradiation time (h)				
	50	100	150	200	300
PVC (control)	0.692	2.277	5.391	15.066	30.765
PVC + Me$_2$SnL$_2$	0.479	1.33	3.375	8.164	17.83

PVC + Bu2SnOHL	0.328	0.9842	2.657	5.086	11.656
PVC + Bu2SnL2	0.23	0.712	1.629	2.785	5.107
PVC + Ph3SnL	0.176	0.604	1.079	1.66	2.841
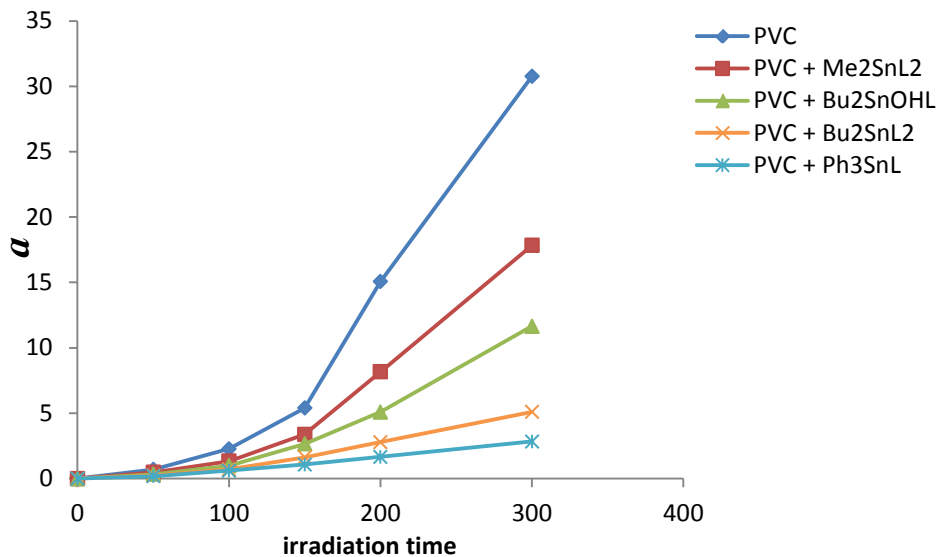
Figure 3.29 Changes in the degree of deterioration (α) for PVC films versus irradiation time.

The degree of polymerization (DP) is usually defined as the number of monomeric units in a macromolecule or polymer. For a homopolymer, there is only one type of monomeric units and the number average degree of polymerization is given by:

$$DP_n = X_n = M_n / M_o \ldots\ldots\ldots (3.8)$$

Where M_n is the number-average molecular weight and M_o is the molecular weight of the monomer unit [101].

The plot of $1/DP_n$ versus irradiation time is adopted to characterize degradation reaction of polymer as shown in Figure (3.30). The curve indicates an increase in the inverse of number average degree of polymerization with irradiation   time [102].

Table 3.13 The variation of DP_n with irradiation time for PVC films with 0.5% of additives, film thickness is (40 μm)

Compound	Irradiation time (h)					
	0	50	100	150	200	300
PVC (control)	2500	1615	1138	691	502	361
PVC + Me2SnL2	2506	1792	1379	1009	713	487
PVC + Bu2SnOHL	2596	2073	1622	1185	929	661
PVC + Bu2SnL2	2631	2239	1830	1449	1192	962
PVC + Ph3SnL	2702	2395	1965	1692	1486	1238

Table 3.14 The variation of $1/DP_n$ with irradiation time for PVC films with 0.5% of additives, film thickness is (40 μm)

Compound	Irradiation time (h)					
	0	50	100	150	200	300
PVC (control)	0.00039	0.00062	0.00087	0.0014	0.00199	0.0027
PVC + Me2SnL2	0.0004	0.00056	0.00073	0.00099	0.0014	0.0021
PVC + Bu2SnOHL	0.00039	0.00048	0.00062	0.00084	0.0011	0.0015
PVC + Bu2SnL2	0.00037	0.00045	0.00055	0.00069	0.00084	0.00104
PVC + Ph3SnL	0.00037	0.00042	0.00051	0.00057	0.00067	0.00081
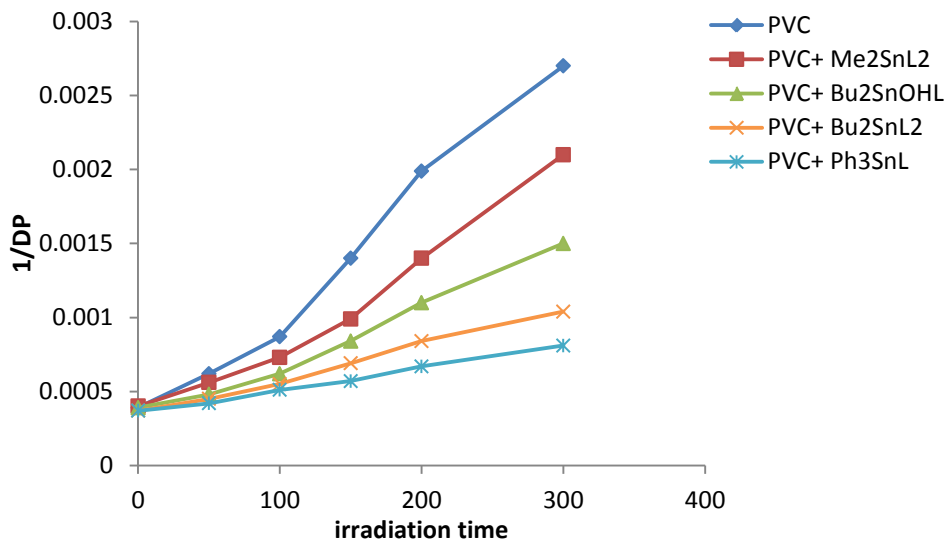
Figure 3.30 Changes in the reciprocal of number average of polymerization (1/DP$_n$) during irradiation of PVC films (40μm) (control) and modified PVC films

The quantum yield of chain scission (Φ_{cs}) for PVC films was represented in Table (3.15). The Φ_{cs} for PVC (control) was found to be higher (5.18×10^{-6}) compared to the ones containing Sn(IV) complexes (1.58×10^{-6}– 9.8×10^{-7}). The higher the Φ_{cs} value the greater the photodegrading of PVC films [103]. The PVC film which contains Ph$_3$SnL complex shows the lowest Φ_{cs} value. It can therefore be suggested that this additive inhibits the photodegrading of PVC upon irradiation. The quantum yield (Φ_{cs}) increases with increasing temperature [103]. It reaches peak around the melting temperature and glass transition temperature (Tg; 80 °C) of the crystalline and amorphous polymers, respectively. The PVC photolysis was carried out at 35–45 °C which is lower than the Tg of PVC. Therefore, the dependence of Φ_{cs} on temperature is not significant [104].

Table 3.15 Quantum yield (Φ_{cs}) for the chain scission for PVC film (40 μm) containing metal complexes (0.5 wt %) after irradiation (300 h).

Compound	Quantum Yield of Main Chain Scission (Φ_{cs}) $\times 10^{-6}$
PVC (control)	5.18
PVC + Me$_2$SnL$_2$	3.79
PVC + Bu$_2$SnOHL	2.95
PVC + Bu$_2$SnL$_2$	1.58

PVC + Ph$_3$SnL	0.98

From the overall results that obtained, the efficiency of organotin complexes as photostabilizers for PVC films can take the following order in photostabilization activity according to their decrease in hydroxyl, polyene, and carbonyl indices for PVC films as shown in Figures 3.17, 3.18 and 3.19:

$$Ph_3SnL > Bu_2SnL_2 > Bu_2SnOHL > Me_2SnL_2$$

3.3 Surface analysis

Polymer macrochains can be completely disordered (amorphous) or partially ordered. Physical and mechanical properties of plastics depend not only on the chemical structure of polymers, but also on their morphology [105].

Microscopic technique such as atomic force microscopy (AFM), permit checking of polymer samples from the scale of micrometres down to angstroms. The arrangement of individual polymer chains is visualized, and in some cases the observation of single atoms is possible [106]. Although microscopic methods are so popular and frequently used in the investigation of polymers, very little is known about their applications to the study of the degradation processes in polymer [107].

The morphological study of the surface of polymers has a lot of advantages. For example, it gives a clear picture about the surface irregularity, defects and the crystalline case. In addition, it allows monitoring the changes within the surface of the polymeric material as a result of photodecomposition or stabilization of polymers when exposed to ultraviolet radiation in which decomposition process can occur as chain scission [108].

The surface morphology images of the non-irradiated PVC films in the presence and absence of organotin (IV) complexes are shown in Figure (3.31). It is clear that the PVC film surface was smooth in which no white spots were detected.
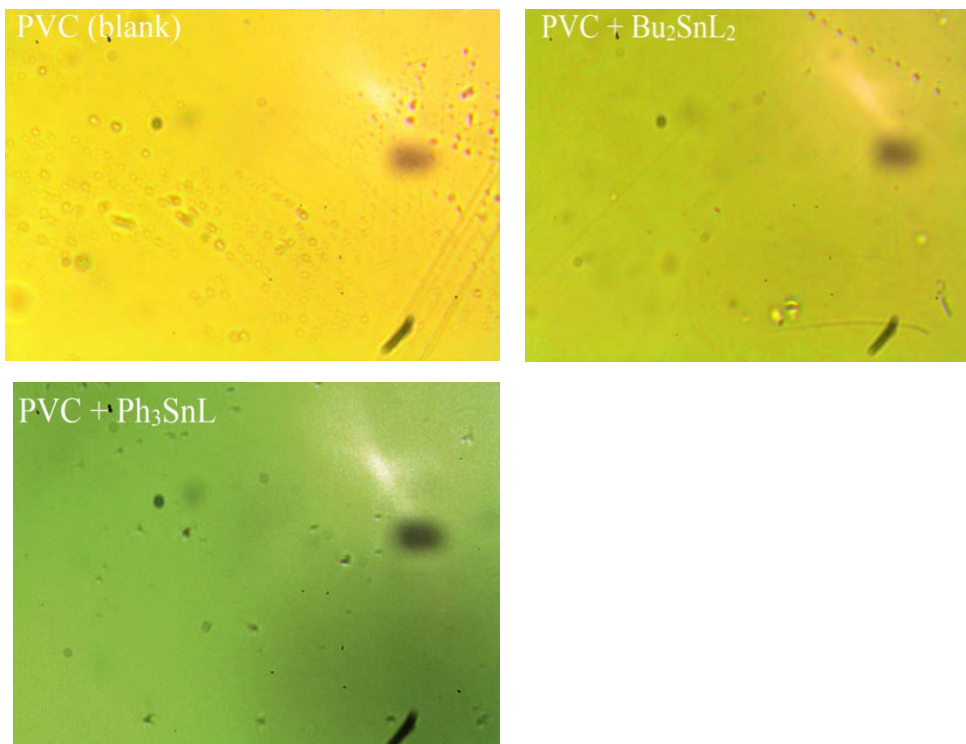
Figure 3.31 Microscope images for the non-irradiated PVC films (40 μm thickness) with organotin (IV) complexes (0.5% by weight) as additives

Figure(3.32) shows the microscopic image of PVC film irradiated for 300 h in air. It is clear that the blank PVC film, irritated for 300 h, was full of white spots and grooves as a result of photodegradation of polymeric materials due to elimination of HCl. In addition, the morphological image of irritated PVC (blank) showed cracks within its surface and color changes [109]. While in the presence of Ph_3SnL and Bu_2SnL_2 as additives, the surface was almost smooth and fewer white spot exist indicating efficient stabilization effects. Clearly, organotin(IV) additives reduce the photodegradation of PVC film through inhabitation of dehydrochlorination.
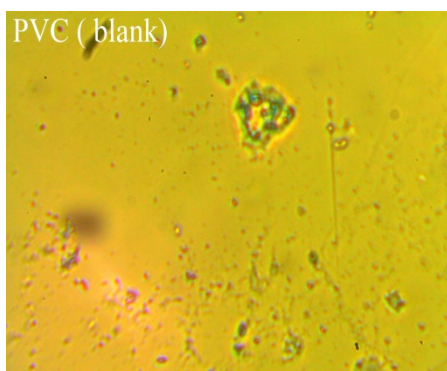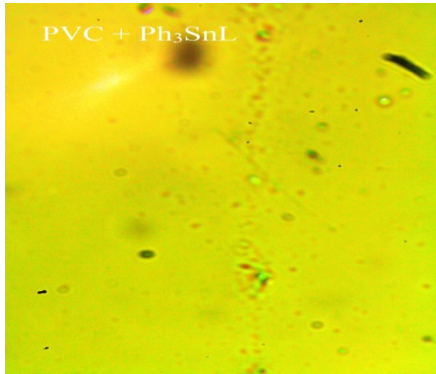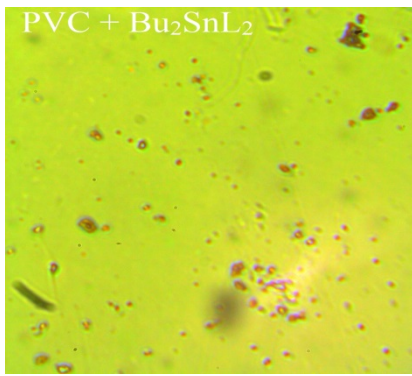
Figure 3.32 Microscope images for the irradiated (300 h) PVC films (40 μm thickness) with organotin (IV) complexes (0.5% by weight) as additives

The morphology of PVC surface (area = 5.0×5.0 μm^2) was inspected using an atomic force microscope (AFM). It provides two- and three-dimensional topographic images of the PVC surface on irradiation (300 h). AFM is helpful to measure the pores size and roughness factor (Rq) of the PVC film [110]. The AFM images for PVC films (control; 40 μm thickness) and that contains Bu$_2$SnL$_2$, Ph$_3$SnL (0.5 wt %) as a photostabilizer after irradiation (300 h) are given in Figures (3.33, 3.34 and 3.35), respectively.
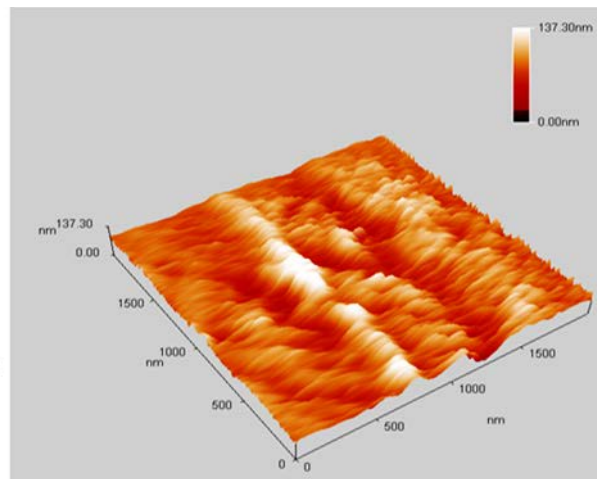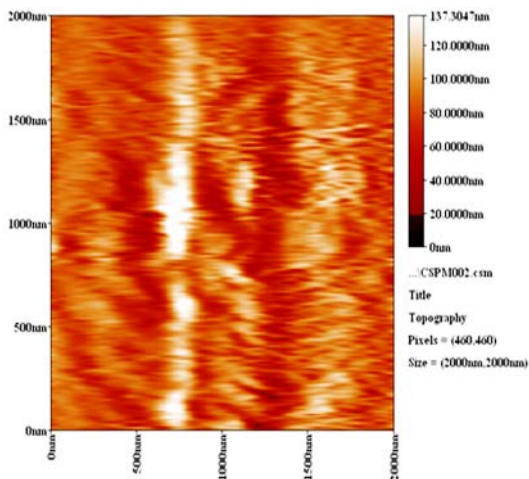
Figure 3.33 AFM images for PVC film (control) after irradiation (300 h).
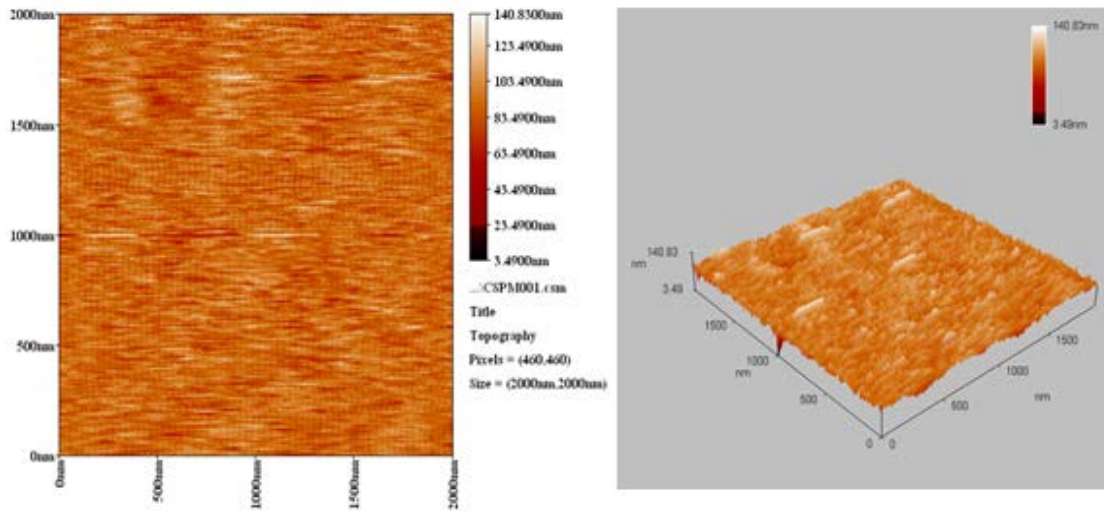
Figure 3.34 AFM images for PVC film containing Bu₂SnL₂ complexes after irradiation (300 h).
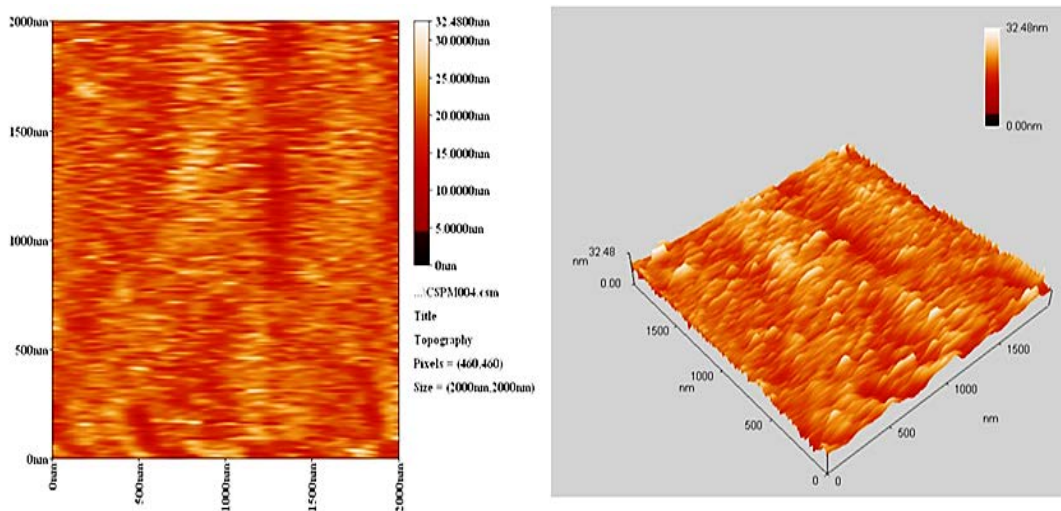
Figure 3.35 AFM images for PVC film containing Ph₃SnL complex after irradiation (300 h).

The surface of PVC film containing Ph_3SnL and Bu_2SnL_2 after irradiation was very smooth (Rq = 2.61 and 9.48), respectively. In contrast, the blank PVC film after irradiation has a rough surface (Rq = 17.3). UV irradiation may have led to bond breakage within polymeric chains and hence the removal of leachable constituents from the PVC surface that can result in a roughened surface [111]. Irradiation of PVC in the absence of photostabilizers could lead to dehydrochlorination [112]. It seems likely that the Sn(IV) complexes inhibits the dehydrochlorination process.

Table 3.16 Rq values of surface modified PVC films

Sample	Rq

PVC (control)	17.3
PVC + Bu$_2$SnL$_2$	9.48
PVC + Ph$_3$SnL	2.61

3.4 Suggested Mechanisms of Photostabilization of PVC by di- and triorganotin complexes

The di- and triorganotin(IV) complexes act as photostabilizers for PVC films and their efficiencies follow the order Ph$_3$SnL > Bu$_2$SnL$_2$ > Me$_2$SnL$_2$. The three Sn(IV) utilized all reduced PVC photodegradation. Such additives can stabilize the polymeric films based on various mechanisms. Tin is a strong Lewis acid, which is also known as a secondary stabilizer, and therefore acts as HCl scavenger (Scheme 4). The photostabilization effect could be due to displacement of chlorine atom within PVC chains by carboxylate oxygen. Various organic compounds are known as long-term PVC stabilizers [113].

R^1 = Ph, Me, Bu
R^2 = Ph, OH, 4-chloro-2-(furan-2-ylmethylamino)-5-sulfamoylbenzoate
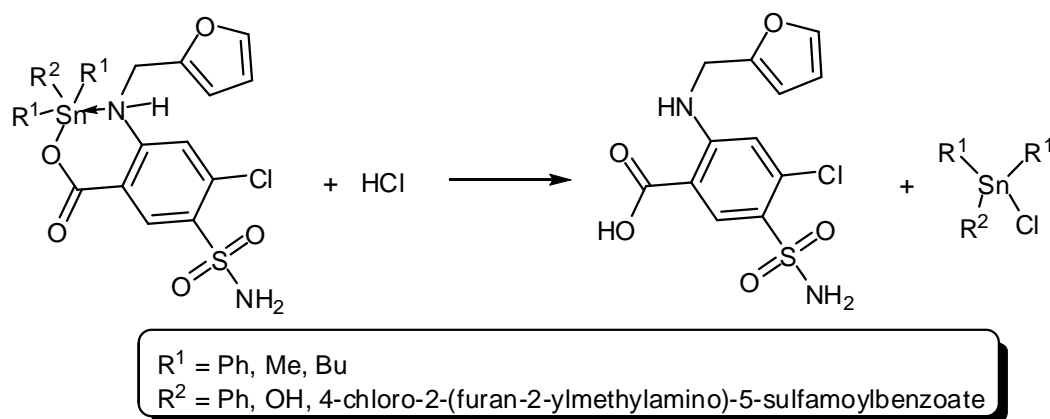
Scheme 4. Organotin complexes act as HCl scavengers.

Photooxidation of PVC can take place in the presence of hydroperoxides. Various additives are known for their reactions with hydroperoxides and therefore inhibit photodegradation of polymers [114]. The organotin(IV) complexes are expected to decompose peroxides (Scheme 5) and therefore, stabilize PVC polymeric chains.
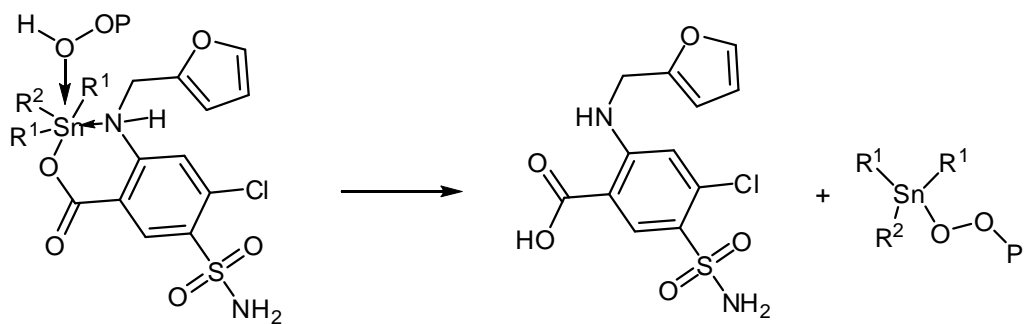
Scheme 5. Organotin complexes as peroxide decomposers.

Attraction between polarized C–O bonds in furan moiety and S–NH$_2$ group within Sn(IV) complexes and polarized C–Cl within PVC chains could stabilize the polymer (Scheme 6). This attraction can aid the conversion of the excited state PVC energy to a level of energy that does not harm the polymeric chain [97].
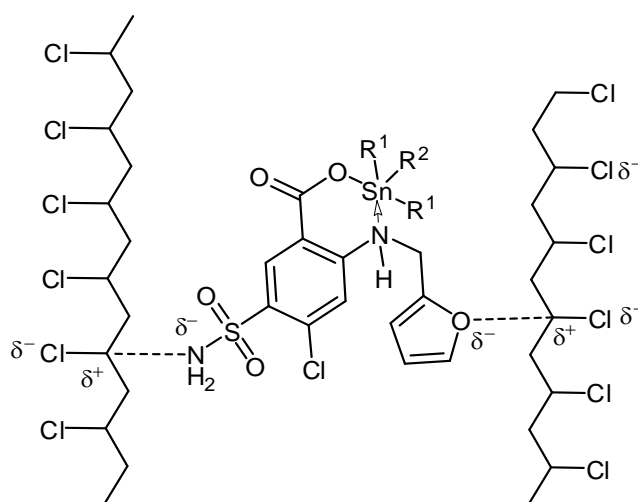
Scheme 6. Organotin complexes as primary stabilizers.

Sn(IV) complexes could also act as radical scavengers (Scheme 6). The additives could form a complex with a chromophore (POO$^•$) in the excited state [115]. This complex could be stabilized via resonance of aryl and furan moieties (Scheme 7).
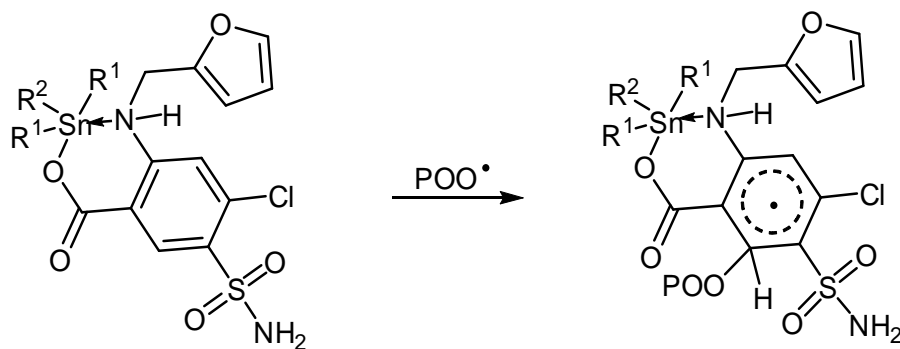
Scheme 7. Organotin complexes as radical scavengers.

Electron rich aromatic moieties within the PVC backbone can absorb UV radiation [97]. These additives can convert the absorbed UV radiation energy into heat energy that is not harmful to PVC. Therefore, it is believed that both furan and aryl ring within Sn(VI) complexes act as UV absorbers (Scheme 8).
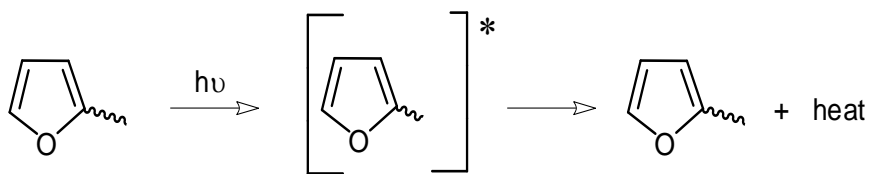
Scheme 8. Furan moiety acts as a UV absorber.

3.5 Conclusion

1. Organotin additives used in this study behave successfully as photostabilizers for PVC films.

2. The additives take the following order in photostabilization activity According to their decrease in carbonyl, hydroxyl, polyene ($I_{C=O}$, I_{OH}, $I_{C=C}$) and the weight loss for PVC films.

$$Me_2SnL_2 < Bu_2SnOHL < Bu_2SnL_2 < Ph_3SnL$$

3. These additives stabilize the PVC films through HCl scavenging, peroxide decomposers, primary stabilizers, free radical scavenger and UV absorber mechanisms.

4. The Ph_3SnL complex was found to be the more efficient in photostabilization process according to the photostability, this supports to use Ph_3SnL complex as a commercial stabilizer for PVC.

3.6 Suggestions for future work

1. Studying the photoactivity of the additives with other polymers such as PS, PVA, LDPE, HDPE comparing the activity of these additives in photostabilization of PVC.

2. Comparing the efficiency of the additives with some commercial stabilizers.

3. Study the effect of additives in the outdoor weathering.

4. Can also study the effect of substitution of the some groups on the aromatic rings in the structure of the complexes and study their effect on polymers.

5. Study the effect of temperature on the efficiency of the additives.

6. Since fixed thickness was used in this work. Further work can be extended   by using different films thickness and studying their effect on the photostabilization process.

7. Extend the study by using different concentration from additives and studying their effect on the photostabilization process

REFERENCES

References

1. Neumnn W. "The Organic Chemistry of Tin" Wiley, New York, **1970**.

2. Tahira K., Ali S., Shahzadi S., Sharma S.K., Qanungo K. Bimetallic organotin(IV) complexes with ferrocene-based azomethines: synthesis, characterization, semi-empirical study, and antibacterial activity. *Journal of Coordination Chemistry.* **2011**, *64*, 1871-1884.

3. Tarassoli A., Talooky S. A. Synthesis and characterization of complexes of organotin(IV) with 2-thiazoline-2-thione. *Journal of Coordination Chemistry*. **2012** doi.org/10.1080/00958972.2012. 717222.

4. Song X., Zapata A., Hoerner J., Dios A., Casabianca L., Eng G. Synthesis, larvicidal, QSAR and structural studies of some triorganotin 2,2,3,3-tetramethylcyclopropanecarboxylates. *Applied Organometallic Chemistry*. **2007**, *21*, 545-550.

5. Sander H., Deelman B., Koten G. Synthetic aspects of tetraorganotins and organotin(IV) halides. *Journal of Organometallic Chemistry*. **2004**, *689*, 2145-2157.

6. Muhammad N. Organotin(IV) Complexes With O'O Donor Atoms From Carboxylic Acid Derivatives (Ph.D. thesis), Department of Chemistry, Quaid-i-Azam University, **2010**.

7. Ugo R., Chiesa A., Fusi A. A highly selective synthesis of R_2SnX_2 (R= alkyl, X = Br, Cl) species directly from tin and alkyl halides. *Journal of Organometallic Chemistry.* **1987**, *330*, 25-30.

8. Sisido K., Kozima S., Hanada T. Direct Synthesis of Organotin Compounds V. Di- and trialkyltin chlorides and bromides. *Journal of Organometallic Chemistry*. **1967**, *99*, 109-115.

9. Davies G., Gielen M., Edward R. "Tin Chemistry: Fundamentals, Frontiers and Applications" John Wiley and Sons, Ltd.1st . 4-5, **2008**.

10. Yousif E., Mehdi B., Yusop R., Salimon J., Salih N., Abdullah B. Synthesis, structure and antibacterial activity of some triorganotin(IV) complexes with a benzamidoalanine ligand. *Journal of Taibah University for Science*. **2014**, *8*, 276-281.

11. Surdy P., Rubini P., Buzas N., Henry B., Pellerito L., Gajda T. Interaction of Dimethyltin(IV)$^{2+}$ Cation with Gly-Gly, Gly-His, and Some Related Ligands. A New Case of a Metal Ion Able To Promote Peptide Nitrogen Deprotonation in Aqueous Solution. *Inorganic Chemistry*. **1999**, *38*, 346-352.

12. Vatsa C., Jain V. K., Kesavadas T., Tiekink E. Structural chemistry of organotin carboxylates XII. Synthesis and characterization of diorganotin(IV) carboxylates containing 2-thiophene- or 2-furan-carboxylic acid. Crystal structure of [Et$_2$Sn(O$_2$CC$_4$H$_3$S)$_2$]. *Journal of Organometallic Chemistry*. **1991**, *410*, 135-142.

13. Osada S., Nishikawa J., Nakanishi T., Tanaka K., Nishihara T. toxicol, Some organotin compounds enhance histone acetyltransferase activity. *Toxicology Letters*. **2005**, *155*, 329-335.

14. Nath M., Jairath R., Eng G., SongX., Kumar A. Spectrochim, New organotin(IV) ascorbates: synthesis, spectral characterization, biological and potentiometric studies, Spectrochimica Acta Part A: *Molecular and Biomolecular Spectroscopy*. **2005**, *61*, 77-86.

15. Pagliarani A., Bandiera P., Ventrella, V., Trombetti F., Pirini M., Borgatti A. Response to alkyltins of two Na$^+$-dependent ATPase activities in Tapes philippinarum and Mytilus galloprovincialis. *Toxicol. in Vitro*. **2006**, *20*, 1145-1153.

16. Nath M., Pokharia S., Yadav R. Organotin(IV) complexes of amino acids and peptides. *Coordination Chemistry Reviews*. **2001**, *215*, 99-149.

17. Omae I. Organotin antifouling paints and their alternative. *Applied Organometallic Chemistry*. **2003**, *17*, 81-105.

18. Shiryaev V., Storozhenko P. Application of organotin compounds for protecting wood and other materials and in nonfouling paints. *Polymer Science Series*. **2012**, *5*, 221-230.

19. Pellerito C., Nagy L., Pellerito L., Szorcsik A. Biological activity studies on organotin(IV)$^{n+}$ complexes and parent compounds. *Journal of Organometallic Chemistry*. **2006**, *691*, 1733-1747.

20. Pellerito L., Nagy L. Organotin(IV)$^{n+}$ complexes formed with biologically active ligands: equilibrium and structural studies, and some biological aspects. *Coordination Chemistry Reviews*. **2002**, *224*, 111-150.

21. Yousif E. Triorganotin(IV) complexes photo-stabilizers for rigid PVC against photodegradation. *Journal of Taibah University for Science*. **2013**, *7*, 79–87.

22. Yousif E. Synthesis, spectroscopic studies and fungicidal activity of some diorganotin(IV) with 2-[(phenylcarbonyl)amino] propanoato. *Journal of King Saud University Science*. **2012**, *24*, 167-170.

23. Yousif E., Farina Y., Graisa A., Salih N., Salimon J. Structure and Fungicidal Activity of Some Diorganotin(IV) with 2-Thioacetic-5-Phenyl-1,3,4-Oxadiazole and Benzamido phenylalanin, *Iranian Journal of Chemistry & Chemical Engineering*. **2011**, *30*, 67-72.

24. Mcurdy R. Successful implementation methods of atmospheric CVD on a glass manufacturing line. *Thin Solid Films*. **1999**, 351, 66-72.

25. Chopra K., Major S., Pandya D. Transparent conductors—A status review, *Thin Solid Films*. **1983**, *102*, 1-46.

26. Huang Z., Ding A., Guo H., Lu G., Huang X. Construction of nontoxic polymeric UV-absorber with great resistance to UV-photoaging. *Scientific Reports.* **2016**, doi:10.1038/srep25508.

27. Saeki Y., Emura T. Technical progresses for PVC production. *Progress in Polymer Science*. **2002**, *27*, 2055–2131.

28. Zhang X., Zhao T., Pi H., Guo S. Mechanochemical preparation of a novel polymeric photostabilizer for poly(vinyl chloride). *Journal of Applied Polymer Science.* **2010**, *116*, 3079–3086.

29. Real L. P., Ferraria A. M., Botelho de Rego A. M. Comparison of different photo-oxidation conditions of poly(vinyl chloride) for outdoor applications. *Polymer Testing.* **2008**, *27*, 743-751.

30. Nicholson, J. W. "The Chemistry of Polymers" 3rd ed.; RSC Pub.: Cambridge, UK, **2012**.

31. Starnes W. H. Structural and mechanistic aspects of the thermal degradation of poly(vinyl chloride). *Progress in Polymer Science*. **2002**, *27*, 2133–2170.

32. Braun D. Thermal Degradation of Poly (vinyl chloride). In Developments in Polymer Degradation; Grassie, N., Ed.; Applied Science Publishers: London, UK, **1981**.

33. Fahmy M. M., Mohamed R. R., Mohamed N. A. Novel antimicrobial organic thermal stabilizer and co-stabilizer for rigid PVC. *Molecules*. **2012**, *17*, 7927–7940.

34. Iván B., Kennedy J. P., Kélen T., Tüdòs F., Nagy T. T., Turcsanyi B. Degradation of PVCs Obtained by Controlled Chemical Dehydrochlorination. *Journal of Polymer Science*. **1983**, *21*, 2177-2188.

35. Yousif E., Hameed A., Rasheed R., Mansoor H., Farina Y., Graisa A., Salih N., Salimon J. Synthesis and photostability study of some modified poly(vinyl chloride) containing pendant benzothiazole and benzimidozole ring. *International Journal of Chemistry*. **2010**, *2*, 65-80.

36. Yousif E., Hasan A., El-Hiti G. A. Spectroscopic, physical and topography of photochemical process of PVC films in the presence of Schiff base metal complexes. *Polymers*. **2016**, *8*, 204, doi:10.3390/polym8060204.

37. Yousif E., El-Hiti G. A., Hussain Z., Altaie A. Viscoelastic, spectroscopic and microscopic study of the photo irradiation effect on the stability of PVC in the presence of sulfamethoxazole Schiff's bases. *Polymers*, **2015**, *7*, 2190-2204.

38. Sabaa M. W., Oraby E. H., Abdel Naby A. S., Mohammed R. R. Anthraquinone derivatives as organic stabilizers for rigid poly(vinyl chloride) against photo-degradation. *European Polymer Journal*. **2005**, *41*, 2530-2543.

39. Tomohito K., Masahiko O. Guid G., Tadaaki M., Toshiaki Y. Antibacterial effect of thiocyanate substituted poly (vinyl chloride). *Journal of Polymer Research*. **2011**, *18*, 945-947.

40. Yousif E. A., Aliwi S. M., Ameer A. A., Ukal J. R. Improved photostability of PVC films in the presence of 2-thioacetic acid-5-phenyl-1,3,4-oxadiazole complexes. *Turkish Journal of Chemistry*. **2009**, *33*, 399-410.

41. Yousif E., Salih N., Salimon J. Improvement of the photostabilization of PVC films in the   presence   of

2*N*-salicylidene-5-(substituted)-1,3,4-thiadiazole. *Journal of Applied Polymer Science*. **2011**, *120*, 2207-2214.

42. Balakit A. A., Ahmed A., El-Hiti G. A., Smith K., Yousif, E. Synthesis of new thiophene derivatives and their use as photostabilizers for rigid poly(vinyl chloride). *International Journal of Polymer Science.* **2015**, doi:10.1155/2015/510390.

43. Folarin O. M., Sadiku E. R. Thermal stabilizers for poly(vinyl chloride): A review. *International Journal of Physical Sciences*. **2011**, *6*, 4323-4330.

44. Chen X., Li C., Zhang L., Xu S., Zhou Q., Zhu Y., Qu X. Main factors in preparation of antibacterial particles /PVC composite. *China Particuol.* **2004**, *2*, 226-229.

45. Cheng Q., Li C., Pavlinek V., Saha P., Wang H. Surface-modified antibacterial TiO_2/Ag^+ nanoparticles: Preparation and properties. *Applied Surface Science.* **2006**, *252*, 4154-4160.

46. Yousif E., Salimon J., Salih N. New photostabilizers for PVC based on some diorganotin(IV) complexes. *Journal of Saudi Chemical Society.* **2015**, *19*, 133-141.

47. Altaee, N.; El-Hiti, G.A.; Fahdil, A.; Sudesh, K.; Yousif, E. Biodegradation of different formulations of polyhydroxybutyrate films in soil. *SpringerPlus*. **2016**, doi:10.1186/s40064-016-2480-2.

48. Yousif E. El-Hiti G. A., Haddad R., Balakit A. A. Photochemical stability and photostabilizing efficiency of poly(methyl methacrylate) based on 2-(6-methoxynaphthalen-2-yl)propanoate metal ion complexes. *Polymers*. **2015**, *7*, 1005-1019

49. Smith K., Al-Zuhairi A. J., El-Hiti G. A., Alshammari M. B. Comparison of cyclic and polymeric disulfides as catalysts for the regioselective chlorination of phenols. *Journal of Sulfur Chemistry.* **2015**, *36*, 74-85.

50. Smith K., Balakit A. A., El-Hiti G. A. Poly(propylene sulfide)-borane: Convenient and versatile reagent for organic synthesis. *Tetrahedron.* **2012**, *68*, 7834-7839.

51. Smith K., Balakit A. A., Pardasani R. T., El-Hiti G. A. New polymeric sulfide–borane complexes: Convenient hydroborating and reducing reagents. *Journal of Sulfur Chemistry.* **2011**, *32*, 287-295.

52. Zimmermann H. Poly(vinyl chloride) polymerization performance-enhancing initiators with emphasis on high activity grades and water-based dispersions. *Journal of Vinyl and Additive Technology.* **1996**, *2*, 287-294.

53. Xie T., Hamielec A., Wood P., Woods D. Suspension, bulk, and emulsion polymerization of vinyl chloride-mechanism, kinetics, and reactor modelling. *Journal of Vinyl and Additive Technology*. **1991**, *13*, 2-25.

54. Naqvi M. Structure and stability of polyvinyl chloride. *Journal of Macromolecular Science*. **1985**, *25*,119-155.

55. Andrady A., Hamid S., Hu X., Torikai A. Effects of increasedsolar ultraviolet radiation on materials, *Journal of Photochemistry and Photobiology A: Chemistry.* **1998**, *46* 96-103.

56. Wiles D. Photostabilization of macromolecules by excited statequenching. *Pure and Applied Chemistry.***1978**, *50*, 291-297.

57. Torikai A., Hasegawa H. Accelerated photodegradationof poly(vinyl chloride). *Polymer Degradation and Stability*. **1999**, *63*, 441-445.

58. Schnabel W. "Polymer Degradation: Principle and Practical Applications" Chapter 14. München: Hanser Int; **1981**.

59. Feldman D. Polymer weathering: photo-oxidation. *Journal of polymer and the environmental*. **2002**, *10*, 163–173.

60. Weidner S., Kuhn G., Freiedrich J., Schroder H. Plasmaoxidative and chemical degradation of poly(ethylene terepthalate) studied by matrix-assisted laser desorption/ionisation mass spectrometry. *Rapid Communications in Mass Spectrometry*. **1996**, *10*, 40–46

61. Chrissafis K., Antoniadis G., Paraskevopoulos K. M., Vassiliou A., Bikiaris D. N. Comparative study of the effect of different nanoparticles on the mechanical properties and thermal degradation mechanism of in situ prepared poly(3-caprolactone) nanocomposites. *Composites Science and Technology*. **2007**, *67*, 2165-2174.

62. Potts J. E. "Plastic environmentally degradation" The Kirk-Othmer Encyclopedia of Chemical Technology, 3rd edn. **1991**.

63. Dindar B., Icli S. Unusual photo reactivity of zinc oxide irradiated by concentrated sunlight. *Journal of Photochemistry and Photobiology A: Chemistry*. **2001**, *140*, 263-268.

64. Vinhas G. M., Souto Maiora R. M., Lapa C. M., Almeida Y. B. Degradation studies on plasticized PVC films submitted to gamma radiation. *Materials Research Bulletin*. **2003**, 6, 497–500.

65. Pinto L., Goi. B., Schmitt C., Neumann M. photodegradation of polystyrene film containing UV- visible sensitizers. *Journal of Research Updates in polymer Science*. **2013**, *2*, 39-47.

66. Schnabel W. "Polymer Degradation: Principle and Practical Applications" Chapter 14. Hanser Int, München. **1981**.

67. El-Tonsy M. M., AlSaati S. A., Oraby A. H. degradation of low density polyethylene due to successive exposure to acid rain and UV radiation. *International Journal of Science and Engineering Applications*. **2015**, *5*, 327-334.

68. Kamiya Y., Niki E. "In Aspects of Degradation and Stabilization of Polymers" Elsevier Scientific Publishing Company, Amsterdam. Ch.3, **1978**.

69. Yousif E., Ahmed A., Mahmoud M. "New Organic Photo-Stabilizers For Rigid PVC Against Photodegradation" LAP LAMBERT, Germany. **2012**.

70. Hoekstra H. D., Breen J. Fracture behavior of exposed HDPE specimens with an embrittled layer due to UV-exposure, *Die Angewandte Makromolekulare Chemie.* **1997**, *252*, 69-88.

71. Wille U., Goeschen C. Damage of polyesters by the atmospheric free radical oxidant NO^3 ˙: a product study involving model systems. *Beilstein Journal of Organic Chemistry*. **2013**, *9,* 1907-1916.

72. Andrei C., Drăguţan I., Balaban A.T. Polyolefins photostabilization with sterically hindered secondary amines (in Roum), Editura Academiei, Bucureşti, **1990**.

73. Yousif E., Salimon J., Salih N. Mechanism of photostabilization of poly(methy methacrylate) films by 2-thioacetic acid benzothiazol complexes. *Arabian Journal of Chemistry*, **2014**, *7*, 206–311.

74. Shneshil M., Redayan M. Photostabilization of PVC films by using some novel tetra Schiff's bases derived from 1,2,4,5-tetra-[5-amino-1,3,4-thiadiazole-2-yl]-benzene. *Diyala j. for pure science*, **2010**, *7*, 34-77.

75. Yousif E.,Shneine J., Ahmed A. Synthesis and Characterization of some Metal Ions of 2-(6-Methoxynaphthalen-2-Yl) Propanoate Complexes, *Journal of Al-Nahrain University*, **2013**, *16*, 46-50.

76. Ganqlitz G., Hubiq S. Chemical Actinometry. *Pure and Applied Chemistry.* **1987**, *61*, 187-195.

77. Andrady A., Searle N. Photodegradation of rigid PVC formulations. II. Spectral sensitivity to light-induced yellowing by polychromatic light, *Journal of Applied Polymer Science.* **1989**, *37*: 2789–2802.

78. Rasheed R., Mansoor H., Yousif E., Hameed A., Farina Y., Graisa A. Photostabilizing of PVC films by 2-(aryl)-5-[4- (aryloxy)-phenyl]-1,3,4-oxadiazole compounds. *European Journal of Scientific Research.* **2009**, *30*, 464-477.

79. Yousif E., Haddad R., Yusop R. M. Ultra Violet Spectra Studies of Polystyrene Films in Presence of Some Transition Metal Complexes with 4-amino-5-pyridyl)-4h-1,2,4-triazole-3-thiol. *Oriental Journal of Chemistry.* **2015**, *31*, 591-596.

80. Aliwi S., Najim T., Naief O. Photostabilization of poly (vinyle chloride) using natural products. *Journal of college education*, **2011**, *1*, 357-390.

81. Ahmed M., Samira T., Ludmila K., Mahmoud A. Itaconamide derivatives as organic stabilizers for poly(vinyl chloride) against photodegradation. *Journal of macromolecular science.* **2016**, *53*, 96-103.

82. Yousif E., Yusop R. M., Ahmed A. Photostabilizing effecincy of PVC based on epoxidized Oleic acid. *Malaysian Journal of Analytical Sciences,* **2015**, *19*, 213-221.

83. Yousif E., Salimon J., Salih N. New stabilizers for polystyrene based on 2-N-salicylidene-5-(substituted)-1,3,4-thiadiazole compounds, *Journal of King Saud University,* **2012**, *24*, 299-306.

84. Kara F., Aksoy E., Yuksekdagd Z., Hasirci N., Aksoy S. Synthesis and surface modification of polyurethanes with chitosan forantibacterial properties. *Carbohydrate Polymer.* **2014**, *112*, 39–47.

85. Nath M., Singh H., Kumar P., Song X., Eng. G. Organotin(IV) tryptophanylglycinates: Potential non-steroidal anti-inflammatory agents; crystal structure of dibutyltin(IV) tryptophanylglycinate. *Applied Organometallic Chemistry*. **2009**, *23*, 347-358.

86. Masood H., Ali S., Mazhar M. ^{1}H, ^{13}C, ^{119}Sn NMR, mass, Mössbauer and biological studies of tri-, di- and chlorodiorganotin(IV) carboxylates. *Turkish Journal of Chemistry*. **2004**, *28*, 75-85.

87. Gölcü A. Spectrophotometric Determination of Furosemide in Pharmaceutical Dosage Forms Using Complex Formation with Cu (II). *Journal of Analytical Chemistry*. **2006**, *61*, 748-754.

88. Coşkun A. The Synthesis of 4-phenoxyphenylglyoxime and 4,4-oxybis(phenylglyoxime) and their complexes with Cu(II), Ni(II) and Co(II). *Turkish Journal of Chemistry*. **2006**, *30*, 461-469.

89. Yousif E., Salih N., Salimon J. Improvement of the photostabilization of PVC films in the presence of 2N-salicylidene-5-(substituted)-1,3,4-thiadiazole, *Journal of Applied Polymer Science*. **2011**, *120*, 2207-2214.

90. Andrady A. L., Searle N. D. Photodegradation of rigid PVC formulations. II. Spectral sensitivity to light-induced yellowing by polychromatic light. *Journal of Applied Polymer Science*. **1989**, *37*, 2789-2802.

91. Yousif E., Bakir E., Salimon J., Salih N. Evaluation of Schiff bases of 2,5-dimercapto-1,3,4- thiadiazole as photostabilizer for poly(methyl methacrylate), *Journal of Saudi Chemical Society*. **2012**, *16*, 279-285.

92. Naif O., Salih H. Synthesis of New Modified PVC and their Photostability Study, *Tikrit Journal of Pure Science*. **2011**, *16*, 1613-1662.

93. Cooray B., Scott G. The effect of thermal processing on PVC-Part VIII: The role of thermally formed peroxides on photo degradation, *Polymer Degradation and Stability*. **1981**, *3*, 127-135.

94. Cooray B., Scott G. The effect of thermal processing on PVC-VI. The role of hydrogen chloride, *European Polymer Journal*. **1980**, *16*, 169-177.

95. Yousif E., Haddad R. Photodegradation and photostabilization of polymers, especially polystyrene: review, *SpringerPlus*. **2013**, *398*, 1-32.

96. Ali M., El-Hiti G. A., Yousif E. Photostabilizing efficiency of poly(vinyl chloride) in the presence of organotin(IV) complexes as photostabilizers. *Molecules*. **2016**, *21*, doi:10.3390/molecules 21091151

97. Balakit A. A., Ahmed A. El-Hiti G. A., Smith K., Yousif E. Synthesis of new thiophene derivatives and their use as photostabilizers for rigid poly(vinyl chloride). *International Journal of Polymer Science* **2015**, doi:10.1155/2015/510390.

98. Naif O., Salih H. Synthesis of New Modified PVC and their Photostability Study, *Tikrit Journal of Pure Science*. **2011**, *16*, 101-117.

99. Braun D., Rabie S. T., Khaireldin N. Y., Abd El-Ghaffar M. A. Preparation and evaluation of some benzophenone terpolymers as photostabilizers for rigid PVC. *Journal of Vinyl and Additive Technology*. **2011**, *17*, 47-155.

100. Saranya K., Rameez M., Subramania A. Developments in conducting polymer based counter electrodes for dye-sensitized solar cells an overview. *European Polymer Journal*. **2015**, *66*, 207-227.

101. Allcock R., Lampe W., Mark P. "Contemporary Polymer Chemistry" 3d ed, Pearson Prentice-Hall. **2003**.

102. Yousif E., Hameed A. Synthesis and Photostability Study of Some Modified Poly(vinyl chloride) Containing Pendant Benzothiazole and Benzimidozole Ring. *International Journal of Chemistry*. **2010**, *2*, 65-80.

103. Yousif E., Hasan A., El-Hiti G. A. Spectroscopic, physical and topography of photochemical process of PVC films in the presence of Schiff base metal complexes. *Polymers*. **2016**, *8*, 204, doi:10.3390/ polym8060204.

104. Jellinek H. G. "Aspects of Degradation and Stabilization of Polymers" Elsevier: Amsterdam, The Netherlands, **1978**.

105. Kaczmarek H. Changes to polymer morphology caused by U.V. irradiation: I. Surface damage, *Polymer*. **1996**, *37*, 189-194.

106. Magonov S., Bar G., Cantow H., Bauer H., Müller I. Atomic force microscopy on polymers and polymer related compounds, *Polymer Bulletin*, **1991**, *26*, 223-230.

107. Kaczmarek H., Linden L., Rabek J. Photo-oxidative degradation of poly(2,6-dimethyl-1,4-phenylene oxide) in the presence of concentrated hydroxy peroxide: the role of

hydroxy (HO.) and hydroperoxy (HOO·) radicals. *Polymer Degradation and Stability.***1995**, *47*: 175-188.

108. Valko L., Klein E., Kovaˇrík P., Bleha T., Šimon P. Kinetic study of thermal dehydrochlorination of poly(vinyl chloride) in the presence of   oxygen: III. Statistical thermodynamic interpretation of the oxygen catalytic activity. *European Polymer Journal*. **2001**, *37*, 1123-1133.

109. Yousif E., A. El-Hiti G., Hussain Z., Altaie A. Viscoelastic, Spectroscopic and Microscopic Study of the Photo Irradiation Effect on the Stability of PVC in the Presence of Sulfamethoxazole Schiff's Bases. *Polymers*. **2015**, *7*, 2190-2204.

110. Júnior G. C., Silva A. S., Guinesi L. S. Synthesis, characterization and electropolymerization of a new polypyrrole iron(II) Schiff-base complex. *Polyhedron* **2004**, *23*, 1953–1960.

111. Kara F., Aksoy E. A., Yuksekdagd Z., Hasirci N., Aksoy S. Synthesis and surface modification of polyurethanes with chitosan for antibacterial properties. *Carbohydrate Polymer*. **2014**, *112*, 39–47.

112. Zheng X. G., Tang L. H., Zhang N., Gao Q. H., Zhang C. F., Zhu Z. B. Dehydrochlorination of PVC materials at high temperature. *Energy Fuels*. **2003**, *17*, 896-900.

113. Folarin O. M., Sadiku E. R. Thermal stabilizers for poly(vinyl chloride): A review. *International Journal of Physical Sciences*. **2011**, *6*, 4323-4330.

114. Pospíšil J., Klemchuk P.P. Oxidation Inhibition in Organic Materials; CRC Press: Boca Raton, FL, USA, **1989**, *1*, 48-49.

115. Shyichuk A. V., White J. R. Analysis of chain-scission and crosslinking rates on the photooxidation of polystyrene. *Journal of Applied Polymer Science*. **2000**, *77*, 3015-3023

<div dir="rtl">

الخلاصــــــــــة

حضرت اربع معقدات من مركبات القصدير العضوية (IV) [(Bu)₂SnO, (Bu)₂SnCl₂, Ph₃SnCl (CH₃)₂SnCl₂)] مع فوروسيميد ليكاند في وسط كحولي.

هذه المعقدات هي :

</div>

Dimethyltin di-[4-hloro-2-(furan-2-ylmethylamino)-5-sulfamoylbenzoic acid], Me$_2$SnL$_2$

Dibutyltin di-[4-chloro-2-(furan-2-ylmethylamino)-5-sulfamoylbenzoic acid], Bu$_2$SnL$_2$

Dibutyltin hydroxy [4-chloro-2-(furan-2-ylmethylamino)-5-sulfamoylbenzoic acid], Bu$_2$SnOHL

Triphenyltin [4-chloro-2-(furan-2-ylmethylamino)-5-sulfamoylbenzoic acid], Ph$_3$SnL

<div dir="rtl">

وقد تم تشخيص هذه المركبات بالطرائق الطيفية (طيف الأشعة تحت الحمراء (FTIR) وطيف الأشعة فوق البنفسجية والمرئية (.UV-Vis) و طيف الرنين النووي المغناطيسي (^{1}H NMR) و قياسات التوصيلية الكهربائية المولارية

</div>

ودرجة الانصهار. ومن خلال القياسات وجد ان المعقدان Me_2SnL_2 و Bu_2SnL_2 ثمانية السطوح اما المعقدان Bu_2SnOHL و Ph_3SnL ياخذان شكل هرمي ثلاثي الزوايا.

تم استعمال معقدات القصدير العضوية كمضافات لتحسين متعدد كلوريد الفينيل ضد التجزئة الضوئية. تم متابعة سرعة التجزئة والتثبيت الضوئي للرقائق البوليمرية بسمك (٤٠) مايكروميتر لمتعدد كلوريد الفينيل يحتوي على تركيز 0.5% من المعقدات التي حضرت. تم دراسة عملية التثبيت الضوئي لرقائق بوليمر كلوريد الفينيل عند درجة حرارة الغرفة استعمال ضوء بطول موجي (313nm) وبشدة 7.75×10^{-7} Einstein dm^{-3} sec^{-1}.

تم تحديد فعالية الاستقرارية الضوئية لمركبات القصدير العضوية بقياس قيم معامل الكاربونيل $I_{C=O}$ والهيدروكسي I_{OH}و البولين $I_{c=c}$ و حسابات نقصان الوزن حيث كانت تزداد مع زيادة زمن التشعيع وان هذه الزيادة تعتمد على نوع المضاف المستعمل.

كما تم خلال البحث دراسة السطح مع زمن التشعيع وكذلك قطع السلسلة البوليمرية وقيم منتوج الكم وذلك بقياس مقدار التغير في متوسط اللزوجة للوزن الجزيئي مع زمن التشعيع، فوجد ان مقدار التغير في متوسط اللزوجة للوزن الجزيئي يقل بزيادة زمن التشعيع.

وجد أن المضافات المحضرة تسلك كمثبتات للتجزئة الضوئية، والتي أخذت الترتيب التالي

$Me_2SnL_2 < Bu_2SnOHL < Bu_2SnL_2 < Ph_3SnL$

$\longrightarrow$

زيادة الاستقرارية الضوئية

من خلال النتائج العملية المستحصلة اقترحت بعض الميكانيكيات اعتماداً على الصيغ التركيبية لمركبات القصدير العضوية لذلك هي قانصات HCl, ممتصات اشعة فوق البنفسجية مجزئات ,البيروكسيد وقانصات الجذور الحر.

جمــــــــــــــــــهورية العراق
وزارة التعليم العالي والبحث العلمي
جامعـــــــــــــــــة النهريـــــــــن
كليــــــــــــــة العــــــــــلوم
قـــــــــسم الكيميــــــاء

استخدام معقدات القصدير العضوية (IV) الثنائية والثلاثية كمثبتات ضوئية لبوليمر متعدد كلوريد الفينيل

رسالة مقدمة الى

كلية العلوم- جامعة النهرين

وهي جزء من متطلبات نيل درجة الماجستير في علوم الكيمياء

من قبل

مصطفى محمد علي

بكالوريوس علوم كيمياء/كلية العلوم/جامعة النهرين

(2014)

المشرف
الاستاذ الدكتور عماد السراج

2017   **1438**